SPRINGER BRIEFS IN
ELECTRICAL AND COMPUTER ENGINEERING

Christoph Guger
Theresa Vaughan
Brendan Allison *Editors*

Brain-Computer Interface Research

A State-of-the-Art Summary 3

Springer

SpringerBriefs in Electrical and Computer Engineering

More information about this series at http://www.springer.com/series/10059

Christoph Guger · Theresa Vaughan
Brendan Allison
Editors

Brain-Computer Interface Research

A State-of-the-Art Summary 3

Springer

Editors
Christoph Guger
Schiedlberg
Austria

Theresa Vaughan
Albany, NY
USA

Brendan Allison
Department of Cognitive Science
UC San Diego
La Jolla, CA
USA

ISSN 2191-8112 ISSN 2191-8120 (electronic)
ISBN 978-3-319-09978-1 ISBN 978-3-319-09979-8 (eBook)
DOI 10.1007/978-3-319-09979-8

Library of Congress Control Number: 2014952785

Springer Cham Heidelberg New York Dordrecht London

Printed on acid-free paper

Springer is part of Springer Science+Business Media (www.springer.com)

Contents

Recent Advances in Brain-Computer Interface Research—The BCI Award 2013

Christoph Guger and Brendan Z. Allison

Keywords Brain-computer interface · BCI Award · State-of-the art in BCI research

1 Introduction

Brain-Computer Interfaces (BCIs) are devices that can enable communication or control without movement. The BCI detects specific patterns of the user's brain activity that reflect different messages or commands that the user wants to send, such as spelling or changing a television channel. Signal processing tools then decode this brain activity to identify the desired message or command, then send this message to an output device. BCIs are closed-loop systems, meaning that the BCI must provide the user with some information in real-time that (hopefully) reflects the intended message or command.

One defining feature of any BCI is the method used to record brain function. Many approaches have been explored, and new ones are often introduced—some later in this book. Most modern BCIs rely on one of the following four methods:

Electroencephalography (EEG) records the brain's electrical activity from electrodes that are usually embedded in an electrode cap. This cap usually requires 5 min to mount on the user and adjust electrodes to get a good signal, although

C. Guger (✉)
g.tec Medical Engineering GmbH/Guger Technologies OG,
Sierningstrasse 14, 4521 Schiedlberg, Austria
e-mail: guger@gtec.at

B.Z. Allison
Cognitive Science Department, University of California at San Diego,
9500 Gilman Drive, La Jolla, San Diego, CA 91942, USA

B.Z. Allison
Electrical and Computer Engineering Department, Old Dominion University,
Norfolk, VA 23529, USA

C. Guger et al. (eds.), *Brain-Computer Interface Research*, SpringerBriefs
in Electrical and Computer Engineering, DOI 10.1007/978-3-319-09979-8_1

newer systems that require less time have been developed. EEG systems are relatively inexpensive and portable, and are the most common neuroimaging method in BCI research.

Electrocorticography (ECoG) involves recording electrical activity from electrodes that are surgically implanted on the surface of the brain. Relative to EEG sensors, ECoG sensors have better spatial resolution, and can accurately detect brain activity at high frequencies that are invisible to EEG electrodes. Once implanted, the electrodes can be ready for BCI use or other tasks without preparation before each use.

Depth electrode recording uses electrodes that are surgically implanted in the brain. This approach has appealing features similar to ECoG, but records activity from a smaller group of neurons. Hence, these two approaches provide a different picture of brain activity.

Functional Magnetic Resonance Imaging (fMRI) does not measure electrical activity, but instead measures the brain's blood flow changes associated with different mental activities. These changes cannot be detected with the temporal precision as the three approaches above. fMRI systems require a very powerful magnetic field, and thus cost millions of dollars and are not portable.

The two middle procedures require neurosurgery to implant the electrodes. Of course, this procedure is only considered when medically necessary, such as prior to epilepsy surgery or for severely disabled patients with few or no other communication and control options. This neurosurgical procedure is expensive, and may not be viable for some patients. Hence, invasive BCIs are only practical for some users. On the other hand, new research in this book and elsewhere is showing that invasive BCIs may provide some communication or rehabilitation options that are otherwise unavailable.

After the signal has been recorded from the brain, signal processing mechanisms must determine which signal the user wanted to send. Signal processing often involves many steps to customize the BCI to a specific user and environment, such as finding the best electrode sites, removing unwanted information (such as electrical noise caused by muscle movement or external devices), determining the best frequencies, and choosing the optimal classifier and classifier parameters. After this, the signal travels to an output device. Early BCIs typically sent signals to monitors, and newer BCIs have been used to control devices including orthoses, wheelchairs, online applications, entertainment systems, or stroke rehabilitation systems. BCIs also differ in the types of mental activities that users perform for control, and the corresponding brain signals. Most BCIs rely on imagined movement or visual attention for control, but new directions are being explored and extended often. Ultimately, the best BCI for each user depends on the user's medical condition (if any), needs, goals, preferences, usage environment, and other factors.

Over the last several years, BCI research has expanded in many different ways. BCI publications are becoming increasingly common in journals and books. The first journal devoted only to BCIs, called the BCI Journal, was launched in late 2013. BCI conferences and workshops are becoming more common and drawing more attendees. Videos and media articles about BCIs are increasingly popular online.

New BCI systems are being tested with a broader range of patient groups, providing new options for communication and rehabilitation. This increase in BCI activity has fostered some exceptional projects that merit additional attention.

2 The BCI Award

To encourage top quality BCI research, g.tec established the annual BCI Awards in 2010. g.tec was formed in 1999 and produces equipment and software used in many BCI labs, as well as numerous research articles. To enter the competition, each team must submit a two-page research summary, detailed on the BCI Award website. The competition is open to any team, and submissions have come from a wide variety of regions and disciplines. The submissions may include different types of hardware and/or software, and must include results from real-world testing and validation.

Each year, a different top research institution is asked to recruit a Chairman of the Jury, who will develop a jury to judge these submissions. This jury consists of respected BCI researchers, which judges the submissions based on the **Award Criteria** below. The jury then chooses ten nominees, who are announced publicly and invited to a gala award ceremony attached to a major BCI conference. Finally, the winning submission is announced at this ceremony. The winning team receives a certificate, trophy, and 3,000 USD. The Award is also a major honor; even being nominated is a significant accolade in the BCI research community. Furthermore, the ten nominees are invited to contribute a chapter to this annual book series, which summarizes their projects along with related work, analyses, discussion, and new directions.

Each jury is asked to select the nominees and winner based on specific **Award Criteria**:

- Does the project include a novel application of the BCI?
- Is there any new methodological approach used compared to earlier projects?
- Is there any new benefit for potential users of a BCI?
- Is there any improvement in terms of speed of the system (e.g., bits/min)?
- Is there any improvement in system accuracy?
- Does the project include any results obtained from real patients or other potential users?
- Is the used approach working online/in real-time?
- Is there any improvement in terms of usability?
- Does the project include any novel hardware or software developments?

The BCI Award has rapidly developed into a top honor within the BCI community. In 2013, 169 projects were submitted, almost triple the number of submissions in 2012. The 2013 Award Ceremony attracted a record number of attendees, and hundreds of BCI researchers and developers awaited the announcement of the winner with great suspense. Our book chapters reviewing the 2011 BCI Award has been downloaded over 10,000 times. The 2014 Award should be more competitive than ever.

3 The 2013 Nominees

This year, the jury was chaired by Theresa Vaughan from the Wadsworth Research Laboratory, who selected Drs. Douglas Weber, Adam Hebb, Donatella Mattia, Andrzej Cichocki, Adam Wilson, and Surjo Soekadar as jury members. Continuing with prior tradition, the jury included the winner of the previous year's award, Dr. Soekadar. These jury members are all from esteemed research institutes around the world, with expertise including signal processing, neuroscience, medicine, invasive and non-invasive BCIs, and real-world BCI use with patients.

Choosing ten nominees out of 169 submissions was very hard, and many interesting submissions from well-known BCI groups had to be rejected. The following projects were nominated for the 2013 BCI Award:

"Give me a sign: The possibilities of using hand gestures as a control signal for implanted brain computer interfaces"

M.G. Bleichner[a], J.M. Jansma[a], Z.V. Freudenburg[a], E.J. Aarnoutse[a], M.J. Vansteensel[a], N.F. Ramsey[a]

[a]Rudolf Magnus Institute of Neuroscience, Dept. of Neurology and Neurosurgery, University Medical Center Utrecht, The Netherlands

"An Ipsilateral, Contralesional BCI in Chronic Stroke Patients"

D.T. Bundy[a], E.C. Leuthardt[a]

[a]Washington University, St. Louis, MO, USA

"A learning-based approach to artificial sensory feedback: intracortical microstimulation replaces and augments vision"

M.C. Dadarlat[a,b], J.E. O'Doherty[a], P.N. Sabes[a,b]

[a]Department of Physiology, Center for Integrative Neuroscience, San Francisco, CA, USA

[b]UC Berkeley-UCSF Bioengineering Graduate Program, University of California, San Francisco, CA, USA

"Motor recovery of chronic writer's cramp by brain-computer interface rehabilitation: A pilot study"

Y. Hashimoto[a], T. Ota[b], M. Mukaino[b], J. Ushiba[c]

[a]Department of Electrical and Electronic Engineering, Kitami Institute of Technology, Kitami, Hokkaido, Japan

[b]Department of Physical Medicine and Rehabilitation, Asahikawa Medical University Hospital, Asahikawa, Hokkaido, Japan

[c]Department of Biosciences and Informatics, Faculty of Science and Technology, Keio University, Yokohama, Kanagawa, Japan

"Cognitive signals for brain-machine interfaces: an alternative paradigm to neuroprosthetics control"

I. Iturrate[a], R. Chavarriaga[b], L. Montesano[a], J. Minguez[a], J. del R. Millán[b]

[a]Instituto de Investigación en Ingeniería de Aragón and Dpto. de Informatica e Ingeniería de Sistemas, University of Zaragoza, Spain

[b]Defitech Foundation Chair in Non-Invasive Brain-Machine Interface, EPFL, Lausanne, Switzerland

"An Accurate, Versatile, and Robust Brain Switch for Neurorehabilitation"

N. Jiang[a], N. Mrachacz-Kersting[b], R. Xu[a], K. Dremstrup[b] and D. Farina[a]

[a]Department of Neurorehabilitation Engineering, Bernstein Center for Computational Neuroscience, University Medical Center, Göttingen, Denmark

[b]Center for Sensory-Motor Interaction, Department of Health Science and Technology, Aalborg University, Aalborg, Denmark

"Ear-EEG: Continuous Brain Monitoring"

D. Looney[a], P. Kidmose[b], M.J. Morrell[a,c], D.P. Mandic[a]

[a]Imperial College London, UK

[b]Aarhus University, Denmark

[c]Sleep Unit, Royal Brompton Hospital, London, UK

"A hybrid brain computer interface for adaptive workload estimation in rehabilitation robotics"

D. Novak[a], B. Beyeler[a], X. Omlin[a], R. Riener[a,b]

[a]Sensory-Motor Systems Lab, ETH Zurich, Switzerland

[b]Spinal Cord Injury Center of Balgrist University Hospital, Switzerland

"A concurrent brain-machine interface for sequential motor function"

M. Shanechi[a,b], R. Hu[d,e], M. Powers[d], G. Wornell[c], E. Brown[d,e,f], Z. Williams[d,e]

[a]Department of Electrical Engineering and Computer Science, University of California, Berkeley, CA, USA

[b]Department of Electrical and Computer Engineering, Cornell University, Ithaca, NY, USA

[c]Department of Electrical Engineering and Computer Science, Massachusetts Institute of Technology, Cambridge, MA, USA

[d]Massachusetts General Hospital, Boston, MA, USA

[e]Harvard Medical School, Boston, MA, USA

[f]Department of Brain and Cognitive Sciences, Massachusetts Institute of Technology, Cambridge, MA, USA

"Exploring an fMRI-guided minimally invasive subdural N200 speller"

D. Zhang[a], H. Song[a], R. Xu[a], B. Hong[a]

[a]Department of Biomedical Engineering, School of Medicine, Tsinghua University, Beijing, China

These ten projects reflect substantial diversity in many ways. The projects include research to help people with visual deficits, hearing deficits, writer's cramp, stroke, and severe movement disabilities. This trend toward broader medical applications is consistent with the overall increase in medical applications for more types of patients. The projects entail a variety of methods for recording brain activity, including conventional methods like scalp recorded EEG and invasively recorded ECoG and unconventional approaches including ear-based EEG recording and activity modulated by direct sensory stimulation. The nominated teams come from a variety of backgrounds and academic disciplines, from China, The Netherlands, Japan, Denmark, Spain, the UK, Switzerland, and various institutes in the USA.

Because of the growing interest in the BCI Awards, and the quality of the nominated projects, we decided to create this annual book series so readers could learn

about the top projects and trends in the BCI community. Each book includes an introduction and conclusion, written by the editors, that summarizes recent BCI trends, the selection procedure, nominees, and winner. The remaining book chapters are written by the nominees themselves, and present each of their projects in more detail than their original two-page submission. These chapters also include newer results, analyses, discussion, and future directions. This year, for the first time, we have added a chapter from a project that received an "Honorable Mention" from the jury, but was not nominated. This chapter includes noteworthy progress since the award submission, and its principal author has been selected as a member of the jury for the 2014 BCI Award.

Give Me a Sign: Studies on the Decodability of Hand Gestures Using Activity of the Sensorimotor Cortex as a Potential Control Signal for Implanted Brain Computer Interfaces

M.G. Bleichner and N.F. Ramsey

The major driving force behind the development of brain computer interfaces (BCI) has been the desire to re-establish communication for severely paralyzed or even locked-in patients. As a consequence, different strategies have been developed to provide a direct link between a still-functional brain and the outside world, bypassing the non-functional muscle system (Wolpaw et al. 2002). The first BCIs used the P300 evoked potential (Farwell and Donchin 1988) and slow cortical potentials (Birbaumer et al. 1999), as they can be measured by electroencephalography (EEG).

In the ideal case, a BCI would enable its user, previously incapable of any communication, to participate in a conversation at the same speed and with the same expressiveness as a non-paralyzed person would. However, the use of electroencephalography (EEG) as the primary recording method has to date limited the potential to decode brain activity, due to its low spatial resolution and signal-to-noise ratio. EEG can only detect prominent changes in brain activity and often has to integrate information over time in order to detect a certain activity pattern. These limitations reduce the speed and flexibility of any communication based on EEG BCI.

M.G. Bleichner (✉) · N.F. Ramsey
Department of Neurology and Neurosurgery, Brain Center Rudolf Magnus, University Medical Centre Utrecht, Utrecht, The Netherlands
e-mail: martin.bleichner@uni-oldenburg.de

N.F. Ramsey
e-mail: n.ramsey@umcutrecht.nl

M.G. Bleichner
Department of Psychology, Neuropsychology Lab, University of Oldenburg, Oldenburg, Germany

C. Guger et al. (eds.), *Brain-Computer Interface Research*, SpringerBriefs in Electrical and Computer Engineering, DOI 10.1007/978-3-319-09979-8_2

In recent years, an alternative to the EEG-based BCIs has emerged that is based on invasive recording techniques such as single-cell/multi-unit recordings (Collinger et al. 2012; Guenther et al. 2009; Hochberg et al. 2012) and electrocorticography (ECoG) (Leuthardt et al. 2004; Vansteensel et al. 2010; Wang et al. 2013). These methods provide a much higher spatial resolution and have a superior signal-to-noise ratio compared to EEG, and provide the potential to differentiate between a greater number of cognitive states and at a faster rate.

The primary objective of invasive BCI research has been the control of artificial limbs using the activity from neurons of the primary motor cortex. Using the combined activity of individual neurons (Hochberg et al. 2012), or larger populations of neurons (Wang et al. 2013), allows tetraplegic patients to control artificial arms and hands with a promising degree of accuracy, enabling them to grasp objects, for example.

Our hands, however, are not only suitable for manipulating objects but also for communication. In sign languages, for example, different hand gestures represent the letters of the alphabet. Sign languages are full-fledged languages that allow anything to be conveyed in the same way that any other language can. With the help of the hands, face and even the entire body, words and meanings are expressed as complex signs. To spell words or names for which no specific signs are available, sign languages also contain a fingerspelling alphabet. For each letter of the alphabet, there exists a specific gesture that can be formed with one hand (see Fig. 1).

The muscles of our body, hands and fingers are controlled by a network of cortical and subcortical structures involving, among others, the cerebellum, the basal ganglia and the primary motor cortex. The topographic representation of body parts in primary motor cortex (Penfield and Rasmussen 1950) makes it easy to differentiate between the movements of the different body parts (legs and arms)

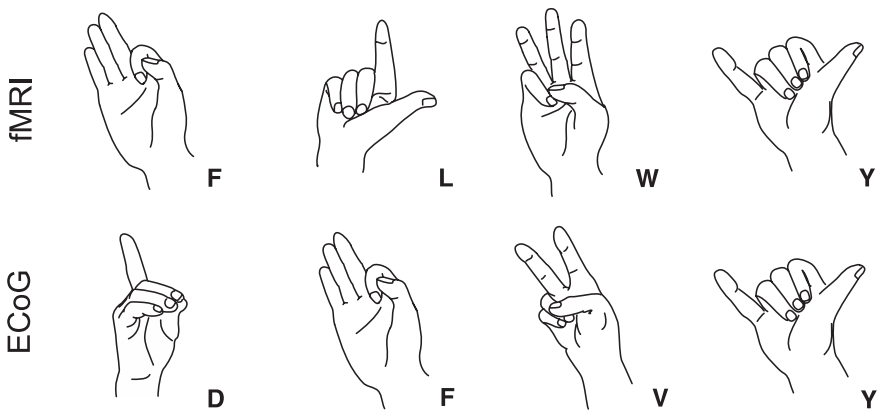

Fig. 1 Participants had to execute one of four hand gestures taken from the American sign language alphabet. For the fMRI study, the gestures '*L*', '*F*', '*W*' and '*Y*' and for the ECoG study '*D*', '*F*', '*V*' and '*Y*' were used

based on neuronal activity, and this topographic representation is also present for individual fingers. The hands and fingers are known to be extensively represented on the sensorimotor cortex at a specific anatomical landmark, the so-called hand knob (Yousry et al. 1997). Moreover, it has been shown that the movement of individual fingers (Kubánek et al. 2009; Miller et al. 2009) and the coordinated movements of all fingers [e.g. during grasping (Chestek et al. 2013; Pistohl et al. 2012)] can be discriminated based on the neuronal activity of the sensorimotor cortex. Consequently it should also be possible to decode communicative hand gestures.

The confined representation of the hand makes it a very interesting target region to extract control states for a permanent BCI using implanted electrodes. Nevertheless, permanent BCIs based on needle or surface electrodes require surgical intervention for the electrode placement. Every surgery comes with a certain risk for the patient, which is especially the case for people with locked-in syndrome. The required surgery should therefore be as short and limited as possible. The hand knob area would be such a region. It is located on the gyrus 'at the cross point between the pre-central sulcus and the central sulcus, and is therefore also visible on the cortical surface' (Yousry et al. 1997), and is also confined to a small area. This makes it surgically comparatively easy to access and therefore only requires a small surgical intervention.

We propose using communicative hand gestures as the control signal for an ECoG based BCI with the purpose of re-establishing communication. If it were possible to decode multiple gestures from their activation pattern over the motor cortex, it would provide an interesting and powerful approach for the control of BCI, specifically aimed at reinstating communication. We therefore studied the feasibility of decoding communicative hand gestures using high-field fMRI and high-density ECoG.

1 fMRI

In a first step towards our goal of using hand gestures for BCI control, we studied the decodability of gestures using functional magnetic resonance imaging (fMRI). Although our objective is an implantable BCI using ECoG electrodes, the fMRI provides valuable information that is difficult to acquire by other means. The primary advantage of using fMRI (compared to invasive recording techniques) is that it allows larger groups of people to be studied. The obtained results are therefore generalizable to the population. fMRI provides a good spatial resolution which, at 7 T field strength, is comparable to what can be measured with high-density ECoG electrodes (1–2 mm inter electrode distance). Furthermore, it allows researchers to record from all parts of the brain (including deeper structures) at the same time. The rather good correspondence between the brain activity patterns on the cortex as measured by fMRI and by ECoG (Hermes et al. 2012; Siero et al. 2013; Vansteensel et al. 2010) makes it possible to use the fMRI results to inform our subsequent ECoG study.

The classification of individual gestures on a single trial basis requires a good signal-to-noise ratio, and the representations we were interested in are presumably rather fine-grained (Dechent and Frahm 2003) necessitating high spatial resolution. We therefore conducted our study using a Philips Achieva MRI 7 T system with a 32-channel head-coil. Given the superiority of 7 T fMRI over typical fMRI at lower field strength, in terms of signal strength and quality (van der Zwaag et al. 2009), we expected to be able to decode individual movements on a single trial basis.

Twelve young healthy right-handed volunteers participated in the study, in which they had to execute four hand gestures taken from the American Sign Language alphabet (corresponding to the letters 'F', 'L', 'W' and 'Y'; see Fig. 1) inside the scanner. The participants were naive to the meaning of the signs prior to the experiment. In a familiarization session, they practiced the gestures and learned the corresponding letters. The execution of the gestures inside the scanner was recorded by an MRI compatible data-glove (5 DT). This data-glove provides information about the flexion of each finger [for a more detailed description of this study, please see Bleichner et al. (2013)].

As we wanted to classify individual gestures, all participants performed two runs. The data from the first run (training run) was used to train a classifier, and the data of the second run (test run) was used to test whether we could predict which gesture was performed on a single trial basis. For this, we computed average activation maps on the training run for each type of gesture. The resulting four activation maps (one for each type of gesture) then served as prototypical templates. Furthermore, to reduce the amount of data, we selected a subgroup of voxels that was considered most informative (i.e. showing a high level of activation of any of the gestures). The individual trials from the test run were then compared with the four prototypes. Using a simple pattern correlation classification, we computed the Pearson correlation between the activity pattern of the individual trial and the activity patterns of the four prototypes. The individual trial was labeled according to the gesture type with which it had the highest correlation.

We found an average classification score for the four gestures of 63 % (range of 35–95 %). This was significantly above the chance level of 25 %, indicating that the gestures could be distinguished on a single trial basis. Noticeably, the classification accuracy varied considerably between participants from barely above chance level (35 %) to almost perfect classification (95 %; Fig. 2a shows the individual classification scores). This wide range of classification scores, however, could be explained by the consistency with which the gestures were executed. The data-glove provided information on the movement of the individual fingers, and allowed us to compute how consistently the gestures of the same type were executed. There was a significant negative correlation ($r = -0.62$, $p < 0.05$) between the classification accuracy and the variability of the gesture execution (Fig. 2b). The less variably the gestures were executed, the higher the classification accuracy. This indicates that the gestures can be classified with high accuracy provided that the gestures are consistently executed.

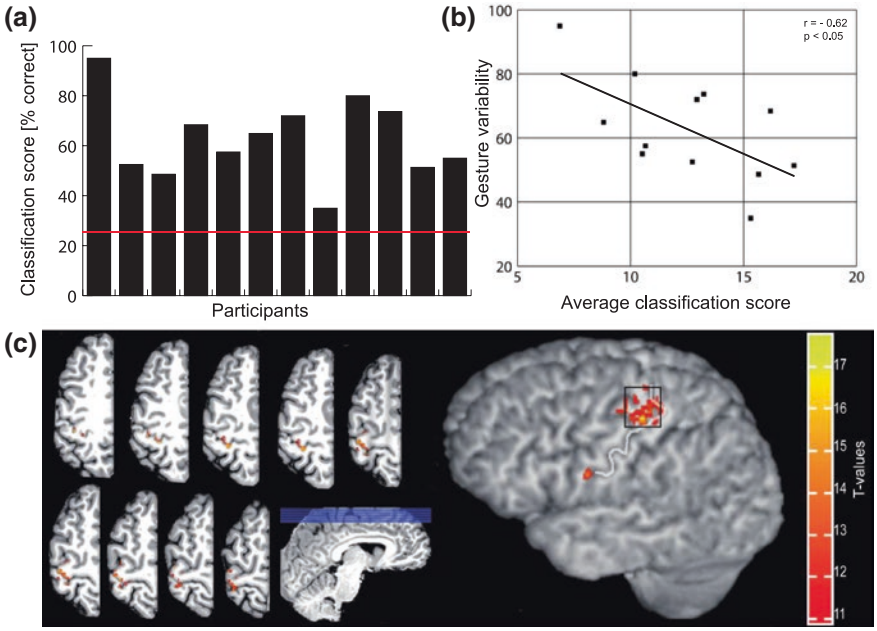

Fig. 2 fMRI results: **a** classification accuracy given as percentage correct for each individual. The *red line* indicates the 25 % chance level. **b** There was a significant negative correlation between the classification accuracy and the variability with which the gestures were executed. Participants who executed the gestures more consistently had a higher classification score. **c** (*Left*) Location of the most informative voxels shown on the axial slices for one participant. The majority of informative voxels are located at the hand knob area. The informative voxels follow the characteristic Epsilon shape of the hand knob. (*Right*) Most informative voxels as projection to the cortex. The *white line* indicates the central sulcus, and the *black square* indicates the possible location of a high density—EcoG grid (2 × 2 cm)

The most informative voxels were confined to a small patch of cortex surrounding the hand-knob area (Fig. 2c). The axial slices show nicely that the informative voxels cluster around the hand knob being partly located within the sulcus as well as on the gyrus.

Unlike fMRI, which provides a complete sample of the entire brain including deeper cortical structures, ECoG electrodes, which are located on the cortical surface, cannot measure from tissue in the sulcus. The ECoG electrodes are most sensitive to the neuronal activity of the tissue directly underneath the electrode, and probably cannot measure much from within the sulcus. To make our fMRI results comparable to the situation with ECoG electrodes, we restricted our voxel selection to those voxels that were located in the upper 6 mm of the cortical surface and we restricted the analysis to a patch of cortex of 2 × 2 cm (centered on the most active voxels). This corresponds to the area that could be covered by a high-density 8 × 8 electrode grid (Fig. 2c: right side, black square).

Using this restriction, we achieved an average classification accuracy of 53 % (range 32.5–92.5 %), which, though significantly lower than the values obtained using all voxels ($p < 0.05$), was still significantly above chance level ($p < 0.01$). For the best participant, that is, the person who performed the gestures most consistently, the classification accuracy was still 92.5 %, which would allow very good BCI control.

These results indicate that it is possible to distinguish different gestures, based on their single trial activation pattern, using a confined area of cortical tissue around the hand-knob region. Consistent execution of the gestures is essential for effectively discriminating the gestures.

2 ECoG

From the fMRI experiment, we learned that the four hand gestures could be classified with a comparably high accuracy using only a small patch of cortex (on the gyrus) that would also be accessible by ECoG surface grids.

In a subsequent study, we had the opportunity to test whether the gestures could also be discriminated using high-density ECoG. In the intensive epilepsy monitoring unit of the University Medical Centre Utrecht/The Netherlands, we recorded from five patients undergoing ECoG monitoring prior to surgery for epilepsy focus detection and functional mapping.

The grids, with an inter-electrode distance of 3 mm, contained 9 times more electrodes than the standard clinical grid (inter electrode distance of 1 cm). The grids contained either 4×8 or 8×8 electrodes and covered the hand-knob region to varying degrees. Only for one patient was the grid optimally located on the hand-knob.

As in the fMRI experiment, we asked participants to perform four hand gestures: ‘D’, ‘F’, ‘V’, ‘Y’ (see Fig. 1). Participants, who were naïve to the meaning of the gestures, underwent a short familiarization period. Due to the limited time we had with the patients, we could only record 40–80 trials in total per patient. To control for the accurate execution of the gestures, the hand movements were recorded using the data-glove as in the fMRI study.

After the normal pre-processing steps of filtering for line noise, and then re-referencing to the common average reference (comprised of all electrodes on the high density grid), the data was epoched into segments of 3 s (1 s before and 2 s after movement onset as determined based on the data-glove recording). For each epoch and electrode, the average power was computed for the frequency range of 70–125 Hz. Based on the literature, this frequency range was expected to be most informative for distinguishing the movements of individual fingers.

In a leave-one-out cross-validation scheme, we performed classification using pattern-correlation. All trials of each condition (excluding one) were used to compute the average activation pattern, leaving us with four averages (one per condition). The excluded trial was than compared with the four averages and classified

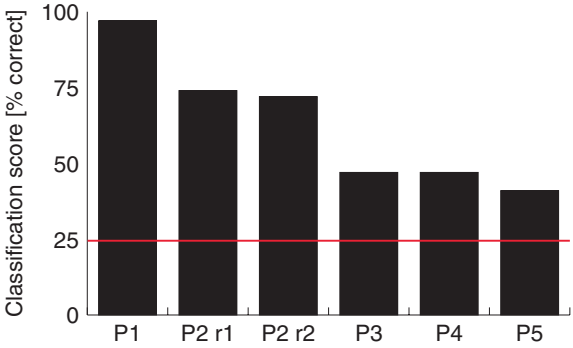

Fig. 3 ECoG classification results shown for each participant. The y-axis presents "classification scores" as percentage correct. The chance level of 25 % is indicated by the *red horizontal line*. Patient 2 (*P2*) did two sessions

as the condition with which it had the highest similarity (as computed by Pearson correlation).

The classification accuracy varied considerably between participants, ranging from 40 to 97 % (see Fig. 3). These large differences are primarily due to the location of the grid. In the fMRI study, we have already seen that the most active voxels cluster around the hand-knob region, being confined to a small area. For patients where the electrode grids did not sufficiently cover the hand-knob, the classification accuracy was low.

The participant with the best classification accuracy had the best coverage (see Fig. 4), which was also confirmed by the 7 T fMRI data we had from this patient. The second best patient also had a sufficiently good coverage, though the electrodes were located primarily on the post-central area. The reason for the lower classification accuracy for this participant was the poor execution of one of the gestures. In both runs (this was the only participant with two runs) the execution of the 'D' gesture entailed considerable problems, leading to hesitation and superfluous movements.

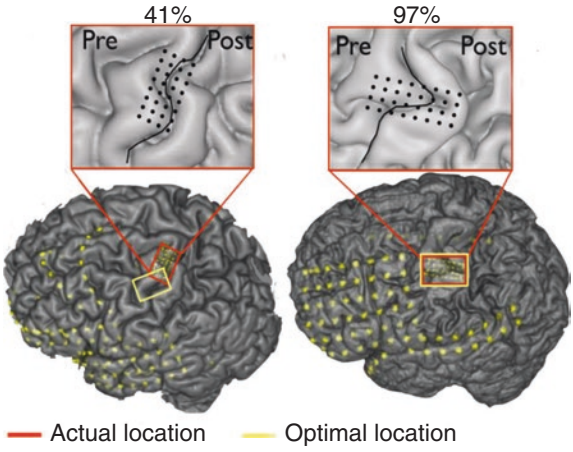

Fig. 4 Electrode locations (*yellow dots*) rendered on the individual anatomy for the worst (41 %) and best (97 %) performing participants. The *red rectangles* indicate the actual location of the high-density grids. The *yellow rectangles* indicate the anatomical location of the hand knob which can be considered optimal

These results show that classification of executed gestures is also possible using high-density surface electrode grids. Our data also suggest that the location of the grid is essential for good classification results. It appeared that high classification accuracy would also have been possible with a sub-selection of electrodes, which could allow the placement of fewer electrodes. Unfortunately, we did not have sufficient data to test this hypothesis.

3 Discussion

The two studies provide converging evidence that hand gestures, as used in the finger spelling alphabet, can be decoded from a small patch (several cm^2) of cortical surface. Using high-density electrode grids, it was possible to achieve almost perfect classification. We take this as evidence that hand gestures are in principle suitable for BCI control.

The small area from which the informative activation was recorded provides an optimal target for subdural grid placement. The burden and risk for the patient should therefore be limited.

The high correspondence between our fMRI and ECoG results provides some interesting opportunities. While this relationship has to be studied in more detail, our results suggest that high-field fMRI can help to pre-localize the optimal location for the electrode grid prior to surgery. The hope is that it will be possible in the future to individually tailor the exact placement of an electrode grid based on the individual cortical representations. Furthermore, a good pre-surgical localisation of the optimal implantation position will increase the chance of success for a patient. This will be especially important for patients with severe paralysis, where the cortical representation might deviate from normal anatomy, due head trauma, tumours or cortical reorganisation after extended periods of paralysis.

Another advantage of this correspondence is the potential to check prior to implantation whether the patient is able to control a BCI using this strategy inside the scanner, by examining the discriminability of the different patterns of activation. This could prevent unnecessary surgical procedures in cases where the chances of success are small. The signal quality allows for realtime feedback of the classifier (Andersson et al. 2012), allowing for presurgical testing.

Using hand gestures to control a BCI has a number of beneficial features. To provide a natural communication speed, BCIs have to be able to discriminate a large number of control signals in a short time. From the user's perspective, it should be possible to generate different control signals effortlessly in fast succession. However, many BCI control strategies require the user to switch between different mental tasks. For example, the fMRI based speller from Sorger et al. (2012) requires the users to switch between three different tasks (e.g. motor imagery, mental calculation and inner speech). This constant task switching, however, is tiring for the user. Using different hand gestures does not require such constant task switching and can be highly automated. Furthermore, the different control signals are just variations of

the same task (i.e. the execution of a gesture), so additional control signals can be introduced by using more gestures. Our approach should therefore be extendable to a larger number of control signals without additional effort for the user.

An important limitation in our experiments is that we studied executed movements in able-bodied participants, while the target group for such BCIs is patients with severe paralysis capable of attempted movements only. We have previously shown that imagined movements, assuming an adequate proxy for an inability to move in paralysis, in abled participants does not activate the primary motor cortex (M1), as measured with fMRI (Hermes et al. 2011). We instead postulate that executed movements are a better proxy for attempted movements in paralyzed people. There are studies that support this notion. Hotz-Boendermaker et al. (2008) have reported that paraplegics showed activation of the primary motor cortex during attempted movements that was comparable to the executed movements in healthy controls. Moreover, Hochberg et al. (2012), Collinger et al. (2012) and Wang et al. (2013) have shown that the sensorimotor cortex in paralyzed people provides sufficient information during attempted movements that allows for control of a robotic arm in several dimensions. Nevertheless, it remains to be shown that the complex hand gestures can also be discriminated during attempted movement and whether our approach is feasible for patients for actual BCI control.

Our approach allows an active BCI [as defined by Zander and Kothe (2011)] to be built. 'The BCI derives its outputs from brain activity which is directly and consciously controlled by the user, independent of external events' (Zander and Kothe 2011). Unlike the P300 speller where the user is dependent on external stimulation (i.e. the flashing of the letters), a gesture controlled BCI allows for self-paced control. The user can generate control signals whenever he wants, providing him with a larger degree of freedom and flexibility. It can also be an option for people that have problems (i.e. due to visual impairments) using the standard P300 speller (Brunner et al. 2010).

Finally, we expect that our approach would only interfere to a limited degree with other tasks. An often underestimated problem of BCI systems is the number of false alarms. BCIs are generally studied under well-controlled conditions in which the user is confronted with little distraction and has to perform a well-defined task (e.g. copy the spelling of a predetermined sentence). Under real circumstances, the control task (e.g. inner speech) might interfere with the task at hand (thinking about what to do), causing unintended reactions from the BCI system. We assume that this interference with general cognitive tasks should be minimal when using attempted movements.

Postulated advantages of using gestures for BCI control

- A small, confined area of cortex is sufficient to discriminate four different hand gestures. This confined area is an optimal target for subdural grid placement.
- The close correspondence between the fMRI and ECoG results suggests that it is possible to pre-localize the best grid position with fMRI prior

to implantation. Furthermore, it is possible to train the patient inside the scanner prior to implantation, using realtime classification feedback.
- Our approach does not require switching between different control tasks (e.g. motor imagery, mental calculation and inner speech), since it is possible to create different control signals by varying the same task (i.e. different gestures).
- Our approach is extendable. Though we have only differentiated between four gestures, it should be possible to differentiate a larger number of gestures.
- Increasing the number of gestures and thereby the number of control signals would not increase the time that is necessary for a selection.
- Our approach can be self-paced. Unlike a P300 speller, external stimulation is not necessary. This also makes it interesting for visually impaired patients.
- Interference effects with other cognitive tasks are expected to be minimal. This may have a positive effect on the false alarm rate.

4 Conclusion

The studies presented here provide a first indication that communicative hand gestures as they are used in the fingerspelling alphabet of sign languages can be distinguished based on their neuronal activity on a small patch of cortex. The hand-knob area, which is anatomically well defined, therefore provides an interesting target area for high-density electrode implantation. We conclude that hand gestures can provide an interesting possibility to control an ECoG based BCI for communication. As our results have been obtained in able-bodied people, considerable work has to be done before this approach can be used in an actual application for people with severe paralysis.

References

Andersson P, Pluim JPW, Viergever MA, Ramsey NF (2012) Navigation of a telepresence robot via covert visuospatial attention and real-time fMRI. Brain Topogr 26(1):177–185. doi:10.1007/s10548-012-0252-z

Birbaumer NN, Ghanayim NN, Hinterberger TT et al (1999) A spelling device for the paralysed. Nature 398:297–298. doi:10.1038/18581

Bleichner MG, Jansma JM, Sellmeijer J et al (2013) Give me a sign: decoding complex coordinated hand movements using high-field fMRI. Brain Topogr 27(2):248–257 doi:10.1007/s10548-013-0322-x

Brunner PP, Joshi SS, Briskin SS et al (2010) Does the "P300" speller depend on eye gaze? J Neural Eng 7:056013–056013. doi:10.1088/1741-2560/7/5/056013

Chestek CA, Gilja V, Blabe CH et al (2013) Hand posture classification using electrocorticography signals in the gamma band over human sensorimotor brain areas. J Neural Eng 10:026002. doi:10.1088/1741-2560/10/2/026002

Collinger JL, Wodlinger B, Downey JE et al (2012) High-performance neuroprosthetic control by an individual with tetraplegia. Lancet. doi:10.1016/S0140-6736(12)61816-9

Dechent P, Frahm J (2003) Functional somatotopy of finger representations in human primary motor cortex. Hum Brain Mapp 18:272–283. doi:10.1002/hbm.10084

Farwell LA, Donchin E (1988) Talking off the top of your head: toward a mental prosthesis utilizing event-related brain potentials. Electroencephalogr Clin Neurophysiol 70:510–523

Guenther FH, Brumberg JS, Wright EJ et al (2009) A wireless brain-machine interface for real-time speech synthesis. PLoS ONE 4:e8218. doi:10.1371/journal.pone.0008218

Hermes D, Vansteensel MJ, Albers AM et al (2011) Functional MRI-based identification of brain areas involved in motor imagery for implantable brain-computer interfaces. J Neural Eng 8:025007. doi:10.1088/1741-2560/8/2/025007

Hermes D, Miller KJ, Vansteensel MJ et al (2012) Neurophysiologic correlates of fMRI in human motor cortex. Hum Brain Mapp 33:1689–1699. doi:10.1002/hbm.21314

Hochberg LR, Bacher D, Jarosiewicz B et al (2012) Reach and grasp by people with tetraplegia using a neurally controlled robotic arm. Nature 485:372–375. doi:10.1038/nature11076

Hotz-Boendermaker S, Funk M, Summers P et al (2008) Preservation of motor programs in paraplegics as demonstrated by attempted and imagined foot movements. Neuroimage 39:383–394. doi:10.1016/j.neuroimage.2007.07.065

Kubánek J, Miller KJ, Ojemann JG et al (2009) Decoding flexion of individual fingers using electrocorticographic signals in humans. J Neural Eng 6:066001. doi:10.1088/1741-2560/6/6/066001

Leuthardt EC, Schalk G, Wolpaw JR et al (2004) A brain-computer interface using electrocorticographic signals in humans. J Neural Eng 1:63–71. doi:10.1088/1741-2560/1/2/001

Miller KJ, Zanos S, Fetz EE et al (2009) Decoupling the cortical power spectrum reveals real-time representation of individual finger movements in humans. J Neurosci 29:3132–3137. doi:10.1523/JNEUROSCI.5506-08.2009

Penfield W, Rasmussen T (1950) The cerebral cortex of man. By wilder penfield and theodore rasmussen. The Macmillan Company, New York, 248 pp

Pistohl TT, Schulze-Bonhage AA, Aertsen AA et al (2012) Decoding natural grasp types from human ECoG. Neuroimage 59:248–260. doi:10.1016/j.neuroimage.2011.06.084

Siero JC, Hermes D, Hoogduin H et al (2013) BOLD consistently matches electrophysiology in human sensorimotor cortex at increasing movement rates: a combined 7T fMRI and ECoG study on neurovascular coupling. J Cereb Blood Flow Metab: Official J Int Soc Cereb Blood Flow Metab 33:1448–1456. doi:10.1038/jcbfm.2013.97

Sorger B, Reithler J, Dahmen B, Goebel R (2012) A real-time fMRI-based spelling device immediately enabling robust motor-independent communication. Curr Biol 22:1333–1338. doi:10.1016/j.cub.2012.05.022

van der Zwaag W, Francis S, Head K et al (2009) fMRI at 1.5, 3 and 7 T: characterising BOLD signal changes. Neuroimage 47:10–10. doi:10.1016/j.neuroimage.2009.05.015

Vansteensel MJ, Hermes D, Aarnoutse EJ et al (2010) Brain-computer interfacing based on cognitive control. Ann Neurol 67:809–816. doi:10.1002/ana.21985

Wang W, Collinger JL, Degenhart AD et al (2013) An electrocorticographic brain interface in an individual with tetraplegia. PLoS ONE 8:e55344. doi:10.1371/journal.pone.0055344.s010

Wolpaw JR, Birbaumer N, McFarland DJ et al (2002) Brain-computer interfaces for communication and control. Clin Neurophysiol 113:767–791

Yousry TA, Schmid UD, Alkadhi H et al (1997) Localization of the motor hand area to a knob on the precentral gyrus. A new landmark. Brain 120(Pt 1):141–157

Zander TO, Kothe C (2011) Towards passive brain-computer interfaces: applying brain-computer interface technology to human-machine systems in general. J Neural Eng 8:025005–025005. doi:10.1088/1741-2560/8/2/025005

An Ipsilateral, Contralesional BCI in Chronic Stroke Patients

David T. Bundy and Eric C. Leuthardt

Abstract Brain-computer interface (BCI) systems have been suggested as a potential method to restore function and enhance communication in motor-impaired patients. This approach has generally been proposed for patients with compromised motor outflow but a fully intact and functioning cortex. Because of this, in BCIs utilizing motor imagery, the BCI control signals have generally relied upon the cortical physiology associated with movements of the contralateral limb. More recently, BCIs have been proposed as a method to restore motor function after hemispheric stroke. In this patient population, the traditional contralateral motor physiology is affected by the cortical lesion, making a different control signal necessary. We review the emerging literature describing the distinct cortical physiology associated with ipsilateral or same-sided motor movements and the technical findings demonstrating the potential for this physiology to be used in BCIs for chronic stroke survivors.

Keywords BCI · Stroke rehabiliation · Hemiplegia · EEG

Disclosures: DTB receives consulting fees from and ECL has stock ownership in the company Neurolutions.

D.T. Bundy · E.C. Leuthardt (✉)
Department of Biomedical Engineering, Washington University in St. Louis,
Campus Box 8057, 660 South Euclid, St. Louis, MO 63130, USA
e-mail: leuthardte@wudosis.wustl.edu

E.C. Leuthardt
Department of Anatomy and Neurobiology, School of Medicine,
Washington University in St. Louis, St. Louis, MO 63130, USA

E.C. Leuthardt
Department of Neurological Surgery, School of Medicine, Washington University in St. Louis,
Campus Box 8057, 660 South Euclid, St. Louis, MO 63130, USA

E.C. Leuthardt
Center for Innovation in Neuroscience and Technology, School of Medicine,
Washington University in St. Louis, St. Louis, MO 63130, USA

C. Guger et al. (eds.), *Brain-Computer Interface Research*, SpringerBriefs
in Electrical and Computer Engineering, DOI 10.1007/978-3-319-09979-8_3

1 Introduction

1.1 Clinical Significance

A major challenge in the treatment of stroke survivors is the rehabilitation of chronically lost motor functions. Stroke is the most common neurological disorder in the United States, affecting 795,000 patients per year in the US alone and with a prevalence in the US of 7,000,000 adult Americans that have experienced a previous stroke (Duncan et al. 1992; Roger et al. 2012). Furthermore, 50 % of the survivors of these strokes experience hemiparesis 6 months after the onset of the stroke (Roger et al. 2012). These deficits are significant as recovery has traditionally been shown to plateau at 3 months after a stroke (Jorgensen et al. 1995). Taken together this means that a large number of stroke survivors have motor impairments and will be unable to experience recovery through traditional means.

1.2 BCI After Stroke

One potential method to restore functionality after stroke would be the use of a brain-computer interface (BCI) system. These systems use signals from the cortex to control a computer or other assistive device and could be used to enhance function either through control of a device independent of the unaffected hand or through pairing BCI operation with motor stimulation to induce recovery from endogenous plasticity. A number of studies have demonstrated the use of motor imagery-based BCI systems utilizing ipsilesional cortex contralateral to the affected limb in stroke survivors (Buch et al. 2008; Daly et al. 2009; Broetz et al. 2010; Caria et al. 2011). Additionally, BCI systems have been utilized in clinical trials to demonstrate the use of ipsilesional BCI systems for rehabilitation after stroke (Ang et al. 2010; Silvoni et al. 2011; Ramos-Murguialday 2012, 2013). While this body of work is promising, stroke-induced motor impairment is associated with a large extent of damage to primary contralateral motor cortices, with damage to the contralateral corticospinal tract, and with changes in functional connectivity in traditional motor networks (Carter et al. 2012). Furthermore, the neural modulation associated with motor imagery after stroke has been related to the remaining integrity of structural and functional motor networks (Buch et al. 2012). Because of this, in patients with dense hemiplegia, that would be the most likely to benefit from use of a BCI system, a novel control signal will likely be necessary for BCI applications. As conceptualized in Fig. 1, our proposal is unique in that it focuses on using ipsilateral motor signals from the contralesional hemisphere as a control signal for a BCI system (Bundy et al. 2012).

2 Motivation for Ipsilateral, Contralesional BCI

There is a variety of evidence that demonstrates that motor areas ipsilateral to a moving limb play a unique role in the planning and execution of motor movements. Wisneski et al. (2008) used electrocorticographic (ECoG) recordings to

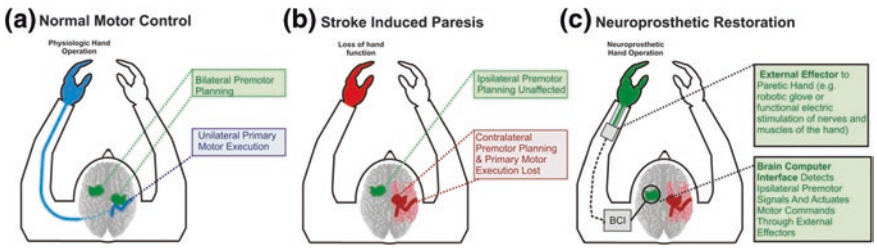

Fig. 1 Conceptual implementation of a BCI using ipsilateral motor areas in the contralesional hemisphere as a control signal in stroke survivors. Reprinted with permission from Bundy et al. (2012). **a** Normal motor control. **b** Stroke-induced paresis. **c** Neuroprosthetic restoration

show that movements of the hand ipsilateral to the electrodes were associated with spectral power changes occurring in lower frequency ranges (average 37.5 Hz), at distinct anatomical locations, and at earlier time points relative to movement onset than movements of the hand contralateral to the electrodes. Because these electrophysiologic activations during movements of the ipsilateral hand occurred earlier and were found in more anterior locations, it was postulated that ipsilateral motor areas are primarily associated with motor planning. An additional line of evidence for the causal input of the ipsilateral hemisphere to movements comes from examination of motor deficits in the ipsilesional, "unaffected" arm after hemispheric stroke. Several studies have demonstrated deficits in the ipsilesional limb after hemispheric stroke that are related to shifts in the location of ipsilateral neural activations (Baskett et al. 1996; Cramer et al. 2002). Additional studies have demonstrated a dissociation of the ipsilesional deficits observed with the side of the hemisphere that was damaged. In particular, in right handed subjects, damage to the left (dominant) hemisphere impaired modulation and adaptation of initial trajectories, while patients with right (non-dominant) hemisphere damage showed an impaired ability to correct their final position accuracy (Schaefer et al. 2007, 2009a, b). Furthermore, these deficits have been shown to be related to the extent of contralesional arm paralysis (Haaland et al. 2009).

In addition to the evidence for an active role of ipsilateral motor cortices in planning and execution of movements in motor intact humans, there are a number of studies that have examined the role of contralesional cortex in recovery from stroke. Traditionally, motor recovery after stroke has been thought to occur with "perilesional awakening" (Weiller et al. 1992; Tecchio et al. 2006) as improved long-term recovery of motor function after stroke is associated with a more normal pattern of contralateral, ipsilesional activity (Ward et al. 2003a, b). Conversely, ipsilateral motor activity in the contralesional hemisphere increases with improvements in motor function in some patients (Cramer et al. 1997; Tecchio et al. 2006). As the potential for recovery in stroke survivors is inversely correlated with corticospinal tract damage (Carter et al. 2011), one hypothesis is that while recovery from stroke ideally involves remodeling of perilesional cortex, that the contralesional hemisphere may provide an alternative path for motor recovery in people with severe or extensive lesions.

Taken together, ipsilateral motor areas contribute to the planning and execution of motor movements of the same-sided hand that is separable from the activity of contralateral motor areas. Furthermore, dense hemiplegics are likely to have more significant damage to the contralateral corticospinal tract (Carter et al. 2011) and decreased neuromodulation of ipsilesional motor areas (Buch et al. 2012), indicating that contralesional cortex would provide an alternative pathway for BCI applications for rehabilitation and an alternative control signal for long-term BCI system use for device control.

3 Ipsilateral, Contralesional BCI After Stroke

3.1 Study Overview

Bundy et al. (2012) demonstrated for the first time that EEG signals from the unaffected hemisphere in chronic stroke survivors that are associated with intended movements of the affected hand can be utilized to control a one-dimensional computer cursor rapidly and accurately. This study used four chronic stroke survivors (17–53 months post-stroke, age 48–61). In each participant, bipolarly derived EEG signals were recorded from scalp locations over frontal and parietal locations. The EEG signals were acquired using g.tec biosignal amplifiers (Graz, Austria) with a sampling rate of 256 Hz (patients 1 and 2) or 512 Hz (patients 3 and 4) using a 0.1 Hz high pass filter.

Patients completed an initial screening task that was utilized to determine features for later BCI control experiments. This screening procedure began with an experiment in which EEG signals were collected while patients performed overt and imagined finger-tapping movements of either the affected or unaffected hand or rested. For the overt movement condition, patients with limited motor function in the affected hand were instructed to perform overt movements of the unaffected hand and intended movements of the affected hand. In a second task, the patients were instructed to perform the same task with all movements imagined. The data was converted to the frequency domain by autoregressive spectral estimation in 2 Hz bins from 1 to 55 Hz. The signed coefficient of determination (r^2) for each channel and frequency bin between ‘rest’ and affected hand movement trials was used to identify the candidate features with the highest r^2 values. Selection of candidate electrode locations was limited to electrode positions over the contralesional hemisphere and, where possible, features were additionally limited to those that discriminated affected hand movement from unaffected hand movement in addition to discriminating affected hand movements from rest.

Using the EEG features selected from the screening procedure described above, the patients participated in closed-loop BCI control experiments in which the objective was to use the neural activity associated with intended movements of the affected hand to move a cursor on a computer screen along a single dimension in order to hit a target presented on either side of the screen. Three different BCI

control experiments were tested, (1) overt affected hand movements versus rest (Patient 1), (2) intended movements of the affected hand versus rest (Patients 2, 3, and 4), and (3) imagined affected hand movements versus imagined unaffected hand movements (Patients 1 and 2). Cursor movement velocity was determined from the EEG features in real-time by the BCI2000 software package (Schalk et al. 2004). Accuracy (the number of successful trials divided by the total number of trials) was calculated for each 2 min block of trials. Performance curves were produced using the entire duration of the closed-loop experiments consisting of multiple blocks with a particular task condition and control features. Subjects performed between 85 and 246 trials of closed-loop BCI control.

Screening task recordings from each subject contained activations in the unaffected hemisphere associated with intended movements of the affected hand (Fig. 2). Notably, when considering cortical activity in the unaffected hemisphere alone, there were spatial and spectral differences in the cortical activity associated with affected (ipsilateral) and unaffected (contralateral) hand movements. When examining all subjects, various features (locations and frequency bins) separated intended movements of the affected hand from both rest and intended movements of the unaffected hand (Fig. 3).

Furthermore, it was qualitatively observed that subjects with more severe motor impairments had contralesional, ipsilateral activity that was located anterior to primary motor areas. Figure 4 demonstrates the significant ($p < 0.05$) activations differentiating screening task conditions at the frequencies utilized for

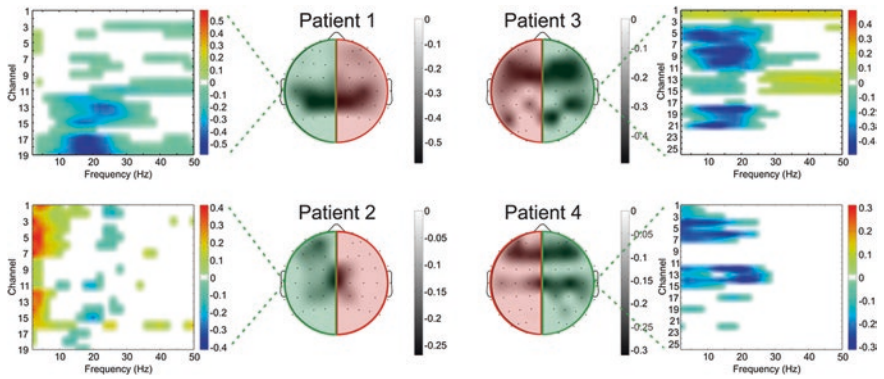

Fig. 2 Screening task activations are illustrated as topographical maps of the maximum coefficient-of-determination (r^2) values of power decreases between 0 and 50 Hz during affected hand movements when compared to rest. As decreases in power in these low frequency ranges have been related to motor intention more negative signed r^2 values are associated with increased neural activity. Feature *plots* demonstrate the coefficient of determination values from electrode locations in the contralesional hemisphere only at all frequency bins between 0 and 50 Hz. Cortical activations are particularly observed in the mu (8–12 Hz) and beta (12–30 Hz) frequency bands. Reprinted with permission from Bundy et al. (2012)

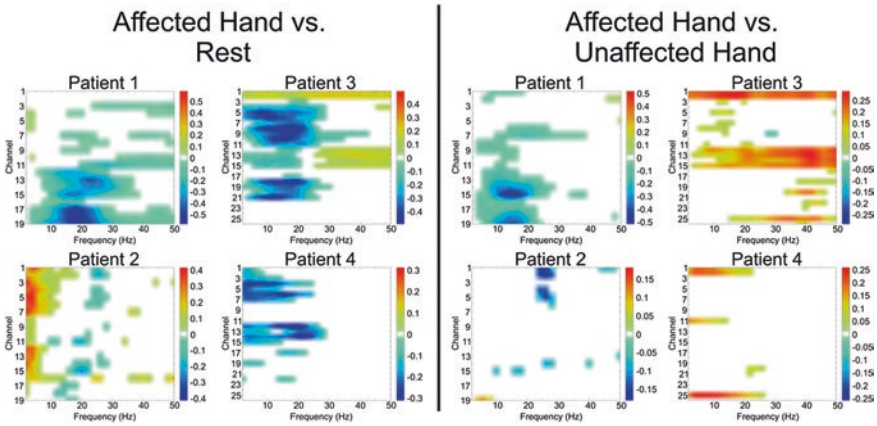

Fig. 3 In addition to differentiating affected hand movements from rest, contralesional cortex is also able to differentiate unaffected hand movements from rest. All 4 patients demonstrate significant ($p < 0.05$) decreases in spectral power in locations over the contralesional cortex associated with affected hand movements when compared to rest (*left plots*). Additionally, 3 of the 4 patients have activity in the unaffected hemisphere that differentiates affected hand movement from unaffected hand movement with the features in two of the patients based upon power decreases (Patients 1 and 2) in low frequencies (<30 Hz). Reprinted with permission from Bundy et al. (2012)

subsequent BCI control. The findings demonstrate wide-spread activity associated with affected hand movement in the contralesional hemisphere that could be used for device control. The time course of closed-loop task performance is shown in Fig. 5. Subjects achieved peak accuracies between 62.5 and 100 % with task durations ranging from 6 to 10 min. Furthermore, post hoc analysis demonstrated that the topography of activations during the closed-loop control and screening tasks were significantly correlated in three of the four patients, indicating that the successful BCI control was achieved through the screened motor task and not an alternative, spurious strategy.

This study provides the first demonstration that neural activity from the unaffected hemisphere associated with intended movements of the ipsilateral affected hand of chronic stroke survivors can be utilized for BCI control. Importantly, this demonstration of closed-loop BCI control was achieved independently from each patient's ability to perform overt movements of the affected hand. Furthermore, the ipsilateral motor signals used for BCI control were observed at distinct locations and frequencies from the motor signals associated with contralateral movements. In particular, utilizing ipsilateral motor activations from the unaffected hemisphere will allow BCI applications to be implemented in stroke survivors with dense hemiplegia and significant damage to contralateral motor areas that have traditionally been used for BCI control. Therefore, the results represent an important step towards translating BCI systems to meeting the significant needs represented by stroke survivors.

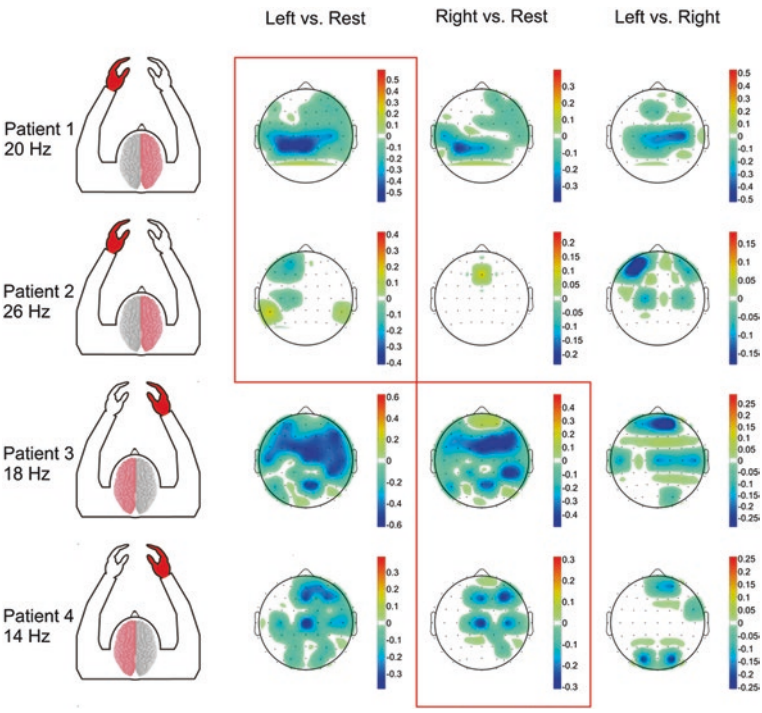

Fig. 4 Topographical maps of screening task activations at frequency bins utilized for BCI control experiments. All patients had significant activity in the contralesional hemisphere associated with intended movements of the affected hand when compared to rest (*red boxes*). Reprinted with permission from Bundy et al. (2012)

4 Future Directions

In the study described above, signals from the unaffected hemisphere were specifically examined as a potential BCI control signal after stroke. The choice of control signal is particularly relevant to the potential use of a BCI system for a rehabilitation tool. There is a variety of evidence in the published literature demonstrating changes in ipsilateral, contralesional activity after stroke. Functional imaging studies examining activity associated with affected hand movements have shown increases in unaffected hemisphere motor areas after recovery in stroke patients both when compared to normal controls (Weiller et al. 1992, 1993; Cramer et al. 1997; Nelles et al. 1999; Tecchio et al. 2006) and when evaluated after improvements in function due to constraint-induced movement therapy (Levy et al. 2001; Schaechter et al. 2002). Furthermore, inhibitory transcranial magnetic stimulation to contralesional cortex can impair movements of the affected hand (Johansen-Berg et al. 2002), indicating an active role of the contralesional cortex in executing movements. Other evidence contradicts the conclusion that contralesional motor activity plays an active role in motor recovery after stroke. Specifically, greater

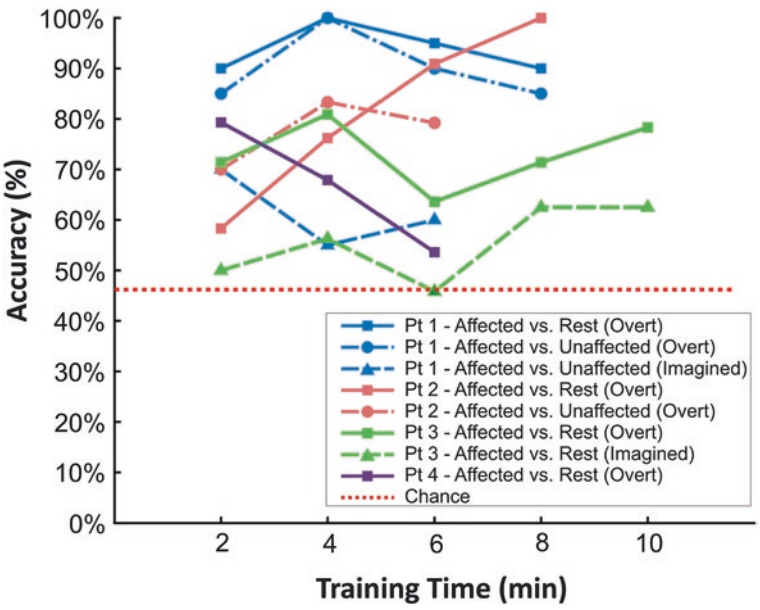

Fig. 5 Performance in closed-loop BCI control tasks over time. Reprinted with permission from Bundy et al. (2012)

ipsilateral excitability measured using TMS in the contralesional hemisphere was found to be associated with poor recovery (Turton et al. 1996; Netz et al. 1997) and both longitudinal and cross-sectional studies of recovery from stroke show decreases in ipsilateral, contralesional motor activity (Ward et al. 2003a, b). Using both of these lines of evidence, a more complicated view can be derived when considering studies that demonstrate both ipsilesional and contralesional changes in activity with recovery from stroke (Green et al. 1999; Levy et al. 2001). Furthermore, patients who recover have been found to show few changes to the locations of their contralesional motor activity, while patients with incomplete recovery have better recovery with increased contralesional motor activity during affected hand motor tasks (Tecchio et al. 2006). This combination of evidence makes sense when considering the association between corticospinal tract damage and motor impairment (Fries et al. 1993; Carter et al. 2011). Taken together, it appears that the ideal, patient-specific rehabilitation strategy may be dependent upon the extent of damage to structural and functional networks. Specifically, we hypothesize that patients with intact contralateral corticospinal tracts may benefit from BCI therapies utilizing ipsilesional activity as control signals as shown previously (Ang et al. 2010; Silvoni et al. 2011; Ramos-Murguialday et al. 2012, 2013), while patients with substantial damage to the corticospinal tract will require an alternative, contralesional pathway for recovery to take place. Future work designed to define the specific rehabilitation strategies (including BCI-based therapies and traditional therapies) associated with optimal outcome dependent upon

the structural and functional areas damaged by the initial lesion will be vitally important to the clinical translation of BCI therapies into patients that can benefit from them.

In addition to assessing the optimal patient-specific rehabilitation strategy, it will be important to gain a greater understanding of ipsilateral motor activity both in healthy patients as well as after stroke. While this project has demonstrated that stroke survivors can utilize their unaffected hemisphere to control a BCI system (Bundy et al. 2012), it is unclear what the extent of information that can be derived from these signals is. While a non-invasive control signal would provide the signal necessary for operation of a BCI for rehabilitation, long-term use of a BCI to control an assistive device would likely require more degrees of freedom than could be derived from non-invasive signals. To address the feasibility of ipsilateral motor areas for BCI control, it will be important to further examine the extent and type of information normally encoded by ipsilateral motor areas using invasive recordings from healthy controls and animal models. Furthermore, in the study described above, patients generally had shifts of the ipsilateral motor activity from the contralesional hemisphere to locations anterior to primary sensorimotor cortices. While this finding is in line with other results demonstrating changes in contralesional motor activity (Cramer et al. 1997; Green et al. 1999; Tecchio et al. 2006), it will be important to fully define the remapping of contralesional motor activity after stroke in order to implement contralesional BCI systems for either rehabilitation or device control.

5 Conclusions

The recovery of chronically lost motor function after stroke represents a significant and growing problem. Recent advances demonstrate the possibility of utilizing ipsilateral motor activity from the unaffected hemisphere of stroke survivors to implement a BCI system for long-term device control or rehabilitation. Creating a system that can be used for either chronic device control or rehabilitation will require further examination of the information encoded in ipsilateral motor signals, examination of the remodeling of ipsilateral motor areas after stroke, and determination of the interplay of lesion location and neural anatomy in determining an optimal rehabilitation strategy after stroke.

References

Ang KK, Guan C et al (2010) Clinical study of neurorehabilitation in stroke using EEG-based motor imagery brain-computer interface with robotic feedback. Conf Proc IEEE Eng Med Biol Soc 2010:5549–5552

Baskett JJ, Marshall HJ et al (1996) The good side after stroke: ipsilateral sensory-motor function needs careful assessment. Age Ageing 25(3):239–244

Broetz D, Braun C et al (2010) Combination of brain-computer interface training and goal-directed physical therapy in chronic stroke: a case report. Neurorehabil Neural Repair 24(7):674–679

Buch E, Weber C et al (2008) Think to move: a neuromagnetic brain-computer interface (BCI) system for chronic stroke. Stroke 39(3):910–917

Buch ER, Modir Shanechi A et al (2012) Parietofrontal integrity determines neural modulation associated with grasping imagery after stroke. Brain 135(Pt 2):596–614

Bundy DT, Wronkiewicz M et al (2012) Using ipsilateral motor signals in the unaffected cerebral hemisphere as a signal platform for brain-computer interfaces in hemiplegic stroke survivors. J Neural Eng 9(3):036011

Caria A, Weber C et al (2011) Chronic stroke recovery after combined BCI training and physiotherapy: a case report. Psychophysiology 48(4):578–582

Carter AR, Patel KR et al (2012) Upstream dysfunction of somatomotor functional connectivity after corticospinal damage in stroke. Neurorehabil Neural Repair 26(1):7–19

Cramer SC, Nelles G et al (1997) A functional MRI study of subjects recovered from hemiparetic stroke. Stroke 28(12):2518–2527

Cramer SC, Mark A et al (2002) Motor cortex activation is preserved in patients with chronic hemiplegic stroke. Ann Neurol 52(5):607–616

Daly JJ, Cheng R et al (2009) Feasibility of a new application of noninvasive brain computer interface (BCI): a case study of training for recovery of volitional motor control after stroke. J Neurol Phys Ther 33(4):203–211

Duncan PW, Goldstein LB et al (1992) Measurement of motor recovery after stroke. Outcome assessment and sample size requirements. Stroke 23(8):1084–1089

Fries W, Danek A et al (1993) Motor recovery following capsular stroke. Role of descending pathways from multiple motor areas. Brain 116(Pt 2):369–382

Green JB, Bialy Y et al (1999) High-resolution EEG in poststroke hemiparesis can identify ipsilateral generators during motor tasks. Stroke 30(12):2659–2665

Haaland KY, Schaefer SY et al (2009) Ipsilesional trajectory control is related to contralesional arm paralysis after left hemisphere damage. Exp Brain Res 196(2):195–204

Johansen-Berg H, Rushworth MF et al (2002) The role of ipsilateral premotor cortex in hand movement after stroke. Proc Natl Acad Sci USA 99(22):14518–14523

Jorgensen HS, Nakayama H et al (1995) Outcome and time course of recovery in stroke. Part II: time course of recovery. The Copenhagen stroke study. Arch Phys Med Rehabil 76(5):406–412

Levy CE, Nichols DS et al (2001) Functional MRI evidence of cortical reorganization in upper-limb stroke hemiplegia treated with constraint-induced movement therapy. Am J Phys Med Rehabil 80(1):4–12

Nelles G, Spiekramann G et al (1999) Evolution of functional reorganization in hemiplegic stroke: a serial positron emission tomographic activation study. Ann Neurol 46(6):901–909

Netz J, Lammers T et al (1997) Reorganization of motor output in the non-affected hemisphere after stroke. Brain 120(Pt 9):1579–1586

Ramos-Murguialday A, Schurholz M et al (2012) Proprioceptive feedback and brain computer interface (BCI) based neuroprostheses. PLoS ONE 7(10):e47048

Ramos-Murguialday A, Broetz D et al (2013) Brain-machine interface in chronic stroke rehabilitation: a controlled study. Ann Neurol 74(1):100–108

Roger VL, Go AS et al (2012) Heart disease and stroke statistics—2012 update: a report from the American Heart Association. Circulation 125(1):e2–e220

Schaechter JD, Kraft E et al (2002) Motor recovery and cortical reorganization after constraint-induced movement therapy in stroke patients: a preliminary study. Neurorehabil Neural Repair 16(4):326–338

Schaefer SY, Haaland KY et al (2007) Ipsilesional motor deficits following stroke reflect hemispheric specializations for movement control. Brain 130(Pt 8):2146–2158

Schaefer SY, Haaland KY et al (2009a) Dissociation of initial trajectory and final position errors during visuomotor adaptation following unilateral stroke. Brain Res 1298:78–91

Schaefer SY, Haaland KY et al (2009b) Hemispheric specialization and functional impact of ipsilesional deficits in movement coordination and accuracy. Neuropsychologia 47(13):2953–2966

Schalk G, McFarland DJ et al (2004) BCI2000: a general-purpose brain-computer interface (BCI) system. IEEE Trans Biomed Eng 51(6):1034–1043

Silvoni S, Ramos-Murguialday A et al (2011) Brain-computer interface in stroke: a review of progress. Clin EEG Neurosci 42(4):245–252

Tecchio F, Zappasodi F et al (2006) Brain plasticity in recovery from stroke: an MEG assessment. Neuroimage 32(3):1326–1334

Turton A, Wroe S et al (1996) Contralateral and ipsilateral EMG responses to transcranial magnetic stimulation during recovery of arm and hand function after stroke. Electroencephalogr Clin Neurophysiol 101(4):316–328

Ward NS, Brown MM et al (2003a) Neural correlates of motor recovery after stroke: a longitudinal fMRI study. Brain 126(Pt 11):2476–2496

Ward NS, Brown MM et al (2003b) Neural correlates of outcome after stroke: a cross-sectional fMRI study. Brain 126(Pt 6):1430–1448

Weiller C, Chollet F et al (1992) Functional reorganization of the brain in recovery from striatocapsular infarction in man. Ann Neurol 31(5):463–472

Weiller C, Ramsay SC et al (1993) Individual patterns of functional reorganization in the human cerebral cortex after capsular infarction. Ann Neurol 33(2):181–189

Wisneski KJ, Anderson N et al (2008) Unique cortical physiology associated with ipsilateral hand movements and neuroprosthetic implications. Stroke 39(12):3351–3359

A Learning-Based Approach to Artificial Sensory Feedback

Maria C. Dadarlat, Joseph E. O'Doherty and Philip N. Sabes

Abstract Proprioception plays an essential role in natural motor control, and we argue that it will serve an equally important function in artificial control of motor prosthetic devices. An artificial sensory feedback signal that could substitute for proprioception in a Brain-Computer Interface (BCI) must be sufficiently informative to be used alone when vision is not available (sensory substitution), and it should integrate with vision to improve motor performance when it is (sensory augmentation). Achieving these qualities with an artificial signal requires a high-bandwidth channel, which can be achieved with an invasive neural interface. With invasive electrode arrays, we can manipulate the activity of populations of neurons using intracortical electrical microstimulation (ICMS), effectively transmitting useful information directly to the neural circuits where it is needed. To date, the dominant strategy for encoding artificial somatosensation has been biomimetic—trying to replicate, at the single neuron level, the neural activity seen during natural sensory processing. Here, we argue for a different, though complementary, learning-based approach. We propose taking advantage of the natural plasticity of the sensorimotor system, and asking the brain to learn, de novo, an artificial input. We hypothesize that the statistical dependencies, such as temporal correlations, that will be imposed on a natural (vision) and an artificial sensory input (ICMS) will be enough to drive learning and, ultimately, integration of the two inputs. Therefore we suggest that such a learning-based approach can achieve sensory substitution and augmentation of vision, the two desired properties of an artificial sensory feedback signal for clinical motor neural prostheses.

M.C. Dadarlat · J.E. O'Doherty · P.N. Sabes (✉)
Department of Physiology, University of California, San Francisco, USA
e-mail: sabes@phy.ucsf.edu

M.C. Dadarlat · J.E. O'Doherty · P.N. Sabes
Center for Integrative Neuroscience, University of California, San Francisco, USA

M.C. Dadarlat · P.N. Sabes
UC Berkeley-UCSF Bioengineering Graduate Program,
University of California, San Francisco, USA

C. Guger et al. (eds.), *Brain-Computer Interface Research*, SpringerBriefs
in Electrical and Computer Engineering, DOI 10.1007/978-3-319-09979-8_4

Keywords Somatosensation, Sensory Feedback, Learning, Multisensory Integration

1 Normal Motor Function Needs Somatosensation

Motor neural prostheses are assistive devices that aim to restore normal movements for persons with injury or disease (Lebedev and Nicolelis 2006; Velliste et al. 2008). These systems harness neural activity to control motor prostheses with the promise of providing natural and effortless mobility with a degree of fluidity that could someday approach that of unimpaired movement. Different motor impairments spare varying degrees of residual function (compare, for example, spinal-cord injury (SCI) to the amputation of a limb), meaning that the most appropriate approach to artificial sensory feedback will be unique in each case. As a result, there is a wide range of neural prosthetic solutions that have been proposed and developed for restoring movements, extending from myoelectric signals extracted from muscles and nerves (Parker and Scott 1986; Kuiken et al. 2009) to direct cortical control (Hochberg et al. 2006, 2012). Despite their diversity, all of these approaches share a common need: somatosensory feedback (Lebedev and Nicolelis 2006; Hatsopoulos and Donoghue 2009; Lebedev et al. 2011; Gilja et al. 2011; Weber et al. 2012).

Somatic sensations (those that originate from the limbs and body, chiefly touch and proprioception) are essential for fine control of movements and the dexterous manipulation of objects (Johansson and Flanagan 2009). They also reduce the effort required to make goal-directed movements while improving their reliability. More specifically, somatosensation relieves the need for constant visual attention to manipulated objects and permits movements made outside of the visual field (into pockets, etc.). It also enables tasks that are difficult to accomplish even with full and direct vision. This critical aspect can perhaps be appreciated by considering the motor impairments exhibited by persons suffering from sensory deafferentation, impairments that persist despite a fully intact motor pathway. For example, the seemingly simple task of lifting an object (Johansson and Westling 1984) or striking a match is more challenging and takes longer to accomplish when attempted without cutaneous sensation from the fingers. Furthermore, without proprioception it is difficult to make spatially precise movement trajectories that require multi-joint coordination (Sainburg et al. 1993). Finally, despite the fact that vision is often viewed as the dominant sensory modality for humans, somatosensation actually offers more precision along some spatial axes (van Beers et al. 2002) and has a shorter feedback latency than vision (Omrani et al. 2013).

As one would predict from its importance for normal limb function, there is growing direct evidence that artificial proprioception would improve motor performance with prosthetic limbs. Monkeys making virtual reaches with a Brain-Computer Interface (BCI) controlled cursor demonstrated better performance levels when an exoskeletal robot passively moved their forelimb to track the cursor movement, compared to performance when their limb was held still or moved randomly (Suminski et al. 2010). Although visual feedback of the state of the cursor

was available in all conditions, BCI control only approached natural levels of performance and fluidity when additional state information was provided by intact proprioceptive feedback. A similar result was observed when decoding movement intention from humans with intact proprioception (Gomez-Rodriguez et al. 2011), where closing the sensorimotor feedback loop improved the user's degree of control over the BCI. We expect that the benefit of proprioceptive feedback on BCI control will persist, even as the BCI control algorithms continue to improve (Gilja et al. 2012; Orsborn et al. 2012)—just as deafferented patients with nominally intact motor systems exhibit motor impairments, a motor neural prosthesis without somatic sensation will remain functionally impaired.

To optimize BCI control, an artificial sensory signal must fulfill the functions of natural proprioception. In particular, we will consider two criteria that we hypothesize will be sufficient for improving BCI control. Namely, we want to design an artificial signal that can provide enough information to be used alone when vision is not available (sensory substitution), and that can be integrated with vision to improve motor performance when both inputs are available (sensory augmentation).

2 Approaches for Artificial Somatosensation

Given the importance of somatosensory feedback for motor neural prosthetic systems, we next ask how such feedback should be provided. As with the selection of a motor decode strategy, the most suitable route for somatosensory feedback will depend on the specifics of the injury and the preferences of the user. For example, an amputee with an upper-limb prosthetic arm may be best served by stimulation of residual peripheral nerve afferents (Schiefer et al. 2010). In contrast, for SCI patients, the peripheral route may not be a viable option and a more central site of stimulation would be required.

In the following, we focus on the problem of restoring somatic sensation for complete SCI or other conditions that result in functionally complete somatosensory loss below the neck. While these strategies may also apply in situations with less severe disability, we choose to focus SCI because there are fewer existing and viable strategies for restoring somatosensation to these individuals. SCI imposes strong restrictions on the design of neural prosthetic devices. Motor commands are only available above the lesion site, so in many cases they must be read out from the brain. Similarly, sensory afferents from below the lesion are few or non-existent. While both invasive and non-invasive devices could be used in this case, we argue next that an invasive approach is preferable for both neural read-out and sensory write-in.

2.1 Non-invasive Approaches

There are several non-invasive ways that a motor command signal could be obtained in SCI, including measurement of eye, head, face, or neck movement—directly or via electromyogram (EMG) or electrooculogram (EOG) recordings—or

with external recording of neural signals from the brain (electroencephalogram, EEG). These controllers can be classified as either "direct" or "indirect." With indirect control schemes, users learn to control the prosthetic device with a substitute effector. Clinically successful examples of indirect control include sip-and-puff systems, head-mounted wands and joysticks, and voice commands. These indirect approaches are simpler and less expensive than other methods, but their information bandwidth is limited. In contrast, direct control schemes measure the control signal from EEG recordings, although eye position control of a computer cursor could also be included. Notably, an EEG-based system has recently achieved information bandwidths comparable to invasive BCIs (Bin et al. 2011). However, these information rates were obtained by analyzing the temporal pattern of visual evoked potentials (VEP) during the serial presentation of a large set of discrete stimuli. The system was able to estimate which of a set of targets was being visually fixated at a rate of approximately every 2 s; significant advances would be needed to use this approach to obtain smooth, continuous control of a prosthetic device.

In principle, restoration of somatosensory feedback via non-invasive BCIs could also include direct and indirect approaches, however in the case of SCI, where the sensory periphery is unavailable, there are currently no viable non-invasive technologies for stimulating the somatosensory pathways of the limb. This leaves only indirect approaches, or "sensory substitution", where sensory information intended for one modality is translated into another. Sensory substitution has employed tactile, auditory, and superficial electrical stimulation to replace systems like natural vision (Nau et al. 2013) and vestibular function (Vuillerme et al. 2011). While non-invasive systems have clear appeal, tactile stimulation can be uncomfortable, and a device of suitably high bandwidth placed on the head or neck is likely to be bulky or awkward. We argue below that a fully implantable invasive device may, in the end, be more tolerable to many patients.

Despite potential limitations for rehabilitation, studies of sensory substitution provide key insight into the central role that sensorimotor learning can play in systems for artificial somatosensation. In a seminal sensory substitution experiment, blind subjects were taught to detect visual objects using a system that translated video input from a camera into a matrix of tactile inputs on the subject's back (Bach-y-Rita et al. 1969; Bach-y-Rita and Kercel 2003). Users of this system had great success, even learning to recognize faces and partially occluded objects, and perceived "the external localization of stimuli," meaning that the objects they sensed seemed to come directly from the camera rather than having to be interpreted from a sense of tingling or touch on their backs (Bach-y-Rita et al. 1969; Bach-y-Rita and Kercel 2002). Importantly, subjects only learned to distinguish objects when they were able to actively manipulate the movement and perspective of the camera, observing the changes in feedback as a result of their actions. If instead the camera was stationary or moved by another person, subjects did not "learn to see," and instead had to interpret the signals in terms of touch and vibration. We conclude that active exploration is essential for learning of new

modalities, but once learned, new modalities can be directly perceived, without the need for a translation step. We believe that these principles can usefully inform invasive approaches for sensory feedback.

2.2 Invasive Approaches

The key challenge for invasive approaches to BCI is the long-term stability and safety of the neural interface. Historically, implanted devices have suffered from mechanical failures (Barrese et al. 2013), neurovascular damage (Kozai et al. 2010), immune response (Woolley et al. 2013; Polikov et al. 2005), infection and other difficulties associated with percutaneous implants. However, recent initiatives aim to solve these problems by improving device design (smaller, more flexible electrodes), taking new approaches to avoid signal degradation (ECOG/LFP-based decoding as well as using robust multi-unit decoding; Schalk et al. 2008; Ledochowitsch et al. 2013; Chestek et al. 2011), and fully-implantable low-power wireless recording systems (Alam et al. 2013) that may alleviate both the medical risks and aesthetic concerns of percutaneous devices. These advances, and others, in the field of neurotechnology suggest that safe and reliable invasive neural interfaces are on the horizon.

A major advantage of using invasive systems is the potential for high-bandwidth readout, due to their high spatial resolution, frequency range, and robustness to noise. Invasive systems now achieve information transfer rates of about 2 bits/s (Mulliken et al. 2008) in the continuous control of cursors and robotic arms, in large part due to improved algorithmic design (Orsborn et al. 2012; Gilja et al. 2012; Li et al. 2011; Shanechi et al. 2013), and continued progress is expected. Still, BCIs have yet to approach the performance levels of natural human movement (4.5 bits per movement, for movements that should take much less than 1 s to perform; Georgopoulos and Massey 1988). We attribute much of the remaining shortcoming in BCI control to the need for somatosensory feedback.

2.3 Biomimetic Encoding of Somatosensory Information

Invasive neural interfaces enable not only high-bandwidth output from the brain, but also multi-channel input into the brain. Electrical stimulation has been used to drive targeted manipulations of neural activity, inducing artificial somatosensation or perturbing natural somatosensation, in both animal models and human (e.g., Penfield and Boldrey 1937; Butovas and Schwarz 2003; Tabot et al. 2013). As the number and density of stimulating electrodes increases, so does the potential complexity of the spatiotemporal pattern of induced activity. This opportunity brings with it the challenge of choosing the right spatiotemporal activity patterns and determining how to create those patterns via stimulation. The dominant strategy so

far has been biomimetic (Fagg et al. 2007)—trying to replicate the patterns of neural activity observed during natural sensory processing. Intuitively, a biomimetic code would be able to provide a sufficiently rich and easily interpreted artificial sensory feedback signal. Preliminary studies using biomimetic stimulation show promise, at least for artificial tactile feedback (Berg et al. 2013; Tabot et al. 2013). However, it not clear how well this approach will extend to proprioception, especially in the context of SCI.

First, it is not possible to simply invert the biophysics of neural activity, i.e. to precisely recreate recorded patterns of activity. Each pulse of electrical current activates a sphere of neural activity around the stimulation site (Stoney et al. 1968; Tehovnik 1996; Tehovnik et al. 2006) or, according to another study, a sparse, distributed population of cells whose processes lie proximal to the stimulation site (Histed et al. 2009). In either scenario, it would be difficult to target individual neurons without undesired and/or unpredictable collateral activity (Butovas and Schwarz 2003). This problem will be particularly acute in brain areas that lack a fine-scale topographic map, i.e. where nearby neurons have different response properties. This appears to be the case in the proprioceptive regions of primary somatosensory cortex (S1) (Kaas et al. 1979; Weber et al. 2012). Even if very small currents could be used to activate single neurons (Houweling and Brecht 2008), the total number of (directly) activated neurons would be limited by the size of the stimulating array. In the near term, then, it seems infeasible to create targeted spatiotemporal patterns that mimic the precision and complexity of natural sensory activity.

A second obstacle faced by biomimetic approaches is our piecemeal understanding of how those natural patterns activity encode the sense touch (Johansson and Flanagan 2009), proprioception (Prud'homme and Kalaska 1994), and their complex interaction (Rincon-Gonzalez et al. 2012; Warren and Tillery 2011). Even in cases where elements of this coding are known—e.g. topographic maps for the digits—SCI with sensory loss raises the additional challenge that the code cannot be simply mapped using natural stimuli. While the problem could be inverted—stimulating individual sites and asking for reports of the subsequent percept—this approach would be slow and coarse.

A third challenge for the biomimetic approach is the cortical remapping that occurs after the loss of sensory afferents. Somatosensory perturbations elicit plastic changes in the adult brain in a matter of months, so that cortical representations of deafferented surfaces become occupied by expanded representations of the surrounding areas (Merzenich et al. 1983a, b). For example, following complete loss of sensory input from the hand, the cortical hand representation ultimately represents somatosensory input from the face (Pons et al. 1991). Further complicating the matter, cortical stimulation itself alters the topography of the sensory cortex (Recanzone et al. 1992), shifting the receptive fields of neighboring cells towards that at the site of stimulation. Thus, neural plasticity must be considering in designing systems for artificial somatosensory feedback: in the absence of a stable cortical map, the target for biomimetic stimulation may itself be non-stationary.

Of course, these forms of neural plasticity could also facilitate artificial somatosensation—for example, allowing the brain to reorganize to use new sensory

signals when they are provided (Frey et al. 2008). Indeed, we argue next that precise biomimetic stimulation may not be needed to achieve artificial sensory feedback. Rather, we suggest taking advantage of ongoing neural plasticity, which should permit the brain to find useful signals in even non-biomimetic patterns of stimulation.

3 Harnessing Neural Plasticity

Despite the difficulties associated with biomimetic stimulation, there is both aesthetic appeal and, possibly, practical expediency in trying to mimic the way that natural systems work. Here we introduce a complimentary approach in which we focus not on how information is naturally encoded in the brain—or how to precisely reproduce that code—but rather on how the brain naturally learns to use new sensory information and how we can harness that process.

This approach should be made possible by the (perhaps counterintuitive) fact that the brain is always learning to use sensory information. Experimental evidence from our lab (Verstynen and Sabes 2011; Sober and Sabes 2005; Simani et al. 2007; McGuire and Sabes 2009) and from others (Ernst and Banks 2002; van Beers et al. 1999; Gu et al. 2008; Burge et al. 2010) demonstrates that sensory streams are integrated to provide statistically efficient feedback, and this process involves continuous recalibration. As described in more detail next, we propose that this ongoing neural plasticity is the key to developing a system for artificial somatosensory feedback. In particular, we propose that with the right training regime, the brain can learn to interpret and use novel artificial sensory signals, even when those signals are not biomimetic.

As an example, consider the problem of reaching to touch an object. To accomplish the reach, the brain must combine sensory estimates of the hand and the object into the appropriate motor command. Humans (van Beers et al. 1999) and animals (Gu et al. 2008) naturally integrate multiple streams of sensory information (e.g., vision and proprioception) about relevant parameters (e.g., position, velocity, etc. of the hand) into a unified estimate. Experimental evidence indicates that—at least to a first approximation—this is a statistically optimal process, in that the individual modalities are combined in order to minimize the variance of the integrated sensory estimate (van Beers et al. 1999; Ernst and Banks 2002; Gu et al. 2008; Fetsch et al. 2012; Alais and Burr 2004). This can be expressed mathematically as

$$\hat{x}_{int} = \left(\frac{\hat{x}_1}{\sigma_1^2} + \frac{\hat{x}_2}{\sigma_2^2} \right) \sigma_{int}^2, \tag{1}$$

where $\hat{x}_1$, $\hat{x}_2$ and $\hat{x}_{int}$ are the mean estimates from the individual modalities and the integrated estimate, respectively. The trial-to-trial variances of these estimates, σ_1^2, σ_2^2, and σ_{int}^2, can also be viewed as measures of the sensory uncertainty associated

with a given estimate. Note that the integrated estimate places more weight on the modality that has the smaller variance, or least uncertainty. The variance of the integrated estimate, σ^2_{int} is given by Eq. 2,

$$\sigma^2_{int} = \left(\frac{1}{\sigma_1^2} + \frac{1}{\sigma_2^2} \right)^{-1}, \tag{2}$$

is guaranteed to be smaller than the variances of the individual estimates, as long as they are finite. This decrease in variance indicates one of the advantages of multisensory integration, and highlights one reason why artificial somatosensation is expected to improve the performance of neural prostheses.

There is preliminary experimental evidence that, at least for some sensory modalities, the coding of multisensory spatial variables reflects minimum-variance integration (Fetsch et al. 2012; Gu et al. 2008), yet the neural mechanisms underlying integration are net yet known. Similarly, although we know that integration is a learned process (Wallace and Stein 1997) and that it continually recalibrates itself (Simani et al. 2007; Burge et al. 2010), the neural basis for these plastic changes is not known.

Our lab has recently proposed a novel model of adaptive multisensory integration in a neural network (Makin et al. 2013). The model stems from the idea that multisensory integration can be viewed as one example of a more general, unsupervised learning problem, namely latent variable density estimation (LVDE). The goal of LVDE is to extract low dimensional representations of incoming data while retaining as much of the original statistical structure as possible. Our model is implemented with a simple neural network that learns LVDE via a biologically plausible Hebbian-like learning rule (Hinton et al. 2006). This model is illustrated in Fig. 1a. It consists of two populations of input neurons—"visual" neurons encoding hand position in extrinsic coordinates, and "proprioceptive" neurons encoding hand position in terms of joint angles—and an output population of multisensory neurons that receive projections from the two input populations. Starting from a state of random connectivity, the links from input to output are learned through exposure to data in which a strong correlation between the two input populations arises from the fact that they both represent the same underlying variable(s), x, for example the state of limb. After learning, the network is able to perform minimum-variance cue combination, as well as a range of other movement-related multisensory computations (Makin et al. 2013).

A key insight from the model in Fig. 1 is that the statistical properties of the input signals, namely the correlation between the activities of the two sensory neural populations, are sufficient to drive the network to learn integrated representations of hand position (Makin et al. 2013), without the need for supervisory signals. We do not know if this model accurately captures the mechanisms implemented in the brain, but its biologically plausible form makes it an exciting candidate and, moreover, it makes several testable predictions of practical importance for BCI.

A testable prediction that is particularly relevant for artificial somatosensation is that correlation between two input signals will drive learning and integration.

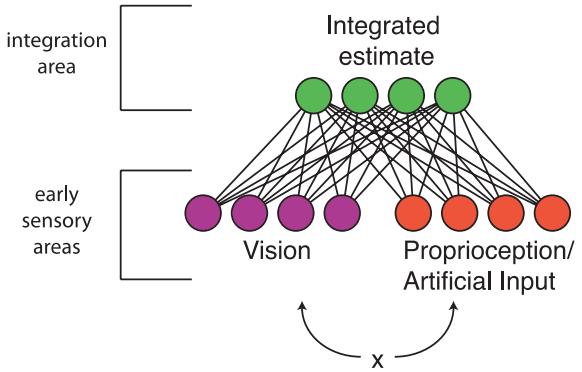

Fig. 1 Learning to integrate natural and artificial sensory signals. A schematic of a neural network model that learns, de novo and in an unsupervised fashion, to integrate visual and proprioceptive feedback of a variable of interest, x, such as the position or velocity of the limb. Learning is driven by correlations between the input populations, which in turn reflect their common encoding of the variable x. The same system would be equally able to learn novel artificial sensory inputs, assuming the inputs remain correlated. This figure is adapted from Makin et al. (2013)

This suggests a powerful learning-based approach for delivering novel sensory signals to the brain: if one provides a novel stream of information, delivered for example by intracortical mircrostimulation, the brain should learn to interpret and integrate that signal as long as it correlates over time with a known sensory signal. Specifically, we propose to deliver an informative artificial feedback signal to a somatosensory area and to correlate this signal with vision. This pairing will drive learning and, ultimately, integration of the two signals, mimicking natural sensory processing.

4 Candidate Neural Structures to Target

In the preceding section we argued for a new, learning-based approach to providing artificial somatosensory feedback, in which cortical stimulation is paired with visual feedback. Here we address the question of where in the brain the stimulation should be delivered. To inform this discussion, the principal cortical areas involved in goal-direction reaching are illustrated schematically in Fig. 2. Briefly, sensory information ascends from the periphery via the thalamus to modality-specific primary sensory areas. These, in turn, project to a number of multisensory cortical areas in the parietal lobe. Motor planning appears to occur across this parietal circuit and in the interconnected pre-motor and primary motor cortex in the frontal lobe. The ideal target for somatosensory stimulation would seem to be one that either lies upstream of, or *is* one of, the multisensory areas involved in movement planning (Fig. 2).

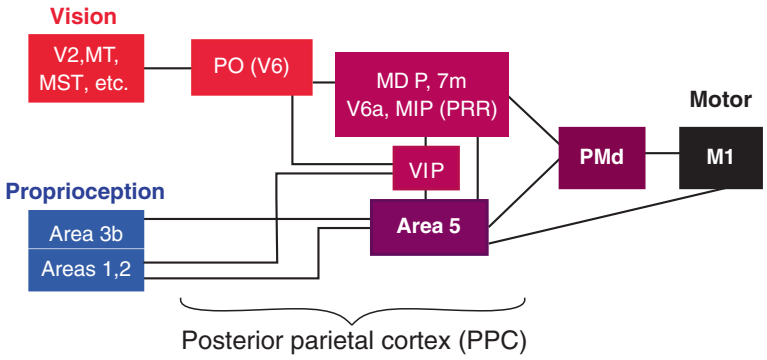

Fig. 2 Possible cortical targets for artificial somatosensory signals. Schematic of the cortical circuit underlying sensory integration and reaching. Visual and proprioceptive information enter the parietal cortex via different pathways, and they are integrated before the information is passed to pre-central motor cortex

Neurons in primary somatosensory cortex (S1) process both touch and proprioceptive information. In primates, S1 is composed of cortical areas 1, 2, 3a, and 3b. Area 3a is largely proprioceptive; 3b mostly cutaneous; and areas 1 and 2 have mixed responses (Krubitzer and Kaas 1990). All of these subdivisions are good candidates for providing artificial somatic sensations, but areas 1 and 2 offer an important practical advantage: easier targeting with electrode arrays because of their superficial location on bank of the post-central gyrus. In contrast, areas 3a and 3b are less accessible: 3b lies on the bank of the central sulcus and 3b is located near its fundus.

Importantly, electrical stimulation of S1 produces sensations referred to the body (Penfield and Boldrey 1937). Stimulating in S1 (and the thalamic regions that project to it) produce sensations at lower thresholds than "higher" cortical areas (Doty 1969). Additionally, S1 projects directly to areas that are known to perform multisensory integration (A5, PMd) as well as to primary motor cortex (Fig. 2). The latter connection, in particular, may play an important role in the ability of somatosensory feedback to elicit rapid corrective responses during movement execution (Omrani et al. 2013). For these reasons, S1 is likely to play a privileged role in providing sensory feedback for BCI control, both for integrating with vision and for establishing a short latency loop between motor output and sensory feedback. Furthermore, neurons in S1 are known to be plastic; for example, they can develop visual responses through somatosensory-visual pairing (Shokur et al. 2013). For these and other reasons, most cortical approaches to providing artificial somatic sensation have targeted S1 (London et al. 2008; O'Doherty et al. 2009, 2011, 2012; Berg et al. 2013; Tabot et al. 2013).

The parietal lobe also contains many multisensory areas. Of these, area 5, which receives projections from S1, may be particularly well suited, as it is situated conveniently on the cortical surface and seems involved in encoding arm postures and movements relative to the body in the context of upcoming motor

responses (Lacquaniti et al. 1995; Kalaska 1996). Furthermore, in intact animals, area 5 may encode feedback from online perturbations during movement execution even earlier than S1 (Omrani et al. 2013). Neurons in area 5 also have larger and more complex receptive fields than S1 (Hyvarinen 1982), suggesting that it employs a more complex, or abstract, representation of proprioceptive space. Finally, area 5 projects directly to dorsal premotor cortex (PMd), and, along with S1, to primary motor (M1) cortex.

Lastly, we note that the thalamus—an earlier subcortical stage of sensory processing—is also an attractive target for stimulation. The percepts evoked by thalamic stimulation correspond to relatively small and localized portions of the body surface (Heming et al. 2011), implying that each channel on a stimulating array could be used as a distinct input channel. Additionally, the neural activity evoked by in cortex by stimulation in the thalamus may more closely resemble "natural" neural activity than that evoked by stimulation of cortex directly (Brockmeier et al. 2012; Choi et al. 2012). Indeed, taking advantage of the information processing performed by the thalamocortical projections may represent the key to obtaining more biomimetic activity patterns in S1. Unfortunately, however, the thalamus is difficult to reach using currently available electrode arrays, and thus far, it seems that evoked percepts more often resemble a numbness or tingle than touch or movement (Heming et al. 2010).

5 Conclusion

In the preceding, we have argued that artificial somatosensory feedback will be needed to optimize clinically viable neural prostheses. Furthermore, we argued that it is practical to provide this feedback through the electrical stimulation of the brain, and indeed that this may be the only viable route for some patient populations, including following SCI with sensory loss. Lastly, we suggested a novel, learning-based approach to providing artificial somatosensory feedback.

Importantly, we are not arguing that the learning-based approach excludes more traditional biomimetic paradigms for stimulation-based feedback. Indeed, we think it is likely that the learning-based system would be learned more quickly as the stimulation protocol drives increasingly biomimetic patterns of activity. Rather, we are arguing that success of this approach need not rely of achieving high-fidelity biomimetic stimulation: the brain's natural mechanisms of plasticity should be able to make up for the difference.

References

Alais D, Burr D (2004) The ventriloquist effect results from near-optimal bimodal integration. Curr Biol CB 14(3):257–262. doi:10.1016/j.cub.2004.01.029

Alam M, Chen X, Fernandez E (2013) A low-cost multichannel wireless neural stimulation system for freely roaming animals. J Neural Eng 10(6):066010. doi:10.1088/1741-2560/10/6/066010

Bach-y-Rita P, Kercel SW (2002) Sensori-"motor" coupling by observed and imagined movement. Intellectica 35:287–297

Bach-y-Rita P, Kercel SW (2003) Sensory substitution and the human-machine interface. Trends Cogn Sci 7(12):541–546

Bach-y-Rita P, Collins CC, Saunders FA, White B, Scadden L (1969) Vision substitution by tactile image projection. Nature 221(5184):963–964

Barrese JC, Rao N, Paroo K, Triebwasser C, Vargas-Irwin C, Franquemont L, Donoghue JP (2013) Failure mode analysis of silicon-based intracortical microelectrode arrays in non-human primates. J Neural Eng 10(6):066014. doi:10.1088/1741-2560/10/6/066014

Berg JA, Dammann JF, Tenore FV, Tabot Ga, Boback JL, Manfredi LR, Peterson ML, Katyal KD, Johannes MS, Makhlin a, Wilcox R, Franklin RK, Vogelstein RJ, Hatsopoulos NG, Bensmaia SJ (2013) Behavioral demonstration of a somatosensory neuroprosthesis. IEEE Trans Neural Syst Rehabil Eng 21(3):500–507. doi:10.1109/TNSRE.2013.2244616 (a publication of the IEEE Engineering in Medicine and Biology Society)

Bin G, Gao X, Wang Y, Li Y, Hong B, Gao S (2011) A high-speed BCI based on code modulation VEP. J Neural Eng 8(2):025015. doi:10.1088/1741-2560/8/2/025015

Brockmeier AJ, Choi JS, Emigh MS, Li L, Francis JT, Principe JC (2012) Subspace matching thalamic microstimulation to tactile evoked potentials in rat somatosensory cortex. In: Annual international conference of the IEEE engineering in Medicine and Biology Society, IEEE Engineering in Medicine and Biology Society, pp 2957–2960

Burge J, Girshick AR, Banks MS (2010) Visual-haptic adaptation is determined by relative reliability. The Journal of neuroscience : the official journal of the Society for Neuroscience 30(22):7714–7721. doi:10.1523/JNEUROSCI.6427-09.2010

Butovas S, Schwarz C (2003) Spatiotemporal effects of microstimulation in rat neocortex: a parametric study using multielectrode recordings. J Neurophysiol 90(5):3024–3039. doi:10.1152/jn.00245.2003

Chestek CA, Gilja V, Nuyujukian P, Foster JD, Fan JM, Kaufman MT, Churchland MM, Rivera-Alvidrez Z, Cunningham JP, Ryu SI, Shenoy KV (2011) Long-term stability of neural prosthetic control signals from silicon cortical arrays in rhesus macaque motor cortex. J Neural Eng 8(4):045005. doi:10.1088/1741-2560/8/4/045005

Choi JS, DiStasio MM, Brockmeier AJ, Francis JT (2012) An electric field model for prediction of somatosensory (S1) cortical field potentials induced by ventral posterior lateral (VPL) thalamic microstimulation. IEEE Trans Neural Syst Rehabil Eng 20(2):161–169. doi:10.1109/TNSRE.2011.2181417 (a publication of the IEEE Engineering in Medicine and Biology Society)

Doty RW (1969) Electrical stimulation of the brain in behavioral context. Annu Rev Psychol 20:289–320. doi:10.1146/annurev.ps.20.020169.001445

Ernst MO, Banks MS (2002) Humans integrate visual and haptic information in a statistically optimal fashion. Nature 415(6870):429–433. doi:10.1038/415429a

Fagg AH, Hatsopoulos NG, de Lafuente V, Moxon KA, Nemati S, Rebesco JM, Romo R, Solla SA, Reimer J, Tkach D, Pohlmeyer EA, Miller LE (2007) Biomimetic brain machine interfaces for the control of movement. J Neurosci Off J Soc Neurosci 27(44):11842–11846. doi:10.1523/JNEUROSCI.3516-07.2007

Fetsch CR, Pouget A, DeAngelis GC, Angelaki DE (2012) Neural correlates of reliability-based cue weighting during multisensory integration. Nat Neurosci 15(1):146–154. doi:10.1038/nn.2983

Frey SH, Bogdanov S, Smith JC, Watrous S, Breidenbach WC (2008) Chronically deafferented sensory cortex recovers a grossly typical organization after allogenic hand transplantation. Curr Biol CB 18(19):1530–1534. doi:10.1016/j.cub.2008.08.051

Georgopoulos AP, Massey JT (1988) Cognitive spatial-motor processes. 2. Information transmitted by the direction of two-dimensional arm movements and by neuronal populations in primate motor cortex and area 5. Exp Brain Res 69(2):315–326

Gilja V, Chestek CA, Diester I, Henderson JM, Deisseroth K, Shenoy KV (2011) Challenges and opportunities for next-generation intracortically based neural prostheses. IEEE Trans Biomed Eng 58(7):1891–1899. doi:10.1109/TBME.2011.2107553

Gilja V, Nuyujukian P, Chestek CA, Cunningham JP, Yu BM, Fan JM, Churchland MM, Kaufman MT, Kao JC, Ryu SI, Shenoy KV (2012) A high-performance neural prosthesis enabled by control algorithm design. Nat Neurosci 15(12):1752–1757. doi:10.1038/nn.3265

Gomez-Rodriguez M, Peters J, Hill J, Schölkopf B, Gharabaghi A, Grosse-Wentrup M (2011) Closing the sensorimotor loop: haptic feedback facilitates decoding of motor imagery. J Neural Eng 8(3):036005. doi:10.1088/1741-2560/8/3/036005

Gu Y, Angelaki DE, Deangelis GC (2008) Neural correlates of multisensory cue integration in macaque MSTd. Nat Neurosci 11(10):1201–1210. doi:10.1038/nn.2191

Hatsopoulos NG, Donoghue JP (2009) The science of neural interface systems. Annu Rev Neurosci 32:249–266. doi:10.1146/annurev.neuro.051508.135241

Heming E, Sanden A, Kiss ZH (2010) Designing a somatosensory neural prosthesis: percepts evoked by different patterns of thalamic stimulation. J Neural Eng 7(6):064001. doi:10.1088/1741-2560/7/6/064001

Heming EA, Choo R, Davies JN, Kiss ZH (2011) Designing a thalamic somatosensory neural prosthesis: consistency and persistence of percepts evoked by electrical stimulation. IEEE Trans Neural Syst Rehabil Eng 19(5):477–482. doi:10.1109/TNSRE.2011.2152858 (a publication of the IEEE Engineering in Medicine and Biology Society)

Hinton GE, Osindero S, Teh YW (2006) A fast learning algorithm for deep belief nets. Neural Comput 18(7):1527–1554. doi:10.1162/neco.2006.18.7.1527

Histed MH, Bonin V, Reid RC (2009) Direct activation of sparse, distributed populations of cortical neurons by electrical microstimulation. Neuron 63(4):508–522. doi:10.1016/j.neuron.2009.07.016

Hochberg LR, Serruya MD, Friehs GM, Mukand JA, Saleh M, Caplan AH, Branner A, Chen D, Penn RD, Donoghue JP (2006) Neuronal ensemble control of prosthetic devices by a human with tetraplegia. Nature 442(7099):164–171. doi:10.1038/nature04970

Hochberg LR, Bacher D, Jarosiewicz B, Masse NY, Simeral JD, Vogel J, Haddadin S, Liu J, Cash SS, van der Smagt P, Donoghue JP (2012) Reach and grasp by people with tetraplegia using a neurally controlled robotic arm. Nature 485(7398):372–375. doi:10.1038/nature11076

Houweling AR, Brecht M (2008) Behavioural report of single neuron stimulation in somatosensory cortex. Nature 451(7174):65–68. doi:10.1038/nature06447

Hyvarinen J (1982) Posterior parietal lobe of the primate brain. Physiol Rev 62(3):1060–1129

Johansson RS, Flanagan JR (2009) Coding and use of tactile signals from the fingertips in object manipulation tasks. Nat Rev Neurosci 10(5):345–359. doi:10.1038/nrn2621

Johansson RS, Westling G (1984) Roles of glabrous skin receptors and sensorimotor memory in automatic control of precision grip when lifting rougher or more slippery objects. Exp Brain Res 56(3):550–564

Kaas JH, Nelson RJ, Sur M, Lin CS, Merzenich MM (1979) Multiple representations of the body within the primary somatosensory cortex of primates. Science 204(4392):521–523

Kalaska JF (1996) Parietal cortex area 5 and visuomotor behavior. Can J Physiol Pharmacol 74(4):483–498

Kozai TD, Marzullo TC, Hooi F, Langhals NB, Majewska AK, Brown EB, Kipke DR (2010) Reduction of neurovascular damage resulting from microelectrode insertion into the cerebral cortex using in vivo two-photon mapping. J Neural Eng 7(4):046011. doi:10.1088/1741-2560/7/4/046011

Krubitzer LA, Kaas JH (1990) The organization and connections of somatosensory cortex in marmosets. J Neurosci Off J Soc Neurosci 10(3):952–974

Kuiken TA, Li G, Lock BA, Lipschutz RD, Miller LA, Stubblefield KA, Englehart KB (2009) Targeted muscle reinnervation for real-time myoelectric control of multifunction artificial arms. J Am Med Assoc JAMA 301(6):619–628. doi:10.1001/jama.2009.116

Lacquaniti F, Guigon E, Bianchi L, Ferraina S, Caminiti R (1995) Representing spatial information for limb movement: role of area 5 in the monkey. Cereb Cortex 5(5):391–409

Lebedev MA, Nicolelis MA (2006) Brain-machine interfaces: past, present and future. Trends Neurosci 29(9):536–546. doi:10.1016/j.tins.2006.07.004

Lebedev MA, Tate AJ, Hanson TL, Li Z, O'Doherty JE, Winans JA, Ifft PJ, Zhuang KZ, Fitzsimmons NA, Schwarz DA, Fuller AM, An JH, Nicolelis MA (2011) Future developments in brain-machine interface research. Clinics 66(Suppl 1):25–32

Ledochowitsch P, Koralek AC, Moses D, Carmena JM, Maharbiz MM (2013) Sub-mm functional decoupling of electrocortical signals through closed-loop BMI learning. In: Annual international conference of the IEEE engineering in Medicine and Biology Society, IEEE Engineering in Medicine and Biology Society, pp 5622–5625. doi:10.1109/EMBC.2013.6610825

Li Z, O'Doherty JE, Lebedev MA, Nicolelis MA (2011) Adaptive decoding for brain-machine interfaces through Bayesian parameter updates. Neural Comput 23(12):3162–3204. doi:10.1162/NECO_a_00207

London BM, Jordan LR, Jackson CR, Miller LE (2008) Electrical stimulation of the proprioceptive cortex (area 3a) used to instruct a behaving monkey. IEEE Trans Neural Syst Rehabil Eng 16(1):32–36. doi:10.1109/TNSRE.2007.907544 (a publication of the IEEE Engineering in Medicine and Biology Society)

Makin JG, Fellows MR, Sabes PN (2013) Learning multisensory integration and coordinate transformation via density estimation. PLoS Comput Biol 9(4):e1003035. doi:10.1371/journal.pcbi.1003035

McGuire LM, Sabes PN (2009) Sensory transformations and the use of multiple reference frames for reach planning. Nat Neurosci 12(8):1056–1061. doi:10.1038/nn.2357

Merzenich MM, Kaas JH, Wall J, Nelson RJ, Sur M, Felleman D (1983a) Topographic reorganization of somatosensory cortical areas 3b and 1 in adult monkeys following restricted deafferentation. Neuroscience 8(1):33–55

Merzenich MM, Kaas JH, Wall JT, Sur M, Nelson RJ, Felleman DJ (1983b) Progression of change following median nerve section in the cortical representation of the hand in areas 3b and 1 in adult owl and squirrel monkeys. Neuroscience 10(3):639–665

Mulliken GH, Musallam S, Andersen Ra (2008) Decoding trajectories from posterior parietal cortex ensembles. J Neurosci Off J Soc Neurosci 28(48):12913–12926. doi:10.1523/JNEUROSCI.1463-08.2008

Nau A, Bach M, Fisher C (2013) Clinical tests of ultra-low vision used to evaluate rudimentary visual perceptions enabled by the BrainPort vision device. Transl Vis Sci Technol 2(3):1. doi:10.1167/tvst.2.3.1

O'Doherty JE, Lebedev MA, Hanson TL, Fitzsimmons NA, Nicolelis MA (2009) A brain-machine interface instructed by direct intracortical microstimulation. Front Integr Neurosci 3:20. doi:10.3389/neuro.07.020.2009

O'Doherty JE, Lebedev MA, Ifft PJ, Zhuang KZ, Shokur S, Bleuler H, Nicolelis MA (2011) Active tactile exploration using a brain-machine-brain interface. Nature 479(7372):228–231. doi:10.1038/nature10489

O'Doherty JE, Lebedev MA, Li Z, Nicolelis MA (2012) Virtual active touch using randomly patterned intracortical microstimulation. IEEE Trans Neural Syst Rehabil Eng 20(1):85–93. doi:10.1109/TNSRE.2011.2166807 (a publication of the IEEE Engineering in Medicine and Biology Society)

Omrani M, Pruszynki AJ, Scott SH (2013) Temporal evolution of task dependent signal in sensory-motor cortices. In: Annual meeting of the Society for Neuroscience, San Diego, 13 November 2013

Orsborn AL, Dangi S, Moorman HG, Carmena JM (2012) Closed-loop decoder adaptation on intermediate time-scales facilitates rapid BMI performance improvements independent of decoder initialization conditions. IEEE Trans Neural Syst Rehabil Eng 20(4):468–477. doi:10.1109/TNSRE.2012.2185066 (a publication of the IEEE Engineering in Medicine and Biology Society)

Parker PA, Scott RN (1986) Myoelectric control of prostheses. Crit Rev Biomed Eng 13(4):283–310

Penfield W, Boldrey E (1937) Somatic motor and sensory representation in the cerebral cortex of man as studied by electrical stimulation. Brain 60:398–443. doi:10.1093/brain/60.4.389

Polikov VS, Tresco PA, Reichert WM (2005) Response of brain tissue to chronically implanted neural electrodes. J Neurosci Methods 148(1):1–18. doi:10.1016/j.jneumeth.2005.08.015

Pons TP, Garraghty PE, Ommaya AK, Kaas JH, Taub E, Mishkin M (1991) Massive cortical reorganization after sensory deafferentation in adult macaques. Science 252(5014):1857–1860

Prud'homme MJ, Kalaska JF (1994) Proprioceptive activity in primate primary somatosensory cortex during active arm reaching movements. J Neurophysiol 72(5):2280–2301

Recanzone GH, Merzenich MM, Dinse HR (1992) Expansion of the cortical representation of a specific skin field in primary somatosensory cortex by intracortical microstimulation. Cereb Cortex 2(3):181–196

Rincon-Gonzalez L, Naufel SN, Santos VJ, Helms Tillery S (2012) Interactions between tactile and proprioceptive representations in haptics. J Mot Behav 44(6):391–401. doi:10.1080/00222895.2012.746281

Sainburg RL, Poizner H, Ghez C (1993) Loss of proprioception produces deficits in interjoint coordination. J Neurophysiol 70:2136–2147

Schalk G, Miller KJ, Anderson NR, Ja Wilson, Smyth MD, Ojemann JG, Moran DW, Wolpaw JR, Leuthardt EC (2008) Two-dimensional movement control using electrocorticographic signals in humans. J Neural Eng 5(1):75–84. doi:10.1088/1741-2560/5/1/008

Schiefer MA, Polasek KH, Tiolo RJ, Pinault GCJ, Tyler DJ (2010) Selective stimulation of the human femoral nerve with a flat interface nerve electrode. J Neural Eng 7(2). doi:10.1088/1741-2560/7/2/026006.Selective

Shanechi MM, Williams ZM, Wornell GW, Hu RC, Powers M, Brown EN (2013) A real-time brain-machine interface combining motor target and trajectory intent using an optimal feedback control design. PLoS ONE 8(4):e59049. doi:10.1371/journal.pone.0059049

Shokur S, O'Doherty JE, Winans JA, Bleuler H, Lebedev MA, Nicolelis MA (2013) Expanding the primate body schema in sensorimotor cortex by virtual touches of an avatar. Proc Natl Acad Sci USA 110(37):15121–15126. doi:10.1073/pnas.1308459110

Simani MC, McGuire LM, Sabes PN (2007) Visual-shift adaptation is composed of separable sensory and task-dependent effects. J Neurophysiol 98(5):2827–2841. doi:10.1152/jn.00290.2007

Sober SJ, Sabes PN (2005) Flexible strategies for sensory integration during motor planning. Nat Neurosci 8(4):490–497. doi:10.1038/nn1427

Stoney SD Jr, Thompson WD, Asanuma H (1968) Excitation of pyramidal tract cells by intracortical microstimulation: effective extent of stimulating current. J Neurophysiol 31(5):659–669

Suminski AJ, Tkach DC, Fagg AH, Hatsopoulos NG (2010) Incorporating feedback from multiple sensory modalities enhances brain-machine interface control. J Neurosci Off J Soc Neurosc 30(50):16777–16787. doi:10.1523/JNEUROSCI.3967-10.2010

Tabot GA, Dammann JF, Berg JA, Tenore FV, Boback JL, Vogelstein RJ, Bensmaia SJ (2013) Restoring the sense of touch with a prosthetic hand through a brain interface. Proc Natl Acad Sci USA 110(45):18279–18284. doi:10.1073/pnas.1221113110

Tehovnik EJ (1996) Electrical stimulation of neural tissue to evoke behavioral responses. J Neurosci Methods 65(1):1–17

Tehovnik EJ, Tolias AS, Sultan F, Slocum WM, Logothetis NK (2006) Direct and indirect activation of cortical neurons by electrical microstimulation. J Neurophysiol 96(2):512–521. doi:10.1152/jn.00126.2006

van Beers RJ, Sittig AC, Gon JJ (1999) Integration of proprioceptive and visual position-information: an experimentally supported model. J Neurophysiol 81(3):1355–1364

van Beers RJ, Wolpert DM, Haggard P (2002) When feeling is more important than seeing in sensorimotor adaptation. Curr Biol CB 12(10):834–837

Velliste M, Perel S, Spalding MC, Whitford AS, Schwartz AB (2008) Cortical control of a prosthetic arm for self-feeding. Nature 453(7198):1098–1101. doi:10.1038/nature06996

Verstynen T, Sabes PN (2011) How each movement changes the next: an experimental and theoretical study of fast adaptive priors in reaching. J Neurosci Off J Soc Neurosci 31(27):10050–10059. doi:10.1523/JNEUROSCI.6525-10.2011

Vuillerme N, Hlavackova P, Franco C, Diot B, Demongeot J, Payan Y (2011) Can an electro-tactile vestibular substitution system improve balance in patients with unilateral vestibular loss under altered somatosensory conditions from the foot and ankle? In: Annual international conference of the IEEE Engineering in Medicine and Biology Society, IEEE Engineering in Medicine and Biology Society, pp 1323–1326. doi:10.1109/IEMBS.2011.6090311

Wallace MT, Stein BE (1997) Development of multisensory neurons and multisensory integration in cat superior colliculus. J Neurosci Off J Soc Neurosci 17(7):2429–2444

Warren JP, Tillery SI (2011) Tactile perception: do distinct subpopulations explain differences in mislocalization rates of stimuli across fingertips? Neurosci Lett 505(1):1–5. doi:10.1016/j.neulet.2011.04.057

Weber DJ, Friesen R, Miller LE (2012) Interfacing the somatosensory system to restore touch and proprioception: essential considerations. J Mot Behav 44(6):403–418. doi:10.1080/00222895.2012.735283

Woolley AJ, Desai HA, Otto KJ (2013) Chronic intracortical microelectrode arrays induce non-uniform, depth-related tissue responses. J Neural Eng 10(2):026007. doi:10.1088/1741-2560/10/2/026007

An Accurate, Versatile, and Robust Brain Switch for Neurorehabilitation

Ning Jiang, Natalie Mrachacz-Kersting, Ren Xu, Kim Dremstrup and Dario Farina

Abstract For the past decade, our group worked towards the development of a non-invasive BCI system for neuromodulation. Until recently, BCIs have been used mainly for communication and replacement or restoration of lost functions for severely disabled people. Using a BCI for neuromodulation requires that the protocol closely matches the steps involved in the motor learning process. However, the underlying mechanisms of motor learning in humans remain elusive, though several possibilities have been proposed. Of these, the most promising was proposed by Hebb (The organization of behavior: a neuropsychological theory, vol. 44, p. 335, 1949), who suggested that synaptic strength is increased when two inputs from two sources arrive at the post-synaptic cell in synchrony. If this occurs repetitively with the necessary intensity, synaptic strength is increased. That is, the same input will produce a greater output. Stefan et al. (Brain J Neurol 123(pt 3):572–584, 2000) were the first to investigate this concept non-invasively in humans, and it has now become accepted that it closely matches what occurs during motor learning. With this knowledge, we developed a BCI system where the user's movement intention is detected through non-invasive electroencephalogram (EEG). When the onset of the intended movement is detected, it is used to drive an external device that produces the intended movement. Through this process, the user is provided with the necessary proprioceptive feedback, timed to coincide with the onset of the intended movement, so that the Hebbian principle of associativity

N. Jiang (✉) · R. Xu · D. Farina
Department of Neurorehabilitation Engineering, Bernstein Center for Computational Neuroscience, University Medical Center Göttingen, Georg-August-University Göttingen, Göttingen, Germany
e-mail: ning.jiang@bccn.uni-goettingen.de

N. Mrachacz-Kersting · K. Dremstrup
Center for Sensory-Motor Interaction, Department of Health Science and Technology, Aalborg University, 9220 Aalborg, Denmark

C. Guger et al. (eds.), *Brain-Computer Interface Research*, SpringerBriefs in Electrical and Computer Engineering, DOI 10.1007/978-3-319-09979-8_5

is satisfied. In this chapter, we outline the development of this BCI system for neuromodulation and show that it can be used to drive any external device while satisfying all the main criteria necessary for a full BCI application, namely: accuracy, flexibility, rapid control, and robustness.

Keywords Brain computer interface · Hebbian plasticity · Movement related cortical potentials · Neurorehabilitation

1 Introduction

Rehabilitation of motor disability for central nervous system injuries, such as stroke and Parkinson's disease, aims to activate the brain areas related to the planning and execution of voluntary movements through consistent and repetitive movements of the affected limb(s), either administered by therapists or produced by robotic devices. Traditional clinical practice of neurorehabilitation, in which therapists manually move the affected limb(s), has limited efficacy. Many patients demonstrate habituation to therapy, physiologically and psychologically. Numerous novel rehabilitation techniques involving advanced technology (Marchal-Crespo and Reinkensmeyer 2009), such as robot-assisted systems (Krebs et al. 2003; Hesse et al. 2005; Sanchez et al. 2006), peripheral and (Ring and Rosenthal 2005; Alon et al. 2007; Yan et al. 2005) cortical electric stimulation (Hummel et al. 2005; Hummel and Cohen 2006; Williams et al. 2009), have been proposed for motor function rehabilitation. However, studies that have successfully demonstrated the clinical advantage of these technology-based approaches over conventional practice are only beginning to emerge. One concern with many of these new approaches is that they are not specifically designed to induce neural plasticity, which is essential to the recovery of motor function and re-learning of motor skills. Plasticity is induced following the Hebbian principle that synaptic connections are strengthened when pre- and post-synaptic neural structures are activated in a highly correlated way: what fires together wires together. Therefore, motor rehabilitation systems need to induce correlated activation of brain areas that are affected by the injuries, and such correlated activation has to be as physiologically realistic as possible.

Another equally important factor in motor rehabilitation is the patients' motivation (Maclean et al. 2000). All previously mentioned methods assign a purely passive role of the patient in the rehabilitation procedure. With this view, methods that would provide the patients a more active role in the rehabilitation process have been proposed by extracting patients' movement intentions using biological signals, such as EEG. This is possible because the cortical areas, which are related to movement planning, sensorimotor processing, attention and task complexity, are shown to be as active in stroke survivors as in controls (Cramer et al. 2002). Therefore, in principle, these active brain state(s) can be identified through processing the associated brain signals, and the patients' motor intentions can be detected. Rehabilitation devices, such as a robotic arm or an electric stimulator, can be controlled, at least in part, by

such a detection, as opposed to being fully controlled by a predefined program or by therapists. In such a way, the patients are in a much more active role in the rehabilitation process and their motivation is likely to be significantly improved.

2 System Overview

With the above principles in mind, our group has been developing a brain switch system that will efficiently induced neural plasticity and at the same time maximize the patients' motivation.

We start with the first principle: creating a rehabilitation approach that complies with the Hebbian rule. In the literature, strong supporting evidence for the Hebbian principle has been obtained in in vivo human experiments, notably the paired associative stimulation (PAS) paradigm (Stefan et al. 2000). In this paradigm, electrical stimulation (ES) was delivered to the peripheral nerve that innervates the target muscle. The ES was applied in a time-locked fashion with non-invasive brain stimulation to the area of the motor cortex with projections to the same muscle. Significant increases in cortical excitability of the target muscle (quantified through transcranial magnetic stimulation, TMS) were observed after a short intervention consisting of repeated pairings of the two stimuli. The enhancement of cortical excitability was rapidly evolving, outlasted the intervention and was specific to the target muscle. In later publications, the dependence on N-methyl-D-aspartate (NMDA) receptor activation was also confirmed, thus satisfying some of the main requirements for an LTP-like (long term potentiation) mechanism. We started the design of our brain switch system inspired by this PAS paradigm. It is known that TMS has the limitation that the stimulation current may spread to non-target brain regions adjacent to the target region. Therefore, the simulation could become 'non-specific' and the efficiency of the intervention can be compromised. To avoid this problem and (more importantly) to design a system that can maximally engage patients, we chose to replace the cortical stimulation with a more natural option: subject's intention of movements, which would activate only the specific cortical regions involved in the movement both spatially but also in a temporally correct manner. Thus, the neuromodulation system we present here consisted of basically two modules: movement intention detection module (a brain switch) and afferent generation module. The function of the movement intention detection module is to detect the intention of movement (imaginary or attempted execution) from scalp EEG, i.e. a brain switch. This is a very challenging goal to achieve in a single trials basis from EEG, particularly in an asynchronous paradigm. In additional to sensitivity and specificity, another key performance requirement for the detection module here is the detection latency from the onset of the movement intention. As discussed in detail in the next section, a short latency is critical for any neuromodulation system to be effective, because the Hebbian plasticity can only be induced when a causal relationship between the movement intention and the corresponding afferents can be

established. Each detection would then trigger the afferent generation module. This module's function is to generate an afferent volley that would mimic, as closely as possible, the natural afferents arising from real movement. It is important to note that the purpose of this module is not to produce functional movements, as a BCI-triggered functional electrical stimulation (FES) is.

3 MRCP and Movement Intention Detection

3.1 MRCP and Voluntary Movements

When voluntary movements, or the imagination of movements, are performed, a type of slow cortical potential (SCP) can be recorded from scalp EEG. This specific signal is usually characterized by a slow negative phase, followed by a faster positive rebound. The negative phase can start as early as 1.5–2 s prior to the onset of movements (or its imagination), and the peak negativity usually occurs at the movement onset. The positive rebound can be as long as 1–1.5 s. This particular signal waveform is often referred to as the movement related cortical potential (MRCP). The different phases of MRCPs are associative to specific neurophysiological mechanisms during voluntary movements. For an in-depth review on the physiology of MRCP, please refer to Johanshahi and Hallettm (2003). In the BCI context, it is important to note that the MRCPs observed from a self-paced movement (in an asynchronous BCI mode) and from a cue-based movement (in a synchronous BCI mode) arises from different physiological processes (Lu et al. 2012). In the former case, it is often referred to Bereitschaftspotential (BP, which means "readiness potential" in German) (Deecke et al. 1976), and the latter is often denoted as the contingent negative variation (CNV) (Walter 1968), or anticipation-related potential (Gangadhar et al. 2009; Garipelli et al. 2013). An example of MRCPs under these two conditions is presented in Fig. 1. In the literature, MRCP or SCP is used to refer to either of the two cases (Johanshahi and Hallettm 2003; Gangadhar et al. 2009; Lew et al. 2012). In our efforts to develop the brain switch system, we are focusing on the self-paced paradigm because it provides the users (patients) a more engaging rehabilitation experience than a cue-based paradigm, and the neurophysiological process involved in a self-paced paradigm is closer to those in everyday activities than in a cue-based paradigm. In the following, MRCP is used in the general case, and BP or CNV is used when a specific condition is discussed where a distinction between the two is necessary.

3.2 Signal Processing of MRCP for Detection of Movement Intentions

The signal processing chain of MRCP for the purpose of movement intention detection is illustrated in Fig. 2. It consists of three modules: pre-processing, training, and detection. The pre-processing step mainly consists of band-pass filtering.

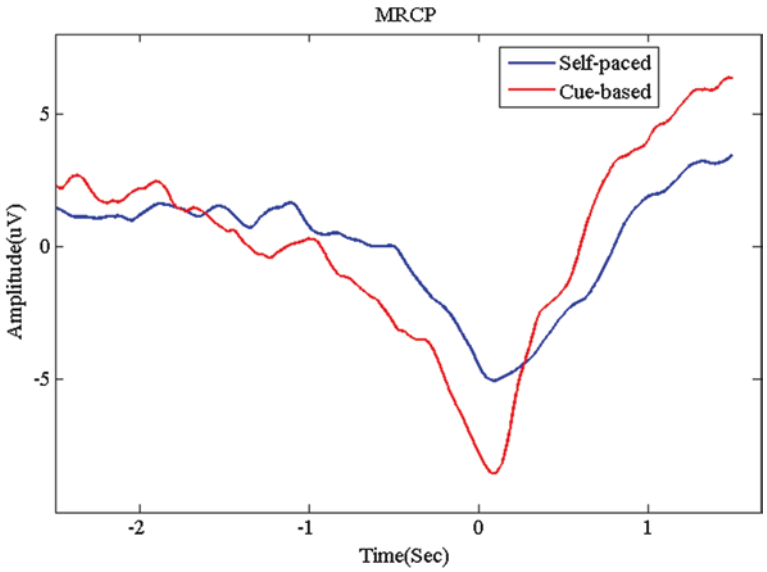

Fig. 1 Self-paced and cue-based MRCPs. The presented MRCPs are epoch averages of 30 trials of execution of dorsiflexions, with self-paced and cue-based paradigms, respectively. Signals were first band-pass filtered at 0.05–3 Hz, and then processed with a large Laplacian spatial filter centered at Cz

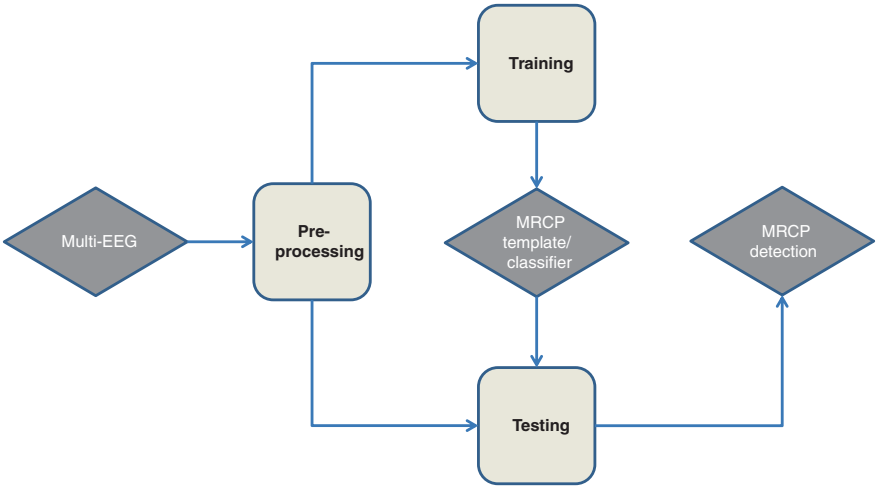

Fig. 2 The schematic diagram for the signal processing chain of MRCP detection

MRCPs are part of the lower end of the EEG spectrum, close to non-physiological DC drift in EEG recording systems. Therefore, a DC-coupled EEG system with a large dynamic range is mandatory for the detection of MRCPs. To extract MRCPs,

it is necessary to band pass filter the raw EEG before any further processing. There is no consensus on the best parameters for the band-pass filter. In a recent study, Garipelli et al. (2013) found that [0.1–1] Hz yielded the best detection accuracy for CNV. In general, [0.05, 5] Hz is acceptable. It is important to note that this type of band-pass filter usually has a very long transient phase (>30 s). Hence, it is highly recommended to check the raw signals at the beginning of a data acquisition session, to ensure that the transient phase has passed, prior to the start of the actual experiments. This is particularly important for online experiments. At this stage, it is also possible to include optional processing steps, such as spatial filtering, independent component analysis etc., which would either enhance the power of the MRCP (Boye et al. 2008), or remove signals corrupted by artifacts, EOG and EMG (Jiang et al. 2014).

Following band-pass filtering, an MRCP detector needs to be trained using a data set from a training session. Usually, during this session, the subject would be instructed to perform a series of single movement execution or imagination (e.g. dorsiflexion, wrist flexion etc.), either following a cue or at a self-selected pace. A typical training session consists of 20–30 such tasks. Usually, signal processing on the training data takes place immediately after the training session. First, data segments consisting of MRCPs are identified. This can be done easily in a cue-based paradigm, for either imagination or execution tasks, because the timing of the movement onset in this paradigm is pre-defined. In a self-paced paradigm, this is only possible for execution tasks, and the EMG from the target muscle is often used to get the timing of movement onset. Once the timing of the movement (either imagination or execution) onset is identified, signals prior to and after the onset ($t = 0$), for example $[-1.5, 1]$ s, are extracted to form an MRCP dictionary, from which an MRCP template can be obtained by taking the epoch-average of the dictionary. Optionally, a further 'noise' dictionary can be obtained by taking signals that are not in the MRCP dictionary. This 'noise' dictionary can be used to obtain an optimal spatial filter for the MRCP in a multi-channel setup by optimizing the power contrast between the MRCP dictionary and the 'noise' dictionary. The 'noise' dictionary can also be used, along with the MRCP dictionary, to train a two-class classifier. Once the detector is trained, either directly using the MRCP template, or through the classifier, the online detection (testing) part can start. After the same pre-processing, testing data will be streamed to the detector, either a matched-filter or a classifier. To improve the robustness of the entire detection process, the raw output of the detector can be subjected to post-processing, such as majority vote (e.g. a final positive detection would occur only when two out of the last three detections were positive).

In the development of our brain switch system, we have conducted a series of studies using this general signal processing framework. We demonstrated the possibility of detecting executed movements and imagined movements (ballistic dorsiflexion) performed by able-bodied subjects, as well as movement attempts by chronic stroke patients in a self-paced paradigm (Niazi et al. 2011). In this study, the initial phase of the MRCP (2 s before the negativity) was used for detection, and spatial filtering was used to enhance detection accuracy. Three spatial

filtering methods were investigated: large Laplacian filter, common spatial patterns, and an optimized spatial filter for MRCP signal-to-noise ratio. The detection algorithm was a simple matched-filter, with a 3-window majority vote (MV) post-processing. The average detection performance of this algorithm for movement execution from healthy controls was 82.5 % true-positive and 1.2 false detections per min. Across all subjects, the detection latency in this case was between −110 and 100 ms, with respect to the cue indicating the movement onset, and the average latency was −66.6 ms. In the movement imagination tasks, the detection performance was significantly lower (64.5 % true-positive and 5.2 false detections per min). For stroke patients, the detection true-positive for movement attempts was lower than healthy controls (56 %), while the false detection rate was similar. Most importantly, the detection latency of stroke patient was similar to that of healthy controls (−56.8 ms), which is critical for plasticity induction.

The detection performance of the simple spatial filtering and matched-filtering was satisfactory, but there was clear room for improvement. More recently, we applied a manifold-based dimensional reduction algorithm called locality preserving projection (LPP) (He and Niyogi 2003) followed by linear discriminant analysis (LDA) for MRCP detection (Xu et al. 2014). The LPP-LDA detector explicitly exploited information from both 'signal' dictionary and 'noise' dictionary, and the resulting detection performance was significantly better. In this self-paced fully online study with healthy volunteers, the average true-positive rate, false positive rate, and detection latency of LPP-LDA was 79 %, 1.4 per minute and 315 ms, respectively. No statistically significant difference was found between movement execution and movement imagination tasks. For all performance measures, LPP-LDA was significantly better than the matched-filter algorithm on the same data set. Note that the detection latency in this study was larger than the one reported previously in Niazi et al. (2013) because the template used also included 0.5 s after the peak negativity.

The online detection of movement intentions (execution or imagination) from MRCPs makes this approach a candidate for our brain switch for neuromodulation. Further, it has been shown that the morphology of the MRCP is modulated by specific task parameters, such as movement type, movement speed, target force level, etc. For example, classification accuracy as high as 81 % was reported for imagination tasks of wrist extension and rotation, while 84 % accuracy was reported for fast and slow imagination of wrist extension (Gu et al. 2009). In a more recent study with healthy subjects, we showed fast and slow executed dorsiflexion can be classified with an average accuracy of 80 %, and high target force and low target force dorsiflexion can be classified with an average accuracy of 75 % (Jochumsen et al. 2013). The classifier used in this study was a Gaussian kernel support vector machine (SVM). These studies demonstrated the potential of the MRCP for online detection of more complex movements. This capability allows for a brain switch that can detect movement intentions with different parameters from the user and provide feedback accordingly. Such as a system is highly desirable for neuromodulation because diversity in movement parameters is an important element of motor learning according to the schema theory (Schmidt 1975; Salmoni et al. 1984; Shea and Wulf 2005).

4 MRCP Triggered Afferent Feedback and Plasticity Induction

With the demonstrated capability of using the MRCP for movement intention detection with a very small time delay, we continued to develop a closed-loop BCI system for neuromodulation. The key objective of such a system is to produce afferent feedback that is as close as possible, both *spatially* and *temporally*, to the afferent volley during normal movement. Spatial similarity means the afferent information has to be task and muscle specific. For example, when the intended movement is dorsiflexion, the afferents have to arise from tibialis anterior or the deep branch of common peroneal nerve; when the intended movement is wrist extension, the afferents have to arise from wrist extensors or radial nerve. This is one of the important distinctions between our brain switch system and other motor imaginary BCI system for communication or controlling external devices, in which the feedback to users is not functionally relevant to their motor intention. Temporal similarity means that the time interval between the movement imagination (or attempt) and the artificially generated afferents arriving at the cortex has to be similar to the time interval between the actual movement and its resulting afferents. This is to ensure that the artificial afferents can be considered as the physiological result of the movement intention. The maximum acceptable delay in a BCI system such as this is not clear. However, studies in myoelectric control indicated the delay should not exceed 250–300 ms for meaningful control (Paciga et al. 1980; Lauer et al. 2000; Velliste et al. 2008). Both spatial and temporal similarities discussed above are necessary for satisfying the Hebbian principle and consequently plasticity induction.

First, we set out to prove that, when these two conditions are met, significant plasticity (cortical output) can be induced using our brain switch (Mrachacz-Kersting et al. 2012). In this study, the subjects performed ballistic dorsiflexion imaginations in a cue-based paradigm. The CNV was extracted and the peak negativity of CNV was used as the reference point for electric stimulation to the deep branch of the common peroneal nerve (dCPN). The BCI intervention consisted of one of three stimulation scenarios: either 2SD-50 ms before, on or 2SD-50 ms after the peak negativity of the CNV, where SD is the standard deviation of the peak negativity of the MRCP. Single pulse motor threshold stimulation was used. The excitability of the cortical projections to the TA muscle was quantified before and after each intervention session using TMS applied at five different stimulation levels. Each subject received 50 paired movement imagination and peripheral stimuli in each scenario. Across all subjects, only when the dCPN stimulation was applied so that the generated afferent volley arrived at M1 during the peak negativity did we observe significant increases in the motor evoked potentials (MEP) for all levels of TMS. Since no alterations of spinal pathways (tested through assessment of the stretch reflex) were found, the induced plasticity was deemed to be at the cortical level. When the afferent volley was timed to arrive at M1 either before or after the peak negativity, there were no significant changes in the recorded TA MEPs.

Additional control conditions were also performed, including movement imagination only, random stimulation only and visual cue only. Neither of these control conditions was shown to have any effect on the TA MEPs. This study demonstrated clearly the necessary temporal and spatial specificity for effective plasticity induction through the brain switch.

We continued with another study using a self-paced paradigm (Niazi et al. 2012) where the matched filter detection algorithm presented in Sect. 3 was used. The subjects were instructed to perform self-paced dorsiflexion imagination, and the corresponding MRCP was detected online. Each detection then triggered an electric stimulation to the dCPN, with the same stimulation parameters as in the previous cue-based study (Mrachacz-Kersting et al. 2012). The subjects also participated in two control conditions: BCI alone and random stimulation. The quantification method of the cortical output to the TA muscle was also the same as in Mrachacz-Kersting et al. (2012). The results again confirmed the efficacy of our brain switch in inducing plasticity. For all subjects, the TA MEPs significantly increased after the BCI intervention, while there was no significant change in both control conditions. Stretch-reflex recordings also revealed no significant change at the spinal level after the BCI intervention.

Following the encouraging results from these studies on healthy subjects, we proceeded to determine whether the same or similar plasticity induction capability of the brain switch also applies to stroke patient. In collaboration with Professor Kostic of the Department of Neurology, University of Belgrade, Serbia, we applied this intervention in a group of 13 chronic stroke subjects who were no longer responding to regular therapy (manuscript in preparation). Each subject participated in four 30-min investigative sessions, separated by at least 24 h. Three of the four sessions were intervention sessions, in which our brain switch protocol was used, and one randomly selected session was a control session, in which the subject was only present in the laboratory for the same amount of time as the intervention sessions, without exposure to the intervention. Both neurophysiological and functional measures were obtained before the first session and after each session. Cortical output to the TA muscle was measured using TMS, with the same procedure as in the earlier studies in healthy subjects (Mrachacz-Kersting et al. 2012; Niazi et al. 2012). In addition, standard motor functional measure tests, including Lower-Extremity Fugl-Meyer assessment (LE-FM), 10 m walk test, a foot tapping task and a finger tapping task, were also performed before and after the intervention sessions. Across all subjects, the MEPs quantified prior to and following the interventions significantly increased. The LE-FM scores of the patients improved significantly, the patients were able to walk significantly faster (on average 8 % in 10 m walk test) and had a significantly higher foot tapping frequency. Interestingly, there was no significant change in the finger tapping frequency, further supporting the specificity of this intervention.

In all the above studies, the afferent flow was elicited with peripheral nerve stimulation. This approach of inducing afferent information has an apparent

problem, because ES is not selective, and the activated nerve fibres and the way in which they are activated during ES are not necessarily similar to what would occur in natural movements, where in essence there is the additional factor of agonist and antagonist activation. More recently, we have investigated the possibility of inducing afferent information by passive dorsiflexion using a motorized ankle-foot orthosis (MAFO). Passive dorsiflexion moves the joint and stretches or compresses the muscle tendons in a more natural fashion than ES. Presumably, it should elicit afferent information more similar to natural movements. Indeed, combined with the LPP-LDA algorithm presented in Sect. 3, the BCI-MAFO brain switch demonstrated a superior capability in inducing cortical plasticity (Xu et al. 2014). With the same intervention protocol and cortical output quantification methods as in the previous studies, our BCI-MAFO brain switch induced a significant level of cortical plasticity with a reduced number of imaginations, thus a shorter intervention (Fig. 3). The MAFO-BCI intervention resulted in an 87 % increase in cortical output following only 50 motor imaginations in a ~14 min intervention, while in Niazi et al. (2012) a 53 % increase was reported with 75 motor imagery in a ~30-min intervention. The observed plasticity outlasted the intervention, as measured 30 min after the cessation of the BCI-MAFO intervention.

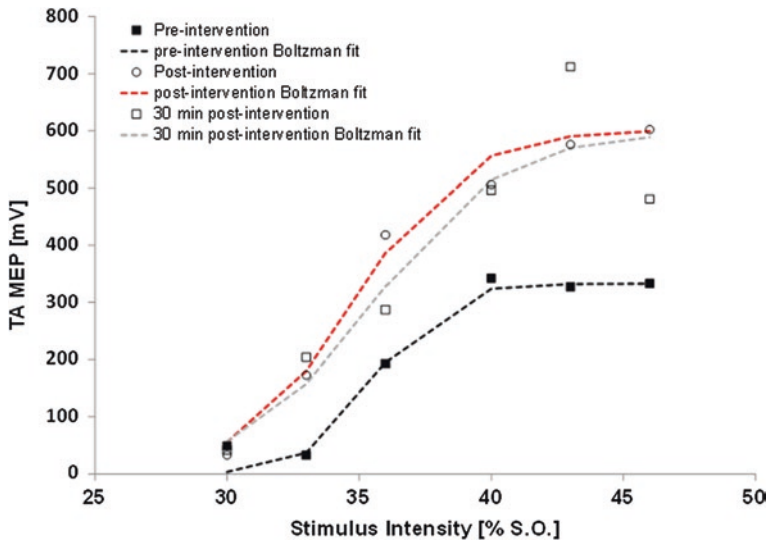

Fig. 3 Tibialis anterior motor evoked potential (*MEP*), recruitment curve, prior to, following and 30 min after the cession of the BCI-MAFO intervention. Each data point represents the average of 10 trials. Data are for n = 1

5 Conclusion Remarks and Long Term Perspectives

We summarized our efforts during the past several years in developing a brain switch that can induce neural plasticity and maximally engage patients during the rehabilitation process. In many aspects, our approach is indeed unique in the literature. In the following, we reiterate and highlight some of these aspects.

5.1 Cortical Versus Peripheral Stimulation

While the non-invasive cortical stimulation protocols such as PAS showed improvements in performance, techniques such as PAS, repetitive TMS or transcranial direct current stimulation (tDCS) have limitations due to current spread to adjacent non-targeted areas. They may thus activate intact areas inappropriately (both temporally and spatially) and thus affect the rehabilitation process. Further, user intention was not incorporated in these protocols. In comparison, our brain switch system relies on voluntary movements, as opposed to cortical stimulation. This choice serves two purposes simultaneously. The user's movement intentions, either imaginary or actual attempts, activate specific brain areas related to the task, and only these areas, resulting in a more efficient dosage. In addition, the entire rehabilitation is controlled, at least to a large extent, by the users, thus providing a very engaging environment for the users. This should help to maximally motivate patients. Metaphorically, the patient is behind the wheel (controlling their own process), and the therapist only needs to point way (defining a protocol).

5.2 Cue-Based Versus Self-paced BCI Paradigm

As discussed in Sect. 3.1, MRCPs are observed in both self-paced (asynchronous) and cue-based (synchronous) paradigms. The former is also called Bereitschaftspotential potential (BP) and the latter is often referred to as contingent negative variation (CNV) or anticipation-related potential. Although the underlying neurophysiological processes of movement under these two conditions are not fully understood, evidences suggested that they are indeed different (Lu et al. 2012). As a result, the morphologies of Bereitschaftspotential and CNV are different (Lu et al. 2012).

We started our development with CNV in the investigation of temporal precision of afferent delivery (Mrachacz-Kersting et al. 2012). However, our ultimate goal is to develop a system that allows maximal control from the patient, and the self-paced paradigm is clearly more suitable for this purpose. More importantly, the neurophysiological processes underlying Bereitschaftspotential are closer to those underlying natural voluntary movements. This is why we mainly focused on the self-paced paradigm (Niazi et al. 2011, 2012; Xu et al. 2014). That said, in

case of users such as stroke patients, who cannot produce any voluntary muscle contractions during movement attempts, a cue-based paradigm must be used in the training phase of the MRCP detector. Only after voluntary muscle activities can be reliably produced are self-paced paradigms possible.

5.3 MRCP Versus Sensory-Motor Rhythm

Sensory-motor rhythm (SMR) is the main signal modality for motor-based BCI. It has been applied widely in various applications, including communications and controlling external devices. In comparison, our choice of signal modality, i.e. MRCP, constitutes a small portion in the literature. Recently, there are several notable efforts towards develop SMR-based neuromodulation systems (Soekadar et al. 2011; Ramos-Murguialday et al. 2013). In Niazi et al. (2012), we demonstrated that MRCP triggered ES induced cortical plasticity within an hour, while previous SMR studies showed similar results with weeks of intervention (Pichiorri et al. 2011). Due to methodological differences, a direction comparison in terms of effective intervention dosage between the two approaches is difficult. That said, we believe that our approach's precise control in the timing when the afferents reach the motor cortex played a critical role in inducing significant cortical plasticity within such a short intervention. In MRCP-based BCI, the detection and triggered afferent flow occurs within a few hundred ms from onset of motor intention, which resulted in effective plasticity induction according to the Hebbian theorem. On the other hand, no special analysis was reported on the detection latency in the above published studies. In addition, MRCP is applicable to naïve subjects (Xu et al. 2014), while SMR usually requires a long training period to get the desirable accuracy (Buch et al. 2008) even before the intervention can start. We acknowledge that, compared with SMR, MRCP-based BCI for neuromodulation is a relatively a new signal modality, and is still an ongoing effort, and more clinical studies on patients are needed for further verifying its effect as well as efficiency.

5.4 Long Term Perspectives

So far, our continued efforts in the development of the brain switch for neuromodulation produced very encouraging results. Currently, we are looking into further development in various aspects of the system. First, we are investigating more advanced EEG signal processing methods that can exploit the morphological differences of MRCP due to different task parameters. In a preliminary study, we demonstrated this potential in a 4-movement class paradigm: fast, slow, high target force and low target force (Jochumsen et al. 2013). It was shown that fast and slow tasks are easier to classify than high-low target force. In the next step, we will investigate

more advanced signal processing and machine learning algorithms, and the possibility of online detecting and classifying movements with different parameters.

Our current efforts have been focused on lower limb muscles, especially the TA muscle. This is because drop-foot is one of the key challenges for the stroke population. However, we will also explore the applicability of the brain switch in upper limb functions. Currently, we are conducting pilot experiments with wrist functions, using the proven protocol for lower limbs. We anticipate challenges both from MRCP detection and afferent elicitation in the case of upper limb motor function.

Because the working principles of our brain switch are the general principles of neurophysiology and motor learning, it might also find application in the rehabilitation of other movement disorders, such as Parkinson's disease. In a very recent study, we demonstrated the possibility of detecting the initiation of gait using only EEG based only on MRCP (Jiang et al. 2014). This can be further developed into an assistive and rehabilitation system for Parkinson's patients who have difficulty initiating gait.

References

Alon G, Levitt AF, McCarthy PA (2007) Functional electrical stimulation enhancement of upper extremity functional recovery during stroke rehabilitation: a pilot study. Neurorehabil Neural Repair 21(3):207–215

Boye AT, Kristiansen UQ, Billinger M, do Nascimento OF, Farina D (2008) Identification of movement-related cortical potentials with optimized spatial filtering and principal component analysis. Biomed Signal Process Control 3(4):300–304

Buch E, Weber C, Cohen LG, Braun C, Dimyan MA, Ard T, Mellinger J, Caria A, Soekadar SR, Fourkas A, Birbaumer N (2008) Think to move: a neuromagnetic brain-computer interface (BCI) system for chronic stroke. Stroke J Cereb Circ 39:910–917

Cramer SC, Mark A, Barquist K, Nhan H, Stegbauer KC, Price R, Bell K, Odderson IR, Esselman P, Maravilla KR (2002) Motor cortex activation is preserved in patients with chronic hemiplegic stroke. Ann Neurol 52(5):607–616

Deecke L, Grözinger B, Kornhuber HH (1976) Voluntary finger movement in man: cerebral potentials and theory. Biol Cybern 23(2):99–119

Gangadhar G, Chavarriaga R, Millán JDR (2009) Fast recognition of anticipation-related potentials. IEEE Trans Biomed Eng 56(4):1257–1260

Garipelli G, Chavarriaga R, Millán J (2013) Single trial analysis of slow cortical potentials: a study on anticipation related potentials. J Neural Eng 10:036014

Gu Y, Dremstrup K, Farina D (2009) Single-trial discrimination of type and speed of wrist movements from EEG recordings. Clin Neurophysiol 120(8):1596–1600

He X, Niyogi P (2003) Locality preserving projections. Adv Neural Inf Process Syst 16:153–160

Hebb DO (1949) The organization of behavior: a neuropsychological theory, vol 44, p 335

Hesse S, Werner C, Pohl M, Rueckriem S, Mehrholz J, Lingnau ML (2005) Computerized arm training improves the motor control of the severely affected arm after stroke a single-blinded randomized trial in two centers. Stroke 36(9):1960–1966

Hummel FC, Cohen LG (2006) Non-invasive brain stimulation: a new strategy to improve neurorehabilitation after stroke? Lancet Neurol 5(8):708–712

Hummel F, Celnik P, Giraux P, Floel A, Wu W-H, Gerloff C, Cohen LG (2005) Effects of non-invasive cortical stimulation on skilled motor function in chronic stroke. Brain 128(Pt 3):490–499

Jiang N, Gizzi L, Mrachacz-Kersting N, Dremstrup K, Farina D (2014) A brain-computer interface for single-trial detection of gait initiation from movement related cortical potentials. Clin Neurophysiol

Jochumsen M, Niazi IK, Mrachacz-Kersting N, Farina D, Dremstrup K (2013) Detection and classification of movement-related cortical potentials associated with task force and speed. J Neural Eng 10(5):056015

Johanshahi M, Hallettm M (eds) (2003) The Bereitschaftspotential: movement-related cortical potentials. Springer, Berlin

Krebs HI, Palazzolo JJ, Dipietro L, Ferraro M, Krol J, Rannekleiv K, Volpe BT, Hogan N (2003) Rehabilitation robotics: performance-based progressive robot-assisted therapy. Auton Robots 15:7–20

Lauer RT, Peckham PH, Kilgore KL, Heetderks WJ (2000) Applications of cortical signals to neuroprosthetic control: a critical review. IEEE Trans Rehabil Eng 8:205–208

Lew E, Chavarriaga R, Silvoni S, Millán JDR (2012) Detection of self-paced reaching movement intention from EEG signals. Front Neuroeng 5:13

Lu M-K, Arai N, Tsai C-H, Ziemann U (2012) Movement related cortical potentials of cued versus self-initiated movements: double dissociated modulation by dorsal premotor cortex versus supplementary motor area rTMS. Hum Brain Mapp 33(4):824–839

Maclean N, Pound P, Wolfe C, Rudd A (2000) Qualitative analysis of stroke patients' motivation for rehabilitation. BMJ 321(7268):1051–1054

Marchal-Crespo L, Reinkensmeyer DJ (2009) Review of control strategies for robotic movement training after neurologic injury. J Neuroeng Rehabil 6(1):20

Mrachacz-Kersting N, Kristensen SR, Niazi IK, Farina D (2012) Precise temporal association between cortical potentials evoked by motor imagination and afference induces cortical plasticity. J Physiol 590(Pt 7):1669–1682

Niazi IK, Jiang N, Tiberghien O, Nielsen JF, Dremstrup K, Farina D (2011) Detection of movement intention from single-trial movement-related cortical potentials. J Neural Eng 8(6):066009

Niazi IK, Mrachacz-Kersting N, Jiang N, Dremstrup K, Farina D (2012) Peripheral electrical stimulation triggered by self-paced detection of motor intention enhances motor evoked potentials. IEEE Trans Neural Rehabil Syst Eng 20(4):595–604

Niazi IK, Jiang N, Jochumsen M, Nielsen JF, Dremstrup K, Farina D (2013) Detection of movement-related cortical potentials based on subject-independent training. Med Biol Eng Comput 51(5):507–512

Paciga JE, Richard PD, Scott RN (1980) Error rate in five-state myoelectric control systems. Med Biol Eng Comput 18:287–290

Pichiorri F, De Vico Fallani F, Cincotti F, Babiloni F, Molinari M, Kleih SC, Neuper C, Kübler A, Mattia D (2011) Sensorimotor rhythm-based brain-computer interface training: the impact on motor cortical responsiveness. J Neural Eng 8:025020

Ramos-Murguialday A, Broetz D, Rea M, Läer L, Yilmaz O, Brasil FL, Liberati G, Curado MR, Garcia-Cossio E, Vyziotis A, Cho W, Agostini M, Soares E, Soekadar S, Caria A, Cohen LG, Birbaumer N (2013) Brain-machine interface in chronic stroke rehabilitation: a controlled study. Ann Neurol 74(1):100–108

Ring H, Rosenthal N (2005) Controlled study of neuroprosthetic functional electrical stimulation in sub-acute post-stroke rehabilitation. J Rehabil Med 37(1):32–36

Salmoni AW, Schmidt RA, Walter CB (1984) Knowledge of results and motor learning: a review and critical reappraisal. Psychol Bull 95(3):355–386

Sanchez RJ, Liu J, Rao S, Shah P, Smith R, Rahman T, Cramer SC, Bobrow JE, Reinkensmeyer DJ (2006) Automating arm movement training following severe stroke: functional exercises with quantitative feedback in a gravity-reduced environment. Neural Syst Rehabil Eng IEEE Trans 14(3):378–389

Schmidt RA (1975) A schema theory of discrete motor skill learning. Psychol Rev 82:225–260

Shea CH, Wulf G (2005) Schema theory: a critical appraisal and reevaluation. J Mot Behav 37(2):85–101

Soekadar SR, Witkowski M, Mellinger JXFR, Ramos A, Birbaumer N, Cohen LG (2011) ERD-based online brain-machine interfaces (BMI) in the context of neurorehabilitation: optimizing BMI learning and performance. IEEE Trans Neural Syst Rehabil Eng 19:542–549

Stefan K, Kunesch E, Cohen LG, Benecke R, Classen J (2000) Induction of plasticity in the human motor cortex by paired associative stimulation. Brain J Neurol 123(Pt 3):572–584

Velliste M, Perel S, Spalding MC, Whitford AS, Schwartz AB (2008) Cortical control of a prosthetic arm for self-feeding. Nature 453:1098–1101

Walter WG (1968) The contingent negative variation: an electro-cortical sign of sensori-motor reflex association in man. Prog Brain Res 22:364–377

Williams JA, Imamura M, Fregni F (2009) Updates on the use of non-invasive brain stimulation in physical and rehabilitation medicine. J Rehabil Med 41(5):305–311

Xu R, Jiang N, Lin C, Mrachacz-Kersting N, Dremstrup K, Farina D (2014) Enhanced low-latency detection of motor intentions from EEG for closed-loop brain-computer interface applications. IEEE Trans Biomed Eng 61(2):288–296

Yan T, Hui-Chan CWY, Li LSW (2005) Functional electrical stimulation improves motor recovery of the lower extremity and walking ability of subjects with first acute stroke: a randomized placebo-controlled trial. Stroke 36(1):80–85

Ear-EEG: Continuous Brain Monitoring

David Looney, Preben Kidmose, Mary J. Morrell and Danilo P. Mandic

Abstract We present a radically new way of recording EEG comfortably and unobtrusively over long time-periods in natural environments. This break-through has been achieved using electrodes embedded on a customized earpiece as typically used in hearing aids (Ear-EEG). We illustrate the potential of Ear-EEG as an enabling technology for a number of uses beyond traditional BCI, which are currently limited by the inconvenience of standard EEG recording methods. We show that Ear-EEG enables both conventional BCI and next-generation applications such as the evaluation of hearing capability and the monitoring of fatigue and drowsiness.

Keywords Ear-EEG · Brain computer interface (BCI) · Non-medical BCI · Wearable EEG · Hearing threshold estimation · Fatigue estimation

1 Introduction

Opportunities for EEG-based BCI are rapidly expanding beyond medical uses, where the primary aim is a high-performance *communication* pathway for paralyzed patients, to numerous non-medical uses wherein the goal is a continuous

D. Looney · M.J. Morrell · D.P. Mandic (✉)
Imperial College London, London, UK
e-mail: d.mandic@imperial.ac.uk

D. Looney
e-mail: david.looney06@imperial.ac.uk

M.J. Morrell
e-mail: m.morrell@imperial.ac.uk

P. Kidmose
Aarhus University, Aarhus, Denmark
e-mail: pki@iha.dk

M.J. Morrell
Sleep Unit, Royal Brompton Hospital, London, UK

C. Guger et al. (eds.), *Brain-Computer Interface Research*, SpringerBriefs in Electrical and Computer Engineering, DOI 10.1007/978-3-319-09979-8_6

Fig. 1 *Left* A 128-channel 'stationary' EEG system (asalab, by ANT neuro) and *right* a wearable system (Emotiv EPOC headset)

measurement of brain state (Blankertz et al. 2010; Allison et al. 2013). Typical applications could include monitoring fatigue or stress to optimize performance at work, or diagnosing sleep disorders (Ward et al. 2012). This all requires overcoming several multi-disciplinary challenges in e.g. machine learning and signal processing, but most crucial of all is the realisation of a robust and portable technology for continuous recording of EEG. The first ambulatory EEG (AEEG) systems appeared in the 1970s (Waterhouse 2003), aided by developments in miniature preamplifiers and continuous analog-recording technology. Digitization of recording platforms, coupled with the integration of computer technology, has provided even greater portability, and current recording systems can operate for 24 h with up to 32 channels. However, conventional recording systems remain bulky and cumbersome, and primarily operate in the laboratory setting (see Fig. 1, left), highlighting the need for so-called wearable systems that allow long-term recordings in natural environments (Casson et al. 2010).

1.1 Towards Wearable EEG

The concept of wearable EEG is of particular value in non-medical BCI applications where a trade-off in performance is acceptable in order to satisfy needs of the user. One of the ways such a trade-off can be achieved is in the design of systems which can accommodate smaller batteries, thereby reducing the system size and increasing its wearability (see Fig. 1, right), either by reducing the number of electrodes or through advanced data compression algorithms which reduce data logging or transmission costs [50 % raw data reduction using lossless compression techniques (Casson et al. 2010)].

Another key advance in wearable EEG is dry electrode technology; standard systems require the use of conductive gel to enable an electrical connection between the electrodes and the scalp, which is time consuming, can cause discomfort and limits the time that the recording system can remain functional as the gel dries out. Dry electrode technologies have been in development since the

late 1960s (Richardson et al. 1968; Bergey et al. 1971) and recent research illustrates that, for motor imagery BCI, dry electrode systems can match the operation of wet electrode systems with only a 30 % reduction in performance (Popescu et al. 2007). More recent work demonstrated that dry electrodes could yield performance comparable to wet electrodes in P300, SSVEP, and motor imagery BCIs (Guger et al. 2012; Edlinger and Guger 2013).

Despite such advances in wearable EEG technology, research has focused on systems which utilise on-scalp electrodes. This methodology is fundamentally limited, as it requires a means for stable attachment (cap and/or adhesive), making the recording process uncomfortable and stigmatising. In order for EEG-based BCI to be adopted more widely and to be robust for use in natural environments, the recording technology must be:

- **discreet**—not clearly visible or stigmatizing;
- **unobtrusive**—comfortable to wear and impeding the user as little as possible; and
- **user-friendly**—users should be able to attach and operate the devices themselves.

2 Ear-EEG

To expand the use of BCI, particularly in non-medical applications where core user requirements (unobtrusive, discreet, user-friendly) are paramount over performance, we have developed the Ear-EEG concept (Looney et al. 2012; Kidmose et al. 2013). The approach, as shown in Fig. 2, is radically new in that EEG is recorded from within the ear canal, which is achieved by embedding electrodes on a customized earpiece (similar to earplugs used in hearing-aid applications). Both in terms of the propagation of the brain electric potentials and the recording technology, Ear-EEG uses the same principles as standard recordings obtained from on-scalp electrodes. In electrophysiological terms, bioelectrical signals from the

Fig. 2 *Left* The right Ear-EEG earplug with electrodes visible and an *arrow* indicating the direction in which it enters the ear canal. *Right* The earplug inserted in the right ear

cortex are attenuated by the cerebrospinal fluid, skull, and skin before reaching the ear canal, as is the case with conventional scalp measurements.

In addition to satisfying the aforementioned BCI user-requirements, crucial advantages of the Ear-EEG platform are as follows (Looney et al. 2012):

- the earpieces are personalized, comfortable to wear, discreet, and are easy to put in place by the users themselves, facilitating everyday use;
- the tight fit between the earpiece and ear canal ensures that the electrodes are held firmly in place, thus overcoming some critical obstacles in scalp EEG—such as motion artifacts and experiment repeatability.

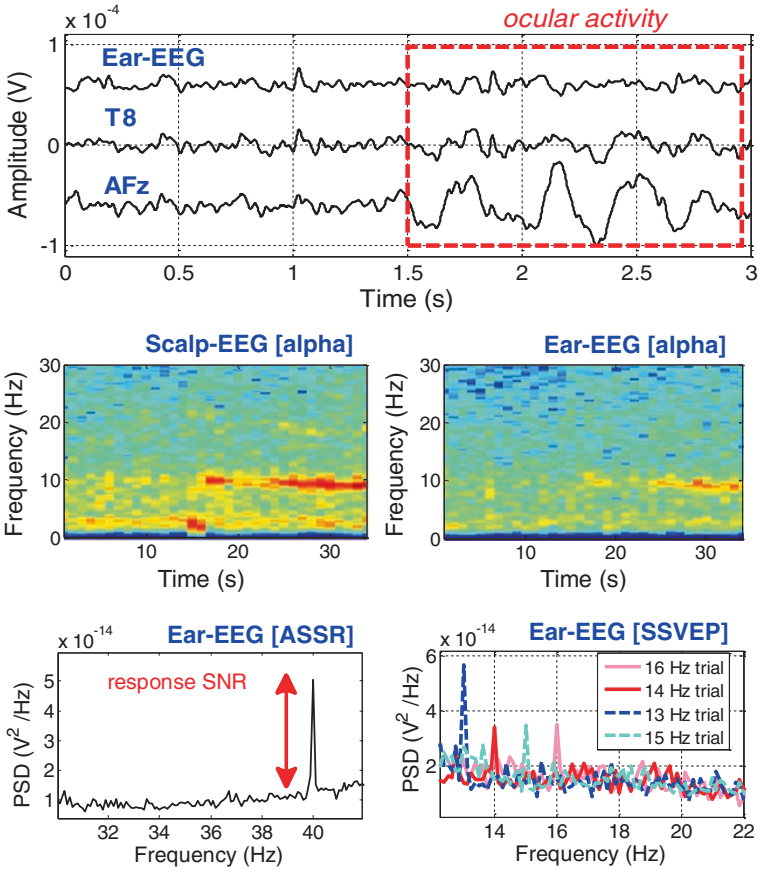

Fig. 3 *Upper* Time waveforms for scalp and Ear-EEG over 3 s with consecutive eye blinking starting at 1.5 s, Ear-EEG exhibits a suppression of ocular artifacts. *Centre* Time-frequency plots as subject closes eyes from 15–35 s, with increased activity visible for scalp (*Centre*, *left*) and Ear-EEG (*Centre*, *right*) in the alpha range (8–12 Hz). *Lower*, *left* The auditory steady state response for Ear EEG (40 Hz stimulus). The SNR (ratio of the response peak to background EEG) matches that of temporal scalp electrodes (Looney et al. 2012; Kidmose et al. 2013). *Lower*, *right* Ear-EEG steady state response to visual (13, 14, 15 and 16 Hz) stimuli, illustrating traditional communication SSVEP-based BCI (Looney et al. 2014)

The current in-ear prototype (see Fig. 2) comprises several electrodes, with areas of approximately 20 mm^2, made of silver (Ag) epoxy glue mounted onto a plastic earpiece [see Kidmose et al. (2013) for more details]. The earpiece does not enter the ear by more than 10 mm and does not approach the part of the ear canal surrounded by bone. Signal acquisition is performed via an external biosignal amplifier (g.tec g.USBamp). When comparing with scalp-EEG, both sets of electrodes are connected to the same amplifier; this facilitates the recording of several independent blocks of inputs, allowing a fair comparison between the two approaches.

The Ear-EEG approach has recently been rigorously validated (Looney et al. 2012; Kidmose et al. 2013) in terms of time, frequency and time-frequency signal characteristics for a range of EEG responses (see Fig. 3); its robustness to common sources of artifacts has also been demonstrated (see Fig. 3, upper). Comparative analysis of the alpha attenuation response (see Fig. 3, centre) shows that Ear-EEG responses match those of neighbouring scalp electrodes located in the temporal region. In general, while signal amplitudes measured from within the ear are weaker, so too is the noise, and for certain auditory responses the signal-to-noise ratios (SNR) are similar (see Fig. 3, lower left). Responses to visual stimuli are also possible (see Fig. 3 lower right). All in all, Ear-EEG offers a unique balance between key user needs and recording quality to enable long-term EEG monitoring in natural environments.

3 Ear-EEG: Towards Continuous Brain Monitoring

The presented results were obtained using a simple prototype system, but with further developments Ear-EEG will be a tiny battery powered brain monitoring device with gel-free electrodes that, like a hearing aid, will perform both the recording and signal processing in situ (see Fig. 4). Moreover, to increase the functionality of Ear-EEG in BCI applications where the user state must be evaluated, other physiological parameters can be inferred by integrating additional non-invasive sensors onto the ear-based platform (Looney et al. 2012):

- cardiovascular function: ear-based PPG devices available (Poh et al. 2010);
- respiratory function: respiratory sounds can be recorded within ear canal (Pressler et al. 2002); and
- movement: accelerometers are sufficiently small size and low-power for in-ear use.

We have already established that Ear-EEG enables conventional communication BCI (see Fig. 3 lower right). Its potential in continuous brain monitoring is illustrated with two case studies via the Ear-EEG prototype shown in Fig. 2. To ensure a fair comparison between scalp and ear-electrodes, EEG was recorded for both approaches using the same amplifier (g.USBamp by g.tec). On-scalp reference and ground electrodes were placed at, respectively, chin and Cz (HTL study) and earlobe and Fpz (fatigue study) based on the 10–20 system. All ear-electrodes were inside the ear, including reference and ground [see Kidmose et al. (2013) for more details].

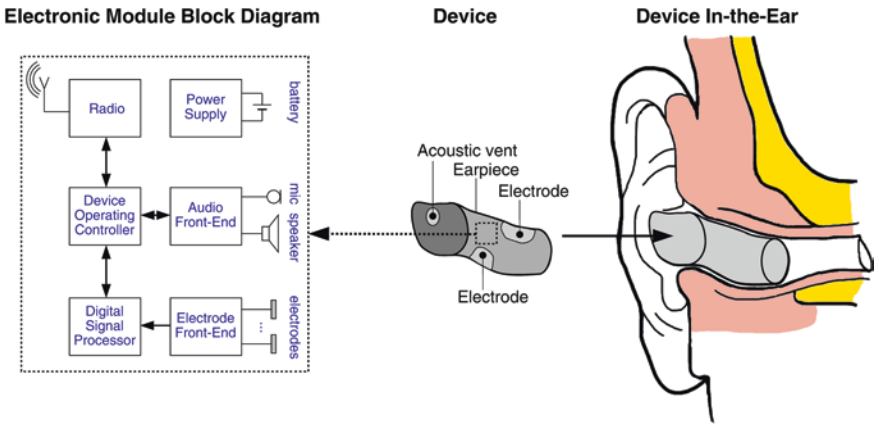

Fig. 4 An illustration of a future Ear-EEG device with an electronic module comprising instrumentation for the electrode signals, analog-to-digital conversion, a signal processing unit, battery, and a radio module

4 Fatigue Estimation

Many occupations and daily activities require prolonged periods of vigilance and concentration. In the transport industry, a lapse in concentration can be fatal. The Royal Society for the Prevention of Accidents estimates that driver fatigue accounts for 20 % of road accidents in Great Britain. Yet there is still no readily available device that can objectively and reliably detect a loss of sustained attention.

We have already shown in Fig. 3 (centre, right) that Ear-EEG can track the evolution of alpha activity with high accuracy. As increases in alpha power are also caused by drowsiness, we next demonstrate how Ear-EEG models drowsiness on a par with a scalp approach: highlighting its role in maintaining vigilance (e.g. phasic alert via a loudspeaker). Our study was based on the Oxford Sleep Resistance Test; a functional test of attention and drowsiness (Davies et al. 1997), wherein a subject was instructed to press a button in response to periodic visual stimuli. A missed stimulus (MS) event denotes the failure of the subject to respond in time to the stimulus and indicates an attention lapse. Fatigue was induced by reducing the sleeping hours of the subject and their vigilance was determined by detecting MS events, or consecutive MS events. Figure 5 shows the button-press errors and the corresponding levels of alpha power in EEG (filtered via a median filter) estimated using scalp- and ear-electrodes.[1] Observe the high similarity in alpha power for ear and scalp EEG and the clear increases in alpha power which accompany error

[1] The in-ear setup used to obtain the results shown in Fig. 5 was electrode ELB referenced to ELH (Kidmose et al. 2013).

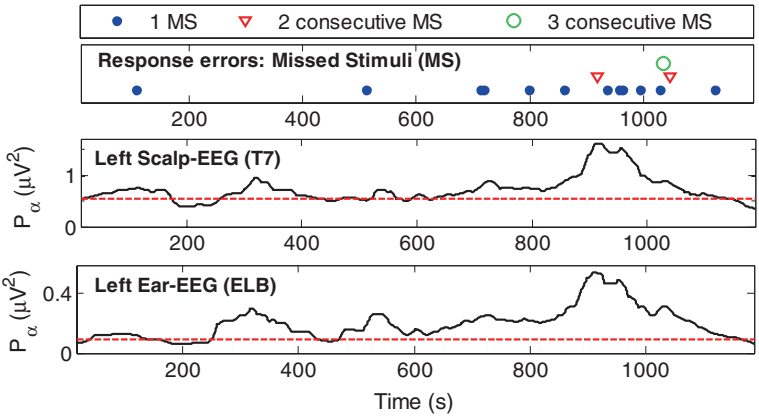

Fig. 5 Fatigue estimation. *Upper* Response errors: missed stimuli (MS) events, single and consecutive. *Centre* and *Lower* Alpha power (*solid black line*) for the scalp and ear electrodes respectively. For reference, the average alpha power of the subject estimated during a non-fatigue state is also given (*dashed red line*)

events and, for instance, how a rise in alpha power at 850 s precedes consecutive MS events. This result is consistent with prior results with on-scalp electrodes (Jung et al. 1997).

5 The Estimation of Hearing Threshold

The World Health Organization (WHO) estimates that hearing impairment affects more than 250 million people worldwide, making it the most common sensory deficit. The operation and fitting of modern hearing devices requires an accurate assessment of hearing capability known as the hearing threshold level (HTL). The HTL is estimated via behavioural hearing tests at an audiology clinic. However, in many cases, hearing loss is progressive or fluctuating (such as in Meniere's disease or auditory neuropathy) and requires continuous assessment.

A well-established HTL-estimation protocol is based on the auditory steady state response (ASSR) (Cone-Wesson et al. 2002). The Ear-EEG platform accommodates a loudspeaker (as in hearing aids) inducing ASSRs as illustrated in Fig. 3 (lower, left), the amplitudes of which reflect the level of the auditory stimuli. This enables a model of HTL and a reference for continuous hearing aid adaptation to match progressive/fluctuating hearing loss without an audiologist. Figure 6 depicts a high level of similarity between the SNR of ASSRs recorded[2] from a scalp

[2] The SNR of the ASSR is defined as the power spectrum ratio of the response peak to the background EEG [see also Fig. 3 (lower, left)].

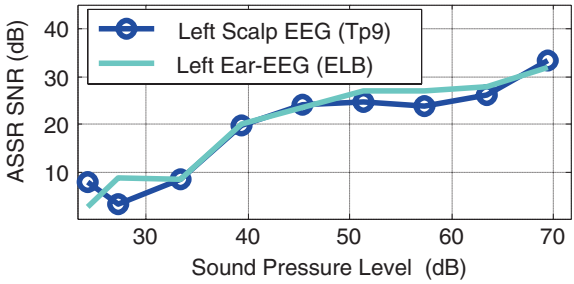

Fig. 6 Hearing threshold estimation. The SNR of the ASSR (an estimate of the response amplitude) for scalp and ear electrodes for ASSR-stimuli of increasing sound pressure levels (SPL)

electrode located in the left temporal region (Tp9) and a left Ear-EEG electrode [ELB referenced to ELH, see Kidmose et al. (2013)] for various ASSR-stimulus sound pressure levels (SPL).

6 Conclusions

Ear-EEG is a breakthrough in wearable sensing that has the potential to be used in non-specialist environments over long time periods—it is robust, discreet and comfortable. We have demonstrated the usefulness of Ear-EEG, with sensing as well as reference and ground electrodes embedded on the earpiece, for current and next-stage BCI—continuous brain monitoring. The estimation of hearing threshold and fatigue have great significance in quality of life and work for a sizeable population. This work illustrates how, when combined with appropriate electronics, the ear-based platform will open up radically new possibilities in future continuous monitoring applications.

References

Allison BZ, Dunne S, Leeb R, Millan J, Nijholt A (2013) Recent and upcoming BCI progress: overview, analysis, and recommendations. In: Towards practical BCIs: bridging the gap from research to real-world applications. Springer, Berlin, pp 1–13

Bergey GE, Squires RD, Sipple WC (1971) Electrocardiogram recording with pasteless electrodes. IEEE Trans Biomed Eng 18(3):206–211

Blankertz B, Tangermann M, Vidaurre C, Fazli S, Sannelli C, Haufe S, Maeder C, Ramsey L, Sturm I, Curio G, Müller KR (2010) The Berlin brain-computer interface: non-medical uses of BCI technology. Front Neurosci 4(198):1–17

Casson AJ, Yates DC, Smith S, Duncan JS, Rodriguez-Villegas E (2010) Wearable electroencephalography. IEEE Eng Med Biol Mag 29(3):44–56

Cone-Wesson B, Dowell RC, Tomlin D, Rance G, Ming WJ (2002) The auditory steady-state response: comparisons with the auditory brainstem response. J Am Acad Audiol 13(4):173–187

Davies RJ, Bennett LS, Stradling JR (1997) What is an arousal and how should it be quantified? Sleep Med Rev 1(2):87–95

Edlinger G, Guger C (2013) Can dry EEG sensors improve the usability of SMR, P300 and SSVEP based BCIs? In: Allison BZ, Dunne S, Leeb R, Millan J, Nijholt A (eds) Toward practical BCIs: bridging the gap from research to real-world applications. Springer, Berlin, pp 303–331

Guger C, Krausz G, Allison BZ, Edlinger G (2012) A comparison of dry and gel-based electrodes for P300 BCIs. Front Neurosci 6(60):1–7

Jung TP, Makeig S, Stensmo M, Sejnowski TJ (1997) Estimating alertness from the EEG power spectrum. IEEE Trans Biomed Eng 44(1):60–69

Kidmose P, Looney D, Ungstrup M, Rank ML, Mandic DP (2013) A study of evoked potentials from ear-EEG. IEEE Trans Biomed Eng 60(10):2824–2830

Looney D, Kidmose P, Park C, Ungstrup M, Rank ML, Rosenkranz K, Mandic DP (2012) The in-the-ear recording concept. IEEE Pulse Mag 3(6):32–42

Looney D, Kidmose P, Mandic DP (2014) Ear-EEG: user-centered, wearable & 24/7 BCI. In: Guger C et al (eds) Brain-computer interface research. Springer, Berlin, pp 41–50

Poh MZ, Swenson NC, Picard RW (2010) Motion-tolerant magnetic earring sensor and wireless earpiece for wearable photoplethysmography. IEEE Trans Inf Technol Biomed 14(3):786–794

Popescu F, Fazli S, Badower Y, Blankertz B, Müller KR (2007) Single trial classification of motor imagination using 6 dry EEG electrodes. PLoS ONE 2(7):e637

Pressler GA, Mansfield JP, Pasterkamp H, Wodicka GR (2002) Detection of respiratory sounds within the ear canal. In: Conference proceedings IEEE engineering in medicine and biology society, pp 1529–1530

Richardson PC, Coombs FK, Adams RM (1968) Some new electrode techniques for long-term physiologic monitoring. Aerosp Med 39(7):745–750

Ward NR, Cowie MR, Rosen SD, Roldao V, De Villa M, McDonagh TA, Simonds A, Morrell MJ (2012) Utility of overnight pulse oximetry and heart rate variability analysis to screen for sleep-disordered breathing in chronic heart failure. Thorax 67(11):1000–1005

Waterhouse E (2003) New horizons in ambulatory electroencephalography. IEEE Eng Med Biol Mag 22(3):74–80

Passive Brain-Computer Interfaces for Robot-Assisted Rehabilitation

Domen Novak, Benjamin Beyeler, Ximena Omlin and Robert Riener

Abstract Stroke patients must exercise intensely with rehabilitation robots to achieve satisfactory rehabilitation outcome, but ensuring appropriate exercise difficulty is a challenging task. Brain-computer interfaces would be suitable for such difficulty adaptations since they capture both conscious and subconscious aspects of workload, but have seen little use in rehabilitation. This chapter reviews previous work on passive brain–computer interfaces and highlights the practical challenges of applying the technology to motor rehabilitation. Preliminary results of a study on workload estimation in a rehabilitation robot with healthy subjects are then presented. Adaptive stepwise regression is used to estimate different types of workload from electroencephalography signals recorded at different sites. Results show that electroencephalography can achieve more accurate workload estimation than autonomic nervous system responses and that adaptive estimation methods can further improve accuracy. However, the number of electrode sites needs to be reduced and issues such as motion artefacts must be resolved before passive brain-computer interfaces can be used in motor rehabilitation.

Keywords Machine learning · Passive brain-computer interface · Psychophysiology · Rehabilitation · Robotics

1 Introduction

1.1 Robot-Assisted Rehabilitation

Stroke affects about 1 million people in Europe each year (Brainin et al. 2000; Thorvaldsen et al. 1995). Though a stroke often causes severe impairment, it is possible to regain lost motor functions and improve quality of life through

D. Novak (✉) · B. Beyeler · X. Omlin · R. Riener
Sensory-Motor Systems Lab, ETH Zurich, Zurich, Switzerland
e-mail: domen.novak@hest.ethz.ch

C. Guger et al. (eds.), *Brain-Computer Interface Research*, SpringerBriefs in Electrical and Computer Engineering, DOI 10.1007/978-3-319-09979-8_7

appropriate therapy. Successful therapy is characterized by intensive, repetitive exercises of long duration (Bütefisch et al. 1995; Kwakkel et al. 2002; Nelles 2004). With respect to these criteria, the normal manually-assisted therapy has several limitations: it is labour-intensive, time-consuming, and expensive. By contrast, robot-assisted rehabilitation can reduce the number of therapist hours and increase the duration and number of training sessions. Furthermore, the robot provides multimodal feedback and supports the assessment of impairment score and functional ability (Guidali et al. 2011).

Despite its advantages, robotic guidance alone is not sufficient to guarantee positive rehabilitation outcome. The patient's motivation is also an important determinant of the outcome (Maclean 2002). Motivation has been highlighted as an additional advantage of robot-assisted rehabilitation, which can be enhanced with virtual environments that are viewed as more fun, engaging and motivating than conventional therapy (Colombo et al. 2007; Mihelj et al. 2012).

1.2 Exercise Difficulty Adaptation

One way to improve patient motivation is to ensure an appropriate exercise difficulty level: the patient should be challenged in a moderate but engaging way without causing undue boredom or stress. Difficulty can be adapted based on the patient's exercise performance (Cameirão et al. 2010; Zimmerli et al. 2012), but this ignores subjective factors such as perceived workload. For example, the patient may be successfully completing the task but only with excessive effort that quickly leads to frustration. An unobtrusive alternative for dynamic difficulty adaptation in motor rehabilitation was proposed in the form of psychophysiological measurements.

Psychophysiological measurements are defined as measurements of the body's responses to psychological factors such as workload, engagement and stress. The first such measurements used in motor rehabilitation were autonomic nervous system (ANS) responses, as the sensors are relatively cheap and can be quickly attached to the patient. Closed-loop rehabilitation difficulty adaptation systems based on ANS responses were first presented in 2011 for both upper limb (Novak et al. 2011a) and lower limb (Koenig et al. 2011) rehabilitation. Since then, other authors have proposed alternative solutions based on ANS responses (Badesa et al. 2012; Guerrero et al. 2013; Shirzad and Van der Loos 2013), but results have been mixed. Since ANS responses are heavily affected by physical workload, which is an integral part of motor rehabilitation, it can be difficult to extract psychological aspects (Novak et al. 2011b). Examples of existing rehabilitation robots that have been used with ANS-based difficulty adaptation are shown in Fig. 1.

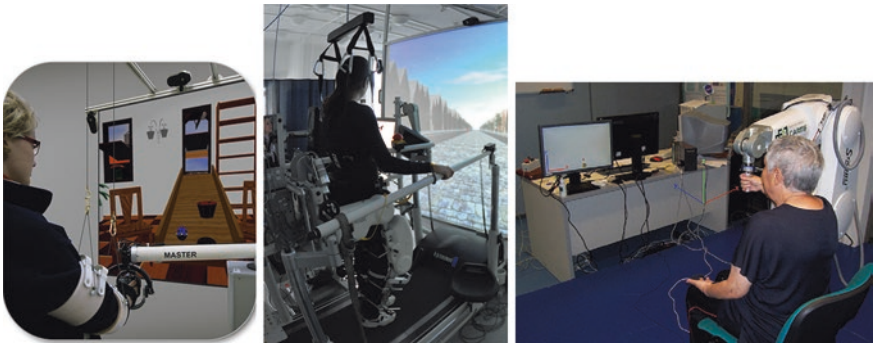

Fig. 1 Existing rehabilitation systems that have been tested with closed-loop difficulty adaptation based on autonomic nervous system responses. *Left to right* HapticMaster (Novak et al. 2010), Lokomat (Koenig et al. 2011), PhysioBot (Guerrero et al. 2013)

1.3 Passive Brain-Computer Interfaces

A promising alternative or complement to ANS responses are passive brain-computer interfaces (BCIs). Unlike classic 'active' BCIs, which measure intentionally generated brain activity (e.g. due to motor imagery), passive BCIs measure brain activity that occurs in response to, for example, stress or workload without conscious user effort (Zander and Kothe 2011). They have been used to classify workload, emotions and attention in many applications, including computer games (Chanel et al. 2011; Girouard et al. 2009), simulated flight (Wilson and Russell 2007) and driving (Zhao et al. 2011). Passive BCIs may represent a more promising and practical application of BCI than active ones since the required temporal resolution is much lower (Van Erp et al. 2012).

Recently, passive BCIs were used in physical human-robot interaction to detect mental workload and adapt robot behaviour accordingly (George et al. 2012). As brain activity should be less vulnerable to physical workload, passive BCI could offer an alternative to ANS responses in motor rehabilitation applications. It may even be possible to combine central and autonomic nervous system responses to obtain the optimal amount of information for exercise difficulty adaptation. Such a combination of passive BCI and ANS responses has already been tested in, for example, computer games (Chanel et al. 2011).

Passive BCIs, however, have their own weaknesses. They can require a significant time to apply, making them problematic in rehabilitation where the goal is to maximize the amount and intensity of exercise in a limited time period. They are vulnerable to motion artefacts, both due to sensor movement and due to electrical activity caused by muscle activation. Even without motion artefacts, inferring useful information from brain signals is not trivial and generally requires advanced machine learning techniques.

In the following sections, we shall discuss the problems of introducing passive BCIs to motor rehabilitation, suggest potential solutions, and finally show our own implementation of a passive BCI in the ARMin rehabilitation robot.

2 Hardware Selection and Setup

The crucial requirements for BCI hardware in motor rehabilitation are non-invasiveness and ease of use. A typical rehabilitation session lasts approximately one hour and should be spent exercising as intensively as possible. To be effective, the BCI should therefore require as little additional setup time as possible. Furthermore, since the added benefit of BCI is simply a more appropriate exercise difficulty (rather than, for example, allowing exercise to be performed at all), patients and therapists are likely unwilling to deal with great inconveniences in applying the equipment. Given these requirements, two promising technologies are electroencephalography (EEG) and functional near infrared spectroscopy (fNIRS), as they are both noninvasive and portable.

2.1 EEG Hardware

EEG is by far the most studied physiological signal for noninvasive BCIs. It measures the brain's electrical activity using electrodes placed on the scalp. Preparation time, however, can be up to 30 min when using a cap with ~15 gelled signal electrodes, a reference, ground, and electrooculography (EOG) electrodes. This is not suitable for motor rehabilitation, so we should aim to minimize the number of electrode sites while making each individual electrode quick and easy to apply.

2.1.1 Electrode Locations

There is no clear agreement on where to place electrodes for passive BCIs, possibly since each passive BCI measures a different aspect of the user's psychological state and thus requires a different electrode placement. Table 1 shows example electrode placements from various passive EEG studies.

We can see from the table that frontal sites are strongly represented, which is convenient as these sites are generally not covered by hair and allow easier electrode application. They are, however, more susceptible to EOG interference. Other popular sites are central (C3, C4, Cz) and parietal (P3, P4, Pz). However, authors often do not make a distinction between workload types, which may range from visual processing to short-term memory recall to decision making under temporal pressure.

Table 1 Signal electrode locations in different passive EEG studies, as well as the psychological variable(s) of interest

Study	Electrode locations	Psychological variable
Missonnier et al. (2003)	F3, F4, Fz, C3, C4, Cz, P3, P4, Pz	Working memory load
Wilson and Russell (2003)	F7, Fz, Pz, T4, T5, Oz	Mental workload
Berka et al. (2004)	Fz, Cz, POz	Vigilance
Ryu and Myung (2005)	Fz, Pz, O1, O2	Mental workload
Fairclough and Venables (2006)	Cz, P3, P4, Pz,	Engagement, distress, worry
Pesonen et al. (2006)	Fp1, Fp2, F3, F4, F7, F8, Fz, C3, C4, Cz, P3, P4, Pz, T3, T4, T5, T6, O1, O2	Auditory memory load
Berka et al. (2007)	F3, F4, Fz, C3, C4, Cz, POz	Engagement, workload
Wilson and Russell (2007)	F7, Fz, Pz, T5, O2	Mental workload
Venables and Fairclough (2009)	F3, F4, C3, C4, P3, P4	Mood, workload
Antonenko et al. (2010)	5 frontal, 4 temporal, 3 central, 2 parietal, 2 occipital	Cognitive load
Heger et al. (2010)	Fp1, Fp2, F3, F4, F7, F8, C3, C4, Cz, P3, P4, Pz, T3, T4, O1, O2	Workload
Wu et al. (2010)	Fp1, Fp2, Fz, Cz, Pz, O1, O2	Arousal
Knoll et al. (2011)	AF3, AF4, F3, F4, F7, F8, FC5, FC6, T7, P7, P8, T8, O1, O2	Cognitive workload
Brouwer et al. (2012)	F3, F4, Fz, FCz, C3, C4, Pz	Workload
Coffey et al. (2012)	F3, F4, Fz, FCz, C3, C4, Cz, Pz	Workload
George et al. (2012)	Fp1, Fp2, F3, F4, F7, F8, C3, C4, Cz, T8, P3, P4, Pz, T7, O1, O2	Mental workload

Robot-assisted rehabilitation involves many brain activities, including motion planning and visual processing. In order to identify the optimal electrode placement, we recommend an initial study of frontal, central and parietal sites with actual rehabilitation tasks. If possible, we should aim to minimize the setup to frontal sites. Though some studies place ground and reference electrodes in spots such as Cz or FCz, we recommend placing them in convenient spots such as the forehead or the ears/mastoids (Berka et al. 2004; Coffey et al. 2012; Ryu and Myung 2005; Wilson and Russell 2007).

2.1.2 Electrode Types

The most convenient device for measuring EEG in rehabilitation would be a low-cost device with integrated electrodes such as the Emotiv EPOC headset (Emotiv Systems, Australia). The Emotiv has previously been used for workload measurement and has successfully shown correlations between frontal signals and task difficulty (Knoll et al. 2011). However, in an evaluation with active BCI, it achieved significantly worse results than a medical EEG device (Mayaud et al. 2013).

As an alternative to low-cost systems, we can consider dry (ungelled) or even noncontact electrode systems, as patients are unlikely to accept gel on the scalp simply for automated difficulty adaptation. Such electrodes have already been shown to be comparable to classic electrodes in active BCI (Chi et al. 2012; Guger et al. 2012).

2.2 fNIRS Hardware

fNIRS has begun gaining ground in passive BCI due to the relatively quick and simple setup (Solovey and Girouard 2009). It provides a measure of blood oxygen concentration indicative of brain activity using one or more infrared light source-detector pairs that probe tissue up to depths of 1–3 cm. Since the light from the source is absorbed by hemoglobin and deoxygenated hemoglobin in the blood, changes in light intensity at the detector can be related to changes in relative concentrations of hemoglobin. The main weakness of fNIRS is that, due to the use of light, ambient lighting or dark hair can easily distort measured signals (Coyle et al. 2004).

2.2.1 Probe Locations

There are many possible placements for fNIRS probes, with the most common being the motor cortex (Sitaram et al. 2007) and the frontal/prefrontal cortex (Ayaz et al. 2012; Ong et al. 2013). The prefrontal cortex has been recommended for passive brain-computer interfaces since it deals with high-level processing such as working memory and problem solving (Solovey and Girouard 2009). fNIRS measurements from the prefrontal cortex are taken by placing the probe on the forehead, which is not covered by hair. This is both user-friendly and prevents problems with dark hair affecting measurements.

Since almost all passive BCI research with fNIRS has been performed with forehead measurements, this is also the best current candidate for motor rehabilitation, though tests with different locations on the forehead should be performed to find the area with the best response to rehabilitation tasks.

2.2.2 Probe Types

The basic fNIRS technology of multiple source-detector pairs is common to all existing probes. The main requirements for practical use are to block out ambient light, which distorts the signal, and to tightly fix the probe to the head. Previous studies have used probes embedded in black hats to block ambient light, and suggestions have been made that probes for applied studies should be embedded in hats or helmets (Solovey and Girouard 2009). At the moment, this appears more

user-friendly for rehabilitation than dimming the light in the room, and is therefore a prime concern in hardware selection.

Another potentially important feature of the probe is the short separation channel. This is an additional source-detector pair whose light does not penetrate deeply enough to measure brain activity, but does measure the same physiological noise as the other channels (Gagnon et al. 2012). It is frequently used to reduce noise, and is practical since it can be built into the same probe as the other channels and therefore does not increase the setup time.

2.3 Hybrid BCIs

It should be reiterated that there is no serious barrier to combining multiple sensor types, creating so-called hybrid BCIs. Hybrid passive BCIs such as EEG combined with ANS responses (Chanel et al. 2011) or even EEG combined with fNIRS (Coffey et al. 2012) have already achieved good results. The only obstacles are increased setup time and possible physical overlapping between sensors (e.g. fNIRS and frontal EEG). However, both can be mitigated with appropriate equipment.

3 Signal Processing

3.1 Artefact Removal

Motor rehabilitation is a noisy environment for passive brain-computer interfaces, and numerous artefacts must be considered. The most problematic ones are motion artefacts due to movement of the head or entire body. While commonly minimized in BCI, motion is an integral part of motor rehabilitation.

Motion affects measured signals either directly (e.g. by causing electrode/probe movement) or indirectly via human physiology. For EEG, the main indirect problem is that the electrodes also measure head and neck muscle activity as well as eye movement and blinking. Neck muscle artefacts are prominent toward the back of the head while eye artifacts are prominent toward the forehead. They cannot be removed by simple bandpass filtering, as frequency bands of the EEG, electromyogram (EMG) and EOG partially overlap (Vaughan et al. 1996). For fNIRS, motion can increase blood flow through the scalp, and head orientation can affect the signal due to gravity's effect on blood (Matthews et al. 2008). fNIRS is notably less vulnerable to eye artefacts than EEG.

Motion artefacts can be reduced using secondary sensors. For instance, eye artefacts can be removed from the EEG by using the EOG as a reference for noise removal algorithms (Croft and Barry 2000). Larger artefacts such as head movement can be detected using accelerometers and reduced in both EEG and fNIRS using

e.g. adaptive finite impulse filtering (Matthews et al. 2008). An alternative approach is to remove artefacts without a secondary sensor using computational methods such as principal or independent component analysis. This has been successfully performed to remove motion artefacts from EEG during walking (Gwin et al. 2010).

Besides motion artefacts, additional noise is caused by cardiorespiratory activity, which is visible in both the EEG (due to e.g. ECG or electrode movement as a result of respiration) and the fNIRS (affecting the blood flow). This noise is commonly removed by measuring cardiorespiratory activity using additional sensors and including this information as an input to adaptive filtering. Most notably, physiological noise could be measured in fNIRS using the short separation channel (Sect. 2.2.2), which may be a simple and convenient solution.

We should, however, consider to what degree physiological noise should be removed at all. Changes in heart rate or respiration also reflect psychological changes, so brain signals containing such physiological 'noise' may actually allow more accurate inference of the subject's psychological state. Similarly, EOG artefacts seen in the EEG reflect eye movement and may provide useful information about visual processing. We believe that physiological noise removal should depend on the research goal. If the goal is to show that brain activity alone can be used to infer workload in rehabilitation, physiological noise should be minimized. However, if the goal is to obtain the most accurate psychophysiological inference, a passive BCI should be evaluated both with and without physiological noise.

3.2 Feature Extraction

In the context of psychophysiology and passive BCI, feature extraction refers to extracting a number of psychologically relevant features from raw physiological signals. They are generally calculated over a certain time period (window) and then fed to the psychophysiological inference algorithms. The length of this window depends on the measured signal and application, with values between 30 s and 5 min being common in psychophysiology (Novak et al. 2012). While EEG responds faster to stimuli than ANS signals and theoretically allows shorter windows, this is probably unnecessary. Feature extraction in closed-loop psychophysiological systems is generally done every time an action is taken by the system. As we should not adapt the rehabilitation task difficulty more than once a minute (or even less frequently), shorter windows are not needed.

3.2.1 EEG Feature Extraction

With regard to signal analysis, passive BCIs differ significantly from active ones. While active BCIs tend to focus on event-related potentials, passive BCIs generally measure brain activity over the entire time period of interest. This activity is examined in multiple frequency bands: delta (0.5–4 Hz), theta (4–8 Hz), alpha (8–13 Hz), beta (13–30 Hz) and gamma (30–70 Hz). The overwhelmingly popular

EEG features for passive BCIs are total power in a particular band (e.g. Antonenko et al. 2010; Wilson and Russell 2007; Wu et al. 2010) and total power in a particular band divided by total power in all bands (e.g. Fairclough and Venables 2006). These features are commonly normalized with respect to a baseline (rest) condition in order to reduce intra- and intersubject variability (e.g. Antonenko et al. 2010).

Not all frequency bands are equally contaminated by motion artefacts. Particularly, frequencies above 20 Hz are significantly affected by EMG (Whitham et al. 2007), reducing their usefulness unless artefact removal methods are applied. This may be problematic since beta and gamma bands are connected to aspects of attention and mental workload (e.g. Herrmann et al. 2004). Though alpha and theta bands still contain a large amount of information about mental workload tasks (Klimesch 1999), this problem should be kept in mind.

3.2.2 fNIRS Feature Extraction

The first step in fNIRS feature extraction is to calculate oxygenated and deoxygenated hemoglobin concentrations using the modified Beer-Lambert law (Villringer and Chance 1997). The commonly extracted features are then simply the mean values of the two concentrations over the time period of interest (Ayaz et al. 2012; Girouard et al. 2009; Ong et al. 2013). As with EEG, the concentrations are often normalized by expressing them as a percentage of change from the baseline level.

4 Psychophysiological Inference

Once a set of potentially relevant features has been extracted from the EEG and/or fNIRS signals, the set should be assigned a label. For motor rehabilitation, this label can be categorical such as "task is too easy/too hard" (Novak et al. 2011a) or "workload is low/high" (George et al. 2012; Koenig et al. 2011). Alternatively, the label can be a continuous number that represents perceived task difficulty or workload (Badesa et al. 2012; Guerrero et al. 2013). The label type affects the actions that can be taken by the robot. Categorical labels are used to trigger discrete actions such as "change difficulty by one level" or "activate/deactivate robotic assistance" while continuous labels can be used for smoother, continuous control such as changing the gain of the robotic assistance.

4.1 Categorical Inference

Categorical labels in psychophysiology and passive BCI are inferred almost exclusively with classifiers based on supervised machine learning. A popular example of such a classifier is linear discriminant analysis (LDA), which has been used in ANS- and EEG-based motor rehabilitation systems despite its simplicity (George et al. 2012; Koenig et al. 2011; Novak et al. 2011a). Other classifiers that have been

previously used for psychophysiological inference include support vector machines, nearest-neighbour classifiers, Bayesian networks and neural networks (Novak et al. 2012). Most of these classifiers are also used in active BCIs (Lotte et al. 2007), with one significant difference. Active BCIs frequently employ hidden Markov models, which take temporal dynamics into account (Lotte et al. 2007; Zimmermann et al. 2013). These are uncommon in passive BCIs and ANS-based psychophysiological systems where dynamics within a time period are not very important.

The best classifier to use in a particular application is uncertain, and our recent review of psychophysiological measures (Novak et al. 2012) did not find a systematic advantage of any specific classifier, though we do not recommend nearest-neighbour classifiers since they are not robust to irrelevant features and features with different numerical ranges. Furthermore, dimensionality reduction methods such as principal component analysis or sequential feature selection are recommended to remove irrelevant input features (Novak et al. 2012). Dimensionality reduction is more relevant for EEG-based passive BCIs, which have a large number of input features compared to fNIRS-based BCIs.

4.2 Continuous Inference

Continuous inference is less common than categorical inference in both ANS-based psychophysiological systems (Novak et al. 2012) and in BCIs (Lotte et al. 2007), but has gained attention in motor rehabilitation since it allows smoother tuning of different parameters (Badesa et al. 2012; Guerrero et al. 2013; Mihelj et al. 2009). While continuous inference can also be based on machine learning techniques such as regression and neural networks (Novak et al. 2012), motor rehabilitation studies have preferred to use fuzzy logic (Badesa et al. 2012; Guerrero et al. 2013; Mihelj et al. 2009).

Fuzzy logic defines the relationship between physiological input features and the output label using if-then rules. Unlike classical logic, fuzzy rules and definitions have degrees of truth. For instance, while a fuzzy rule may state "if blood oxygenation is high, workload is high", blood oxygenation can be 70 % 'high' and 30 % 'low' at a certain time. The if-then rules are manually defined by experts and are appropriate for noisy systems where a precise mathematical model does not exist, but experts can identify general rules underlying the system—which is the case in passive BCIs. Furthermore, fuzzy logic does not require training data, which can potentially simplify the design of the system.

5 Preliminary Implementation

This section describes our own preliminary experiment with a passive BCI in the ARMin arm rehabilitation robot. To illustrate the principle, we present first results; a more detailed analysis is planned for the future as a journal publication.

5.1 Goal

Passive BCIs have potential in rehabilitation robotics, but several application-specific issues remain. Outstanding questions include:

1. Passive BCIs commonly involve regular rest periods to allow physiological activity to return to a baseline state. These must be avoided at all costs in motor rehabilitation, as they decrease the amount of exercise performed by the patient. However, can passive BCIs still provide useful information without them?
2. Given the high levels of physical activity in motor rehabilitation, how heavily contaminated by motion artefacts are the measured signals?
3. What measurement locations are needed to obtain useful information? Specifically, are frontal locations (user-friendly, dominant in fNIRS) sufficient?
4. What psychological quantities do we wish to infer from the BCI data? Previous work has focused on workload (George et al. 2012; Koenig et al. 2011) or arousal/valence (Badesa et al. 2012; Guerrero et al. 2013; Mihelj et al. 2009). However, workload has many aspects [e.g. physical, temporal, mental (Hart and Staveland 1988)] that may be correlated with each other in a rehabilitation task. Furthermore, perceived workload may not always positively correlate with the effort the user puts into the task; for instance, users may become frustrated and give up as workload becomes too high.
5. What level of accuracy can the psychophysiological inference achieve? In one of our previous studies, for instance, using physiological measurements for closed-loop adaptation of a rehabilitation task was less accurate than simply using the task performance, but combining both sources of information gave the best accuracy (Novak et al. 2011a). Can a passive BCI outperform or at least complement task performance information and ANS responses?

Though we naturally cannot satisfactorily answer all questions at once, we designed a first study to obtain exploratory information.

5.2 Study Protocol

Ten healthy subjects (8 males, 2 females, 27.6 $\pm$ 3.7 years of age) were asked to perform a "whack a mole" game with the ARMin III rehabilitation robot. The ARMin III (Nef et al. 2009) has an exoskeletal structure with seven actuated degrees of freedom, including a hand module. The subject's dominant arm is connected to the robot with cuffs on the upper arm and forearm. The hand is fixed to the hand module with elastic straps. The dimensions of the device are adjustable to the individual subject, and gravity and friction compensation allow the arm to be moved in all directions without resistance. A photo of the subject performing the task is shown in Fig. 2.

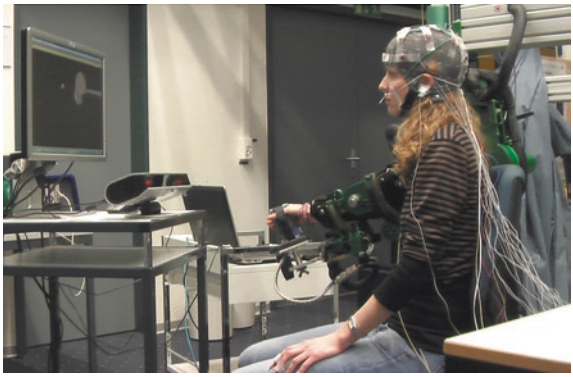

Fig. 2 A subject performing the task with the ARMin robot while monitored with sensors

Fig. 3 A screenshot of the "whack a mole" task

The principle of the game is to hit monsters with a hammer before they disappear (Fig. 3). The hammer is moved around the screen with the end-effector of the robot, and a 'hitting' movement is performed by turning the forearm. Monsters appear at one of nine locations (3 × 3 layout) and disappear if not hit within a certain amount of time. Each monster has a mathematical equation attached to it, and the subject should only hit a monster if the equation is correct. 50 % of all equations are correct.

The task has two adjustable parameters: the equation difficulty and the frequency with which monsters are spawned. A new monster can spawn every 1.5, 2.5, 4 or 6 s. An individual monster remains on the screen 2.5 times the spawn interval, so there are at most three monsters on the screen at any time. The equation difficulty has five possible levels, from very easy (e.g. $2 + 5 = 7$) to very difficult (e.g. $45 + 33 + 63 = 141$). With 5 equation difficulty levels and 4 temporal difficulty levels, there are 20 possible conditions in total.

The study protocol began with a practice round where the subject played until he/she was comfortable and understood the task. The questionnaire was demonstrated, and the sensors were applied and calibrated. There was then a 60-s baseline

period during which subjects were asked to relax, not move, keep their eyes open, and remain silent. After the baseline period, subjects performed 19 60-s task periods, with each task period having a different combination of equation difficulty and monster spawn difficulty. Of the 20 possible combinations, only the easiest one (level 1 equations, one monster per 6 s) was omitted as it was found to be extremely boring for the subjects. The 19 combinations were presented in a random order that was generated differently for each subject.

Physiological measurements were taken continuously during the study. Each task period was followed by the questionnaire (Sect. 5.3) before the next task period began. Subjects were told to answer it for the preceding task period, not the entire task to then. After the 19th task period and questionnaire, the experiment was concluded.

5.3 Measurements

5.3.1 Questionnaire

The NASA-TLX (Hart and Staveland 1988) was used to obtain reference self-report values of workload during the task. It has been extensively used in human workload studies, including previous closed-loop psychophysiological work (Wilson and Russell 2007). It consists of six scales: mental workload, temporal workload, physical workload, performance, effort and frustration. Subjects rate each on a visual scale from 'very low' to 'very high'. A computerized version was presented, with the subjects moving a slider along the visual scale by pronating/supinating their forearm in the robot. The selections were saved as numerical values from 0 to 100.

The task difficulty levels should affect the different NASA-TLX scales. Equation difficulty should affect mental and temporal workload, as subjects have to perform more complex mental arithmetic in the same amount of time. The monster spawn difficulty should affect both temporal and physical workload, as subjects must perform calculations faster and move their arm more often. Effort should increase with all workload types, though only up to a point; excessive workload may lead to a decrease in effort as subjects give up. Similarly, performance should decrease and frustration should increase with increasing workload.

5.3.2 Physiology

The primary measurement was EEG, which was measured with the g.GAMMAcap (g.tec Medical Engineering GmbH, Austria) and g.Butterfly active electrodes. Electrodes were placed at 14 locations of the International 10–20 system: Fz, F3, F4, F8, F7, Cz, C3, C4, Pz, P4, POz, O1 and O2. All signals were referenced to an electrode at position FPz and grounded with an electrode on the left earlobe.

Additionally, the EOG was recorded with two electrodes (Grass Technologies, USA): one to the upper right of the right eye and one to the lower left of the left eye. EOG was used only to correct ocular artefacts in the EEG. Both EEG and EOG were sampled at 600 Hz using a g.USBamp signal amplifier (g.tec).

In addition to EEG, four ANS responses were measured: the electrocardiogram (ECG), skin conductance, respiration and skin temperature. ECG was measured with three surface electrodes placed on the trunk. Respiration was measured using a thermistor flow sensor beneath the nose. Skin conductance was measured using a g.GSR sensor (g.tec). Electrodes were placed on the medial phalanges of the second and third fingers of the nondominant hand. Peripheral skin temperature was measured using a g.TEMP sensor (g.tec) attached to the distal phalanx of the fifth finger of the nondominant hand. All ANS signals were sampled at 600 Hz using a second g.USBamp amplifier.

Finally, eye tracking was performed using the SMI RED 250 (SensoMotoric Instruments, Germany), a remote eye tracker placed underneath and slightly in front of the screen. Though it is more commonly mounted directly below the screen, it was moved forward to ensure that the distance between the eyes and tracker is within the optimal operating conditions. The sampling frequency was 250 Hz.

5.4 Feature Extraction

Several features were extracted from the raw physiological signals for the baseline period and the 19 task periods. Each feature was calculated over the entire 60-s period.

5.4.1 EEG

The EEG was first bandpass-filtered between 1 and 30 Hz. Eye movement and blink artifacts were then removed using a recursive least-squares filter with EOG as the noise reference. The power spectral density of each EEG channel was then calculated using Welch's method. For each EEG channel, we calculated four features used in previous studies:

- alpha power divided by total power,
- theta power divided by total power,
- alpha power divided by theta power,
- 1/(alpha power + theta power).

These features can optionally be individualized for each subject by using the peak frequency method to set the borders of the alpha band (Goljahani et al. 2012). Additional features based on the beta and gamma band were considered but later omitted due to concerns over data quality (see Sect. 5.6.1).

5.4.2 ANS Responses

From the ECG, intervals between two normal heartbeats (NN intervals) were extracted. Then, *mean heart rate* as well as three standard measures of heart rate variability (HRV) were calculated (Task Force, 1996): the *standard deviation of NN intervals* (*SDNN*), the *square root of the mean squared differences of successive NN intervals* (*RMSSD*), and the *number of interval differences of successive NN intervals greater than 50 ms divided by the total number of NN intervals* (*pNN50*).

From the skin conductance signal, we detected all skin conductance responses (SCRs). A SCR is a transient increase in skin conductance whose amplitude exceeds 0.05 microsiemens and whose peak occurs less than 5 s after the beginning of the increase. *SCR frequency* and *mean SCR amplitude* were calculated.

From the respiration signal, we calculated *mean respiratory rate* and *standard deviation of respiratory rate*.

From the temperature signal, we calculated the *final skin temperature* as the mean temperature during the last 5 s of each period. Additionally, the *mean derivative of skin temperature* was calculated over the entire period.

5.4.3 Eye Tracking

Eye tracker feature extraction was done by the manufacturer's provided software, BeGaze 3.1, which first segments the recorded signals into blinks, saccades (rapid gaze shifts from point to point) and fixations. It then outputs the *number of blinks*, *number of saccades*, and *number of fixations* as well as the *mean blink duration*, *mean saccade duration*, and *mean fixation duration*.

For saccades, BeGaze outputs the *mean saccade velocity*, saccade velocity variability and *mean saccade amplitude*. For fixations, it outputs the *mean pupil diameter*, the *standard deviation of pupil diameter* and *mean gaze dispersion* (the amplitude of small movements performed by the eyes during a fixation). Finally, it outputs the *ratio of total fixation time and total saccade time*.

All of these features can optionally be individualized for each subject by setting different thresholds for fixations, saccades and blinks in BeGaze 3.1.

5.5 Psychophysiological Inference

Though we have previously worked extensively with classification algorithms (Koenig et al. 2011; Novak et al. 2011a), we chose to assign continuous values to each task period as suggested by other authors in rehabilitation robotics (Badesa et al. 2012; Guerrero et al. 2013). This was partially also why we selected the NASA-TLX as a reference—it measures each workload scale as a value between 0 and 100.

Stepwise linear regression was used to predict NASA-TLX reported values from the extracted physiological features. Since data were analyzed offline, cross-validation was used to obtain the results. The regression algorithm was trained with three approaches:

- Leave period out: Trained with data from all but one task period of one subject, then tested on the subject's remaining task period. Repeat for all subjects. In leave-period-out crossvalidation, EEG and eye tracking features were individualized to each subject as described in Sect. 5.4.
- Leave subject out: Trained with data from all but one subject, then tested on the remaining subject. Repeat for all subjects. In leave-subject-out crossvalidation, features were normalized for each task period. This was done for a period by subtracting the feature's baseline value (obtained during the initial baseline period) from the current value and dividing the result by the baseline value.
- Adaptive leave subject out: Same as leave subject out, but after each task period, the regression weights are updated using information from that task period through Kalman filtering. It thus gradually adapts to the current subject. The approach is computationally the same as in our previous adaptive LDA (Koenig et al. 2011; Novak et al. 2011a), except with a regression rather than classification function.

The measure of regression quality was the mean absolute error between the reported and predicted workload; the lower the error, the better. Regression functions were created separately for EEG, ANS and eye tracking data. Furthermore, to evaluate what accuracy would be achieved by a completely random regression function, regression functions were also created using twelve randomly generated features. These features' values were generated randomly for each time period from either a normal (6 features) or a uniform (6 features) distribution.

5.6 Initial Results and Discussion

5.6.1 EEG Data Quality

An examination of the EEG data found major motion artefacts: regardless of the task difficulty, measured power in the beta and especially gamma bands was much higher during any task period than during rest (up to nearly triple the baseline value). Tests before and after the official measurement protocol showed that high gamma activity is present even when no task is displayed and subjects simply move their arm inside the robot in a circular motion. Power in alpha and theta bands did not significantly increase when performing circular motions, and sometimes actually decreased during task periods.

From these observations, we conclude that beta and gamma band features cannot be used in motor rehabilitation without extensive artefact removal. It is currently unclear how much effort this would require. Rehabilitation robots already

measure arm movement, which could be used as an input to a noise reduction algorithm. However, this would only help with arm motions, not with head motions, which likely have a larger effect. For our first investigation, we chose to only utilize alpha and theta band information.

5.6.2 Correlations Between Game Difficulty and NASA-TLX

Pearson correlation coefficients were calculated separately for each subject, then averaged across subjects to obtain the final result. The mean correlation coefficient between *equation difficulty and mental workload* was 0.65 (range: 0.49–0.81) while the mean correlation coefficient between *monster spawn frequency and temporal workload* was 0.67 (range: 0.49–0.82). Workload was thus indeed induced by the task as desired.

However, there were also significant correlations between the different NASA-TLX scales. The mean correlation coefficient between *mental* and *temporal workload* was 0.41 (range: 0.07–0.71) while the mean correlation coefficient between temporal and physical workload was 0.42 (range 0.01–0.86). Effort was significantly correlated with all three workload types, though interestingly the correlation coefficients were negative in some subjects. The mean absolute correlation coefficients were 0.55 for *effort* and *mental workload* (range: −0.59 to 0.87), 0.46 for *effort* and *physical workload* (range: −0.36 to 0.74) and 0.54 for *effort* and *temporal workload* (range: −0.60 to 0.90). Finally, the mean absolute correlation coefficient between *effort* and *frustration* was 0.52 (range: −0.62 to 0.85). The same subjects who have negative correlations between effort and workloads (3 out of 10) also have negative correlations between effort and frustration.

While these results depend on the task, they suggest two things. First of all, it is not necessary to try and measure all types of workload in rehabilitation robotics, as they are correlated with each other. Second, subjects do sometimes respond to high workload by giving up and no longer putting as much effort into the task, as evidenced by negative correlation coefficients between effort and workload in some subjects.

For a motor rehabilitation task such as ours, we therefore suggest inferring two psychological dimensions from physiological measurements: the workload the subject is experiencing and how he/she is coping with it (actively or passively). This reinforces the suitability of the arousal/valence emotion model, which was used by previous studies (Badesa et al. 2012; Guerrero et al. 2013; Mihelj et al. 2009), but was suggested to be suboptimal due to the inability of ANS responses to accurately measure valence (Novak et al. 2010). An EEG-based passive BCI could measure valence more accurately than ANS responses, making this model more suitable. As different workload dimensions are difficult to separate in haptic and rehabilitation robotics (Novak et al. 2011b), such a two-dimensional model would likely be sufficient in most cases. A model with more dimensions, however, would be suitable for rehabilitation scenarios that consist of alternative mental and physical challenges (e.g. Koenig et al. 2011; Mihelj et al. 2012). A promising

candidate in such a case would be the proposed but untested arousal/valence/physical workload model of Mihelj et al. (2009).

5.6.3 Accuracy of Psychophysiological Inference

Since the NASA-TLX scales are significantly correlated, we present first results for estimation of *mental workload* and *effort* in Fig. 4. An example of reported and estimated (through leave-period-out linear regression) workload is shown for two subjects in Fig. 5.

All three physiological modalities estimated *mental workload* significantly better than random in leave-period-out cross validation where the regression function is trained on other data from the same subject. The accuracy of both EEG and eye tracking was significantly better than that of ANS responses. However, no modality provided significantly better than random results in leave-subject-out cross validation where the regression function is trained on data from other subjects.

ANS and EEG estimated *effort* significantly better than random, but again only in leave-period-out cross validation. ANS achieved a slightly better result than EEG, though the difference between the two was not significant. Leave-subject-out results were poor and actually significantly worse than random estimation in the case of EEG and eye tracking. However, the adaptive algorithm was able to greatly decrease leave-subject-out error, reaching approximately the same accuracy as in the leave-period-out case.

These results suggest that both mental workload and effort can be estimated better than random with EEG or other physiological data. The estimation can be done in the presence of physical activity and with only a single initial baseline, though user-specific models are needed. Furthermore, they demonstrate that EEG has advantages over previously used ANS responses in a rehabilitation robot: it

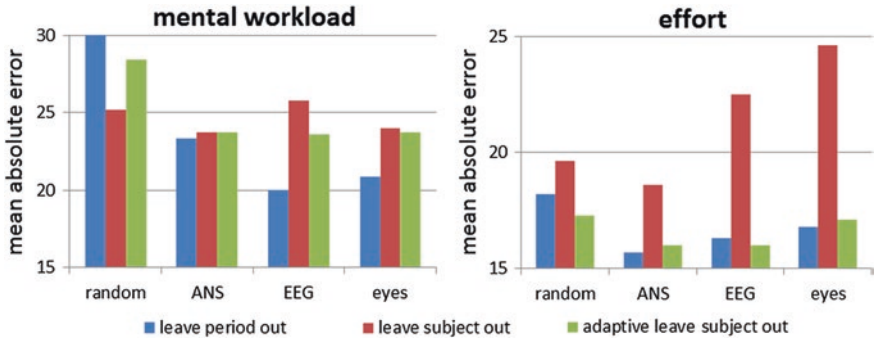

Fig. 4 Mean absolute error (difference between estimated and self-reported value in questionnaire units) for regression of mental workload (*left*) and effort (*right*) using autonomic nervous system responses, electroencephalography and eye tracking. The error when using random input data is shown for comparison

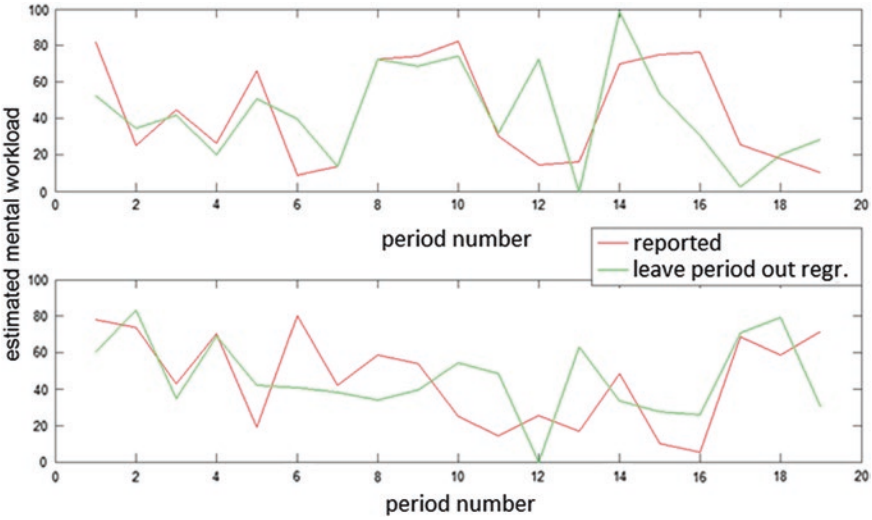

Fig. 5 Reported and estimated workload (through leave-period-out linear regression) for two subjects over the entire study. The *top* graph represents a subject with relatively low estimation error while the *bottom* graph represents a subject with high error

is able to estimate mental workload significantly better than ANS responses. If subject-specific models are not available, the adaptive algorithm can be used to greatly increase the error. However, the current offline implementation assumes that the algorithm can always adapt perfectly after each task period, which would not be the case in reality.

6 Conclusion and Outlook

In our review of the state of the art, we identified both EEG and fNIRS as promising passive BCI modalities for rehabilitation robotics. As the sensors need to be set up quickly in a rehabilitation environment, we should aim to minimize the number of electrodes/probes, use only frontal sites (not covered by hair), and use only dry (non-gelled) sensors, though not all of these goals may be achievable in practice. The two main practical problems in rehabilitation are the high level of physical activity, which results in motion artefacts, and the lack of baseline periods due to the need to maximize rehabilitation intensity.

In our first implementation with the ARMin III, we showed that EEG in the beta and especially gamma bands is strongly contaminated by motion artefacts, to the degree where such artefacts would be difficult to remove even with reference motion sensors. We therefore only used alpha and theta bands. Nonetheless, we were able to show that information from these two bands allows both mental

workload and effort to be estimated significantly better than random, with EEG outperforming ANS responses (previously used for task adaptation in rehabilitation robotics) in mental workload estimation. The estimation algorithms are computationally inexpensive and suitable for real-time use. However, subject-specific models or an adaptive (learning) algorithm are required. This may be due to the fact that subjects respond differently to workload, with some actually decreasing their effort as workload increases.

The immediate next step of our study is to compare the accuracy of EEG-based workload inference with the accuracy that can be achieved using nonphysiological data such as task score and movement information. Furthermore, we will attempt to identify the EEG channels that contribute the most to workload inference and thus attempt to minimize the number of channels used. We will develop algorithms to try and reduce motion artefacts in the EEG using either the robot's built-in position sensors or additional sensors to measure head movement. At the same time, we will conduct a second study to test whether fNIRS could provide a more convenient alternative to EEG. Finally, once an optimal, minimum-configuration setup is available, we will test it with actual patients undergoing motor rehabilitation to test both accuracy compared to healthy subjects and acceptance by the target population.

Acknowledgments This work was supported by the Swiss National Science Foundation through the National Centre of Competence in Research Robotics and by the Clinical Research Priority Program "NeuroRehab" University of Zurich.

References

Antonenko P, Paas F, Grabner R, Gog T (2010) Using electroencephalography to measure cognitive load. Educational Psychol Rev 22(4):425–438

Ayaz H, Shewokis PA, Bunce S, Izzetoglu K, Willems B, Onaral B (2012) Optical brain monitoring for operator training and mental workload assessment. NeuroImage 59(1):36–47

Badesa F, Morales R, Garcıa-Aracil N, Sabater J, Perez-Vidal C, Fernandez E (2012) Multimodal interfaces to improve therapeutic outcomes in robot-assisted rehabilitation. IEEE Trans Syst Man Cybern Part C Appl Rev 42(6):1152–1158

Berka C, Levendowski D, Cvetinovic M, Petrovic M, Davis G, Lumicao M et al (2004) Real-time analysis of EEG indexes of alertness, cognition, and memory acquired with a wireless EEG headset. Int J Hum Comput Interact 17(2):151–170

Berka C, Levendowski DJ, Lumicao MN, Yau A, Davis G, Zivkovic VT, Craven PL (2007) EEG correlates of task engagement and mental workload in vigilance, learning, and memory tasks. Aviat Space Environ Med 78(5 Suppl):B231–B244

Brainin M, Borstein N, Boysen G, Demarin V (2000) Acute neurological stroke care in Europe: results of the European stroke care inventory. Eur J Neurol 7:5–10

Brouwer A-M, Hogervorst M, Van Erp JBF, Heffelaar T, Zimmerman PH, Oostenveld R (2012) Estimating workload using EEG spectral power and ERPs in the n-back task. J Neural Eng 9(4):045008

Bütefisch C, Hummelsheim H, Denzler P, Mauritz K (1995) Repetitive training of isolated movements improves the outcome of motor rehabilitation of the centrally paretic hand. J Neurol Sci 130:59–68

Cameirão MS, Badia SBI, Oller ED, Verschure PFMJ (2010) Neurorehabilitation using the virtual reality based rehabilitation gaming system: methodology, design, psychometrics, usability and validation. J Neuroeng Rehabil 7:48

Chanel G, Rebetez C, Bétrancourt M, Pun T (2011) Emotion assessment from physiological signals for adaptation of game difficulty. IEEE Trans Syst Man Cybern Part A Syst Hum 41(6):1052–1063

Chi YM, Wang Y-T, Wang Y, Maier C, Jung T-P, Cauwenberghs G (2012) Dry and noncontact EEG sensors for mobile brain-computer interfaces. IEEE Trans Neural Syst Rehabil Eng 20(2):228–235

Coffey EBJ, Brouwer A-M, van Erp JBF (2012) Measuring workload using a combination of electroencephalography and near infrared spectroscopy. In: Proceedings of the human factors and ergonomics society 56th annual meeting, vol 56(1), pp 1822–1826

Colombo R, Pisano F, Mazzone A, Delconte C, Micera S, Carrozza MC et al (2007) Design strategies to improve patient motivation during robot-aided rehabilitation. J Neuroeng Rehabil 4:3

Coyle S, Ward T, Markham C (2004) Physiological noise in near-infrared spectroscopy: implications for optical brain computer interfacing. In Proceedings of the 26th annual international conference of the IEEE engineering in medicine and biology society, pp 4540–4543

Croft RJ, Barry RJ (2000) Removal of ocular artifact from the EEG: a review. Clin Neurophysiol 30(1):5–19

Fairclough SH, Venables L (2006) Prediction of subjective states from psychophysiology: a multivariate approach. Biol Psychol 71(1):100–110

Gagnon L, Cooper RJ, Yücel MA, Perdue KL, Greve DN, Boas DA (2012) Short separation channel location impacts the performance of short channel regression in NIRS. NeuroImage 59(3):2518–2528

George L, Marchal M, Glondu L, Lecuyer A (2012) Combining brain-computer interfaces and haptics : detecting mental workload to adapt haptic assistance. In: Proceedings of EuroHaptics 2012, pp 124–135

Girouard A, Solovey E, Hirshfield L (2009) Distinguishing difficulty levels with non-invasive brain activity measurements. In: Proceedings of INTERACT 2009, pp 440–452

Goljahani A, D'Avanzo C, Schiff S, Amodio P, Bisiacchi P, Sparacino G (2012) A novel method for the determination of the EEG individual alpha frequency. NeuroImage 60(1):774–786

Guerrero CR, Fraile Marinero JC, Turiel JP, Muñoz V (2013) Using "human state aware" robots to enhance physical human-robot interaction in a cooperative scenario. Comput Methods Programs Biomed 112(2):250–259

Guger C, Krausz G, Allison BZ, Edlinger G (2012) A comparison of dry and gel-based electrodes for P300 BCIs. Front Neurosci 6:60

Guidali M, Duschau-Wicke A, Broggi S, Klamroth-Marganska V, Nef T, Riener R (2011) A robotic system to train activities of daily living in a virtual environment. Med Biol Eng Comput 49(10):1213–1223

Gwin JT, Gramann K, Makeig S, Ferris DP (2010) Removal of movement artifact from high-density EEG recorded during walking and running. J Neurophysiol 103(6):3526–3534

Hart S, Staveland LE (1988) Development of NASA-TLX (task load index): results of empirical and theoretical research. In: Hancock PA, Meshkati N (eds) Human mental workload. North Holland Press, Amsterdam

Heger D, Putze F, Schultz T (2010) Online workload recognition from EEG data during cognitive tests and human-machine interaction. Lect Notes Comput Sci 6359:410–417

Herrmann CS, Munk MH, Engel AK (2004) Cognitive functions of gamma-band activity: memory match and utilization. Trends Cogn Sci 8(8):347–355

Klimesch W (1999) EEG alpha and theta oscillations reflect cognitive and memory performance: a review and analysis. Brain Res Rev 29(2–3):169–195

Knoll A, Wang Y, Chen F, Xu J, Ruiz N, Epps J, Zarjam P (2011) Measuring cognitive workload with low-cost electroencephalograph. In: Proceedings of INTERACT 2011, pp 568–571

Koenig A, Novak D, Omlin X, Pulfer M, Perreault E, Zimmerli L, Riener R (2011) Real-time closed-loop control of cognitive load in neurological patients during robot-assisted gait training. IEEE Trans Neural Syst Rehabil Eng 19(4):453–464

Kwakkel G, Kollen B, Wagenaar R (2002) Long term effects of upper and lower limb training after stroke: a randomised trial. J Neurol Neurosurg Psychiatry 72:473–479

Lotte F, Congedo M, Lécuyer A, Lamarche F, Arnaldi B (2007) A review of classification algorithms for EEG-based brain-computer interfaces. J Neural Eng 4(2):R1–R13

Maclean N (2002) The concept of patient motivation: a qualitative analysis of stroke professionals' attitudes. Stroke 33(2):444–448

Matthews F, Pearlmutter BA, Ward TE, Soraghan C, Markham C (2008) Hemodynamics for brain computer interfaces. IEEE Signal Process Mag 25(1):87–94

Mayaud L, Congedo M, Van Laghenhove A, Orlikowski D, Figère M, Azabou E, Cheliout-Heraut F (2013) A comparison of recording modalities of P300 event-related potentials (ERP) for brain-computer interface (BCI) paradigm. Neurophysiol Clin 43(4):217–227

Mihelj M, Novak D, Munih M (2009) Emotion-aware system for upper extremity rehabilitation. In: Proceedings of virtual rehabilitation 2009, pp 160–165

Mihelj M, Novak D, Milavec M, Ziherl J, Olenšek A, Munih M (2012) Virtual rehabilitation environment using principles of intrinsic motivation and game design. Presence Teleoperators Virtual Environ 21(1):1–15

Missonnier P, Leonards U, Gold G, Palix J, Ibáñez V, Giannakopoulos P (2003) A new electrophysiological index for working memory load in humans. NeuroReport 14(11):1451–1455

Nef T, Guidali M, Riener R (2009) ARMin III—arm therapy exoskeleton with an ergonomic shoulder actuation. Appl Bionic Biomech 6(2):127–142

Nelles G (2004) Cortical reorganization—effects of intensive therapy. Arch Phys Med Rehabil 22:239–244

Novak D, Mihelj M, Ziherl J, Olenšek A, Munih M (2011a) Psychophysiological measurements in a biocooperative feedback loop for upper extremity rehabilitation. IEEE Trans Neural Syst Rehabil Eng 19(4):400–410

Novak D, Mihelj M, Munih M (2011b) Psychophysiological responses to different levels of cognitive and physical workload in haptic interaction. Robotica 29(03):367–374

Novak D, Mihelj M, Munih M (2012) A survey of methods for data fusion and system adaptation using autonomic nervous system responses in physiological computing. Interact Comput 24:154–172

Novak D, Ziherl J, Olenšek A, Milavec M, Podobnik J, Mihelj M, Munih M (2010) Psychophysiological responses to robotic rehabilitation tasks in stroke. IEEE Trans Neural Syst Rehabil Eng 18(4):351–361

Ong M, Russell PN, Helton WS (2013) Frontal cerebral oxygen response as an indicator of initial attention effort during perceptual learning. Exp Brain Res 229(4):571–578

Pesonen M, Björnberg CH, Hämäläinen H, Krause CM (2006) Brain oscillatory 1–30 Hz EEG ERD/ERS responses during the different stages of an auditory memory search task. Neurosci Lett 399(1–2):45–50

Ryu K, Myung R (2005) Evaluation of mental workload with a combined measure based on physiological indices during a dual task of tracking and mental arithmetic. Int J Ind Ergon 35(11):991–1009

Shirzad N, Van der Loos HFM (2013) Adaptation of task difficulty in rehabilitation exercises based on the user's motor performance and physiological responses. In Proceedings of the 2013 IEEE international conference on rehabilitation robotics

Sitaram R, Zhang H, Guan C, Thulasidas M, Hoshi Y, Ishikawa A, Birbaumer N (2007) Temporal classification of multichannel near-infrared spectroscopy signals of motor imagery for developing a brain-computer interface. NeuroImage 34(4):1416–1427

Solovey E, Girouard A (2009) Using fNIRS brain sensing in realistic HCI settings: experiments and guidelines. In: Proceedings of UIST 2009, pp 157–166

Thorvaldsen P, Asplund K, Kuulasmaa K, Rajakangas AM, Schroll M (1995) Stroke incidence, case fatality, and mortality in the WHO MONICA project. Stroke 26(3):361-367

Van Erp JBF, Lotte F, Tangermann M (2012) Brain-computer interfaces: beyond medical applications. IEEE Comput 41:26–34

Vaughan TM, Wolpaw JR, Donchin E (1996) EEG-based communication: prospects and problems. IEEE Trans Rehabil Eng 4(4):425–430

Venables L, Fairclough SH (2009) The influence of performance feedback on goal-setting and mental effort regulation. Motiv Emot 33(1):63–74

Villringer A, Chance B (1997) Non-invasive optical spectroscopy and imaging of human brain function. Trends Neurosci 20:435–442

Whitham EM, Pope KJ, Fitzgibbon SP, Lewis T, Clark CR, Loveless S, Willoughby JO (2007) Scalp electrical recording during paralysis: quantitative evidence that EEG frequencies above 20 Hz are contaminated by EMG. Clin Neurophysiol 118(8):1877–1888

Wilson GF, Russell C (2003) Real-time assessment of mental workload using psychophysiological measures and artificial neural networks. Hum Factors 45(4):635–643

Wilson GF, Russell C (2007) Performance enhancement in an uninhabited air vehicle task using psychophysiologically determined adaptive aiding. Hum Factors 49(6):1005–1018

Wu D, Courtney CG, Lance BJ, Narayanan SS, Dawson ME, Oie KS, Parsons TD (2010) Optimal arousal identification and classification for affective computing using physiological signals: virtual reality Stroop task. IEEE Trans Affect Comput 1(2):109–118

Zander TO, Kothe C (2011) Towards passive brain-computer interfaces: applying brain-computer interface technology to human-machine systems in general. J Neural Eng 8(2):025005

Zhao C, Zheng C, Zhao M, Tu Y, Liu J (2011) Multivariate autoregressive models and kernel learning algorithms for classifying driving mental fatigue based on electroencephalographic. Expert Syst Appl 38(3):1859–1865

Zimmerli L, Krewer C, Gassert R, Müller F, Riener R, Lünenburger L (2012) Validation of a mechanism to balance exercise difficulty in robot-assisted upper-extremity rehabilitation after stroke. J Neuroeng Rehabil 9:6

Zimmermann R, Marchal-Crespo L, Edelmann J, Lambercy O, Fluet M-C, Riener R et al (2013) Detection of motor execution using a hybrid fNIRS-biosignal BCI: a feasibility study. J Neuroeng Rehabil 10:4

A Concurrent Brain-Machine Interface for Enhanced Sequential Motor Function

Maryam M. Shanechi, Rollin C. Hu, Marissa Powers, Gregory W. Wornell, Emery N. Brown and Ziv M. Williams

Abstract Brain-machine interfaces (BMIs) have largely been designed for performing single-targeted movements. However, many tasks involve planning a sequence of such targeted movements before execution. Hence a BMI that can concurrently decode the complete planned sequence before its execution can enable subjects to also perform these sequential movements. Moreover, such concurrent decoding may allow the BMI to consider the higher-level goal of the task to reformulate the motor plan and perform it more effectively. Here, we demonstrate that concurrent BMI decoding is possible. Using population-wide modeling, we discovered two distinct subpopulations of neurons in the rhesus monkey premotor cortex that allowed two planned targets of a sequential movement to be simultaneously held in working memory without degradation. Interestingly, this simultaneous representation occurred because each subpopulation encoded either only currently held or only newly added target information regardless of the exact sequence. Capitalizing on this stable representation, we developed a BMI that

This work was published in part in Nature Neuroscience (Shanechi et al. 2012a).

M.M. Shanechi (✉)
Ming Hsieh Department of Electrical Engineering, University of Southern California, Los Angeles, CA, USA
e-mail: shanechi@usc.edu

R.C. Hu · M. Powers · E.N. Brown · Z.M. Williams
Massachusetts General Hospital, Boston, MA, USA

R.C. Hu · E.N. Brown · Z.M. Williams
Harvard Medical School, Boston, MA, USA

G.W. Wornell
Department of Electrical Engineering and Computer Science, Massachusetts Institute of Technology, Cambridge, MA, USA

E.N. Brown
Department of Brain and Cognitive Sciences, Massachusetts Institute of Technology, Cambridge, MA, USA

C. Guger et al. (eds.), *Brain-Computer Interface Research*, SpringerBriefs in Electrical and Computer Engineering, DOI 10.1007/978-3-319-09979-8_8

concurrently decodes a full motor sequence in advance of movement and can then accurately execute it as desired.

Keywords Brain-machine interface · Neuroprosthetics · Working memory · Sequential motor function · Premotor cortex

An important motivation for the design of brain-machine interfaces (BMIs) has been their potential to restore lost motor function in individuals with neurological injury or disease (e.g., due to motor paralysis or stroke). In such cases, the envisioned role of the BMI is to decode intended motor function from neural activity in the relevant areas of the brain, and use this information to control an affected limb or prosthetic.

The design of such BMIs has received considerable attention in recent years (Chapin et al. 1999; Wessberg et al. 2000; Serruya et al. 2002; Hochberg et al. 2006; Carmena et al. 2003; Taylor et al. 2002; Ganguly and Carmena 2009; Wolpaw and McFarland 2004; Velliste et al. 2008; Moritz et al. 2008; Mulliken et al. 2008; Kim et al. 2008; Li et al. 2009; Chase et al. 2009; Musallam et al. 2004; Santhanam et al. 2006; Shanechi et al. 2013, 2014). Work to date has principally focused on achieving the motor goal in tasks that involve single-targeted movements, such as the task of moving a cursor on a display to an individual target location. However, in many natural tasks—such as playing a succession of notes on a piano—the goal is more complex, and the motor plan for achieving it can be viewed as a sequence of such simpler plan elements to be executed in order.

Our focus is on the design of BMIs that can achieve the goal of these sequential motor plans. Planned sequential behavior is a fundamental motor process in which all targets of a movement sequence are planned ahead of its initiation. Hence a BMI for performing this behavior would allow a person to *plan a full motor sequence* ahead of execution. For example, when picking up a cup and bringing it to one's lips, a person normally formulates the full motor plan prior to its execution as opposed to planning and performing each of its elements individually and separately. Hence, the objective of such a BMI would be to perform the sequential behavior by decoding the full sequence of elements of the motor plan concurrently and in advance of movement—thus requiring the consideration of a *concurrent* BMI architecture.

This concurrent BMI functionality is thus distinct from that in prior BMIs whose objective is to decode and execute individual single targeted movements one by one, and hence have a *sequential* BMI architecture (Chapin et al. 1999; Wessberg et al. 2000; Serruya et al. 2002; Hochberg et al. 2006; Carmena et al. 2003; Taylor et al. 2002; Ganguly and Carmena 2009; Wolpaw and McFarland 2004; Velliste et al. 2008; Moritz et al. 2008; Mulliken et al. 2008; Kim et al. 2008; Li et al. 2009; Chase et al. 2009; Musallam et al. 2004; Santhanam et al. 2006; Shanechi et al. 2012b, 2013). Because this latter objective corresponds to a low-level interpretation of the overall motor goal of the individual, such a sequential architecture is inherently limited. While such a BMI has the potential to restore or match original motor functionality, a compelling objective is the design

of a BMI that may be able to enhance such natural motor functionality by considering the motor goal at a higher-level.

A concurrent architecture could allow the BMI to consider the overall motor goal at a higher-level. This is a result of the BMI having information about all the motor plan elements at once and in advance of execution. This may allow the BMI to analyze the entire sequence prior to action to determine ways to perform the task more effectively. For example, the BMI might determine a way to accomplish the task more quickly, or more efficiently. Alternatively, based on additional sensor inputs, the BMI might determine that the planned sequence of movements would result in an accident with an obstacle, and thus modify the execution of the task to avoid such an accident.

The realization of BMIs that can perform and more effectively execute sequential motor function in this way will obviously require significant technological innovations. But as a key initial step, it requires considering a concurrent BMI architecture in which the elements of a planned motor task are decoded in parallel (i.e., at once), in contrast to the serial process of a sequential BMI. Hence, the feasibility of such BMIs hinges on the degree to which the elements of a motor plan sequence can, in fact, be decoded concurrently. This is the starting point for this work.

Prior work has demonstrated that premotor neurons in primates display selective responses to planned single-targeted movements before their initiation (Kurata 1993; Messier and Kalaska 2000; Crammond and Kalaska 1994, 1996, 2000; Boussaoud and Bremmer 1999; Crutcher et al. 2004; Hocherman and Wise 1991). Such responses have been successfully exploited in the design of BMIs for single-target tasks (Musallam et al. 2004; Santhanam et al. 2006). In comparison, the neural encoding of tasks requiring a sequence of targeted movements to be formulated prior to execution is less well understood, and the design of real-time BMIs that can concurrently decode and then execute such sequential motor plans remains unexplored. Prior work has shown that an individual neuron can display a response that is selective to one or more elements of a sequential motor plan (Batista and Andersen 2001; Ninokura et al. 2003; Tanji and Shima 1994; Shima et al. 2007; Shima and Tanji 2000; Baldauf et al. 2008; Averbeck et al. 2002, 2006; Mushiake et al. 1990, 2006; Ohbayashi et al. 2003; Kettner et al. 1996; Lu and Ashe 2005; Nakajima et al. 2009; Saito et al. 2005). However, little is known regarding how information about multiple elements of a sequential motor plan is simultaneously distributed across the whole premotor population during working memory, and whether these plan elements can be accurately and robustly decoded from the neural population in a concurrent manner.

Here, we find that sequential motor plans can be decoded simultaneously, accurately, robustly, and in advance of movement from the neural activity in the premotor cortex of monkeys. Additionally our study reveals a surprisingly structured encoding mechanism that is used by the premotor populations for these sequential plans and that, in turn, enables their accurate and concurrent decoding. Based on these findings, we develop and implement a real-time BMI that can concurrently decode a dual sequence of motor targets and then execute them as desired.

1 Methods

1.1 Experimental Task

In the study, rhesus monkeys were trained to perform a task in which two targets were presented, in sequence, on a computer display. Each of the targets could randomly appear in one of four possible spatial locations ("up", "down", "left", or "right"). Repeated locations were precluded, so there were a total of 12 possible combinations (sequences) of two consecutive distinct target locations. After a blank-screen variable delay, a "go" cue appeared directing the monkeys to sequentially move a cursor from the center of the screen to each of the two remembered targets, in order (Dual-target task; Fig. 1a, b). We define the working memory period as the 500 ms blank-screen interval following presentation of the second target and before the earliest possible "go" cue. Therefore, the task here was a working-memory task in which the monkeys were required to serially add to working memory two *randomly* selected target locations in each trial and then simultaneously retain them in working memory prior to execution.

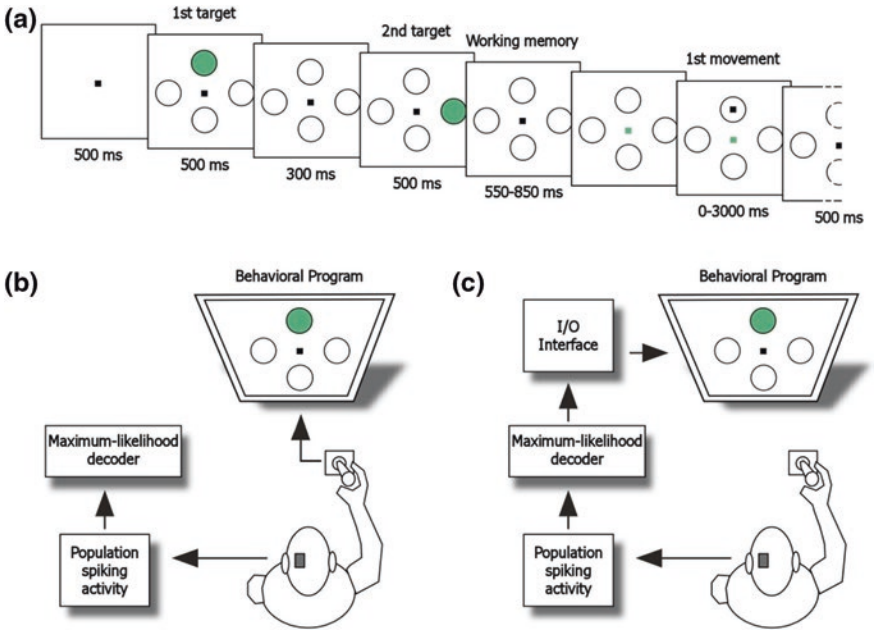

Fig. 1 Task design and experimental setup. **a** Schematic illustration of a standard dual-target task over a single trial. Task periods and their timings are displayed over a single trial from *left* to *right*. The *right end* of the panel in which the second movement is made is truncated to conserve space. **b** Experimental setup for the standard training sessions. **c** Experimental setup for the BMI sessions

1.2 Neural Recordings

Multiple-unit responses were recorded from the premotor cortex as the primates performed this task. Multiple planar silicone multi-electrode arrays (NeuroNexus Technologies Inc., MI) were surgically implanted in each monkey into the dorsal premotor (PMd) and the supplementary motor (SMA) areas. A Plexon multichannel acquisition processor was used to amplify and band-pass filter the neuronal signals (150 Hz–8 kHz; Plexon Inc., TX). Signals were digitized at 40 kHz and processed to extract action potentials in real time by the Plexon workstation. Classification of the action potential waveforms was performed using template matching and principle component analysis based on waveform parameters. Only single, well-isolated units were used.

1.3 Model Construction Using the Expectation-Maximization (EM) Algorithm

We model the activity of each neuron under any given sequence as an inhomogeneous Poisson process whose likelihood function (using the theory of point processes) is given by (Truccolo et al. 2005)

$$p(N^c_{1:K}|S_i) = \prod_{k=1}^{K} (\lambda_c(k|S_i)\Delta)^{N^c_k} \exp(-\lambda_c(k|S_i)\Delta) \quad i = 1{:}12, \tag{1}$$

where Δ is the time increment taken to be small enough to contain at most one spike, N^c_k is the binary spike event of the cth neuron in the time interval $[(k-1)\Delta, k\Delta]$, $\lambda_c(k|S_i)$ is its instantaneous firing rate in that interval, S_i is the ith sequence, and K is the total number of bins in a duration $K\Delta$.

For each sequence and neuron, we estimate the firing rate $\lambda_c(k|S_i)$ using the neuronal data observed. One can find this using the peristimulus time histogram (PSTH) that simply averages the number of spikes over any given window. However, to get a good estimate using the PSTH, one has to pick relatively large windows. This in turn masks the fine-scaled evolution of the firing rate. Also, there is no principled way for selecting a window size. Hence we instead use a state-space algorithm to find the firing rate (Smith and Brown 2003; Smith et al. 2010). This approach consists of two models: A prior or state model that in general enforces any prior information available about the unobservable states—such as a simple continuity condition—and an observation model that relates the neuronal observations to these states. We take the state at time increment k, x_k, to be the logarithm of the firing rate, i.e., $x_k = \log(\lambda_c(k|S_i))$, or equivalently

$$\lambda_c(k|S_i) = \exp(x_k), \tag{2}$$

and enforce a continuity condition on it by assuming that it evolves according to a linear first-order Gaussian model,

$$x_k = x_{k-1} + \epsilon_k,$$

where ϵ_k is the zero-mean white Gaussian noise with variance σ_ϵ^2. The observation model is in turn given by substituting (2) in (1). Here, $\theta = \sigma_\epsilon^2$ is an unknown parameter of the model and should be estimated jointly with the state. Hence we use the expectation-maximization (EM) iterative algorithm to find the maximum likelihood estimate of θ and in turn estimate the firing rate (Smith and Brown 2003; Dempster et al. 1977). Denoting the estimate of θ in the ith iteration by $\theta^{(i)}$, its estimate in the $i+1$th iteration after the maximization step is given by

$$\theta^{(i+1)} = \frac{1}{K}\left(\sum_{k=1}^{K} W_k + W_{k-1} - 2W_{k,k-1}\right), \tag{3}$$

where $W_k = E[x_k^2|N_{1:K}^c; \theta^{(i)}]$ and $W_{k,k-1} = E[x_{k-1}x_k|N_{1:K}^c; \theta^{(i)}]$ are found from the forward filter, fixed-interval smoothing, and covariance recursive algorithms in the expectation step as follows. Assuming that there are J total trials and denoting the causal filter state estimate by $x_{k|k} = E[x_k|N_{1:k}^c; \theta^{(i)}]$ and its variance by $w_{k|k}$, and the smoothed state estimate by $x_{k|K} = E[x_k|N_{1:K}^c; \theta^{(i)}]$ and its variance by $w_{k|K}$, the recursions in the E-step are given by the forward filter recursions (Eden et al. 2004),

$$\begin{aligned}
w_{k|k-1} &= w_{k-1|k-1} + \theta^{(i)} \\
x_{k|k-1} &= x_{k-1|k-1} \\
w_{k|k} &= (w_{k|k-1}^{-1} + J\exp(x_{k|k-1})\Delta)^{-1} \\
x_{k|k} &= x_{k|k-1} + w_{k|k}\sum_{j=1}^{J}(N_k^c(j) - \exp(x_{k|k-1})\Delta),
\end{aligned}$$

for $k = 1, \ldots, K$, where $N_k^c(j)$ is the spike event in trial j, and by the fixed interval smoothing recursions (Smith and Brown 2003; Brown et al. 1998),

$$\begin{aligned}
A_k &= w_{k|k}w_{k+1|k}^{-1} \\
x_{k|K} &= x_{k|k} + A_k(x_{k+1|K} - x_{k+1|k}) \\
w_{k|K} &= w_{k|k} + A_k^2(w_{k+1|K} - w_{k+1|k}),
\end{aligned}$$

for $k = K-1, \ldots, 0$ and with initial condition $x_{K|K}$ and $w_{K|K}$ from the filter recursions. We pick the initial conditions for the forward filter at each iteration of the EM algorithm as $x_{0|0}^{(i+1)} = x_{0|K}^{(i)}$ and $w_{0|0}^{(i+1)} = w_{0|K}^{(i)}$. Finally the state-space covariance algorithm gives all the terms needed for the M-step to find $\theta^{(i+1)}$ in (3) using these recursions (Brown et al. 1998; Jong and Mackinnon 1988),

$$W_k = w_{k|K} + x_{k|K}^2,$$

for $k = 0, \ldots, K$ and

$$W_{k+1,k} = A_k w_{k+1|K} + x_{k|K} x_{k+1|K},$$

for $k = 0, \ldots, K-1$. The iterations of the EM algorithm are run until convergence. The estimated firing rate at any time bin $k = 1, \ldots, K$ is in turn the smoothed estimate, $\hat{\lambda}_c(k|S_i) = \exp(x_{k|K})$ evaluated at the estimate of θ in the final iteration.

Repeating this procedure for all neurons under each sequence and fitting the inhomogeneous Poisson models results in a continuous smoothed estimate of the rate function for each neuron under any given sequence and over the entire length of a trial.

1.4 Maximum-Likelihood Decoder

Once models are fitted, a maximum-likelihood decoder is used to decode the intended sequence based on the neuronal activity in any period of interest. Using the likelihood model in (1) and assuming that neurons are conditionally independent given the sequence, the population likelihood under any sequence is given by

$$p(N_{1:K}^{1:C}|S_i) = \prod_{c=1}^{C} \prod_{k=1}^{K} (\lambda_c(k|S_i)\Delta)^{N_k^c} \exp(-\lambda_c(k|S_i)\Delta) \quad i = 1{:}12$$

The predicted sequence, $\hat{S}$, is thus given by

$$\hat{S} = \arg\max_{S_i} p(N_{1:K}^{1:C}|S_i).$$

2 Results

We recorded 281 well-isolated neurons from the supplementary motor area (SMA) and dorsal premotor cortex (PMd) over 11 sessions, for an average of 26 ± 6 cells (mean $\pm$ S.D.) per recording session. Using the inhomogeneous Poisson models for each neuron and under each sequence, we employed a maximum-likelihood decoder to quantify the probabilities that groups of neurons could correctly identify the first and second targets on a trial-by-trial basis during the working memory period (leave-one-out cross-validation). We used decoding accuracy as our measure of the amount of information encoded by a population of neurons about each target. Specifically, for an individual (first or second) target, we measured the percentage of trials in which the maximum-likelihood decoder correctly predicted the respective target from that population's activity. Likewise, we measured the amount of information encoded about the full sequence as the percentage of trials in which both targets were correctly decoded.

2.1 Accurate and Concurrent Encoding of the Motor Sequence by the Premotor Population

We find that neural population activity within the premotor cortex accurately encoded the location of both targets during the working memory period. During this period, the population correctly encoded the first and second targets on up to 85 and 82 % of the trials in a session, respectively. When considering all 12 possible target combinations, the population encoded both targets correctly on up to 72 % of the trials in a session (Fig. 2a). Across all tested sessions, the population correctly encoded the first and second targets on average on 76 ± 11 and 56 ± 17 % of trials, respectively, both of which were significantly above chance (one-sided Z-test, $P < 10^{-15}$). Also, the population encoded both targets correctly on average on 45 ± 12 % of the trials across all sessions, which was also far higher than chance at 1/12 ≈ 8 % (one-sided Z-test, $P < 10^{-15}$). These results were consistent across the two monkeys ($P < 10^{-15}$ for both).

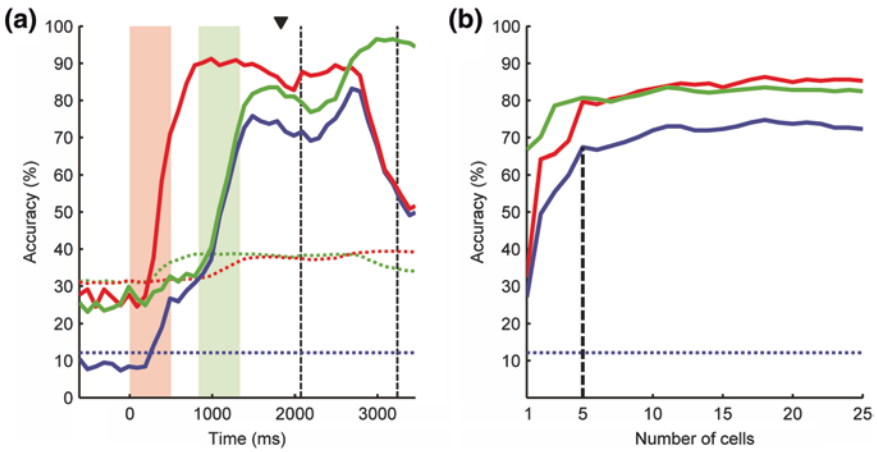

Fig. 2 Population decoding accuracy for a selected session. **a** Population decoding accuracy over time for the first target (*red curve*), second target (*green curve*), and the full sequence (*blue curve*). Each point on the *curves* indicates the decoding accuracy for the population over the *preceding* 500 ms window. Time at zero is aligned to the start of first target presentation. The *red* and *green vertical bars* indicate the times during which the first and second targets were presented, respectively. The first and second *dashed black lines* indicate the mean times at which the first and second "go" cues were given, respectively. The *arrow* indicates the time point of decoding for the preceding working memory period (i.e., 0–500 ms from the end of the second target presentation). The *dotted lines* indicate the 99 % chance upper confidence bounds for the first target, second target, and sequence (out of 12 possibilities), with the same respective color scheme used above. **b** Number of cells sufficient to reach decoding accuracy asymptote during the working memory period for the same session. The first target (*red curve*), second target (*green curve*), and sequence (*blue curve*) accuracies are displayed as a function of the cumulative number of cells, in descending order of single-cell sequence accuracy. The number of cells needed to reach over 90 % of the population accuracy is indicated by the *vertical dashed line*

2.2 Robustness of the Encoding

Only a small number of cells were needed to decode the target sequence with high accuracy. When performing the decoding analysis over all trials, which employed all 12 possible target combinations, only 29 % of the population (7.5 cells) was needed, on average, to achieve higher than 90 % of the population sequence accuracy (Fig. 2b). When performing the decoding analysis over subsets of all trials that employed only 4 or 8 target combinations, population sequence accuracies in the best session were as high as 93 and 80 %, respectively. In these cases, decoding from only 2 and 4 cells, respectively, was sufficient to achieve higher than 90 % of these sequence accuracies.

2.3 Real-Time Concurrent BMI for Sequential Movement Decoding and Execution

Motivated by the observation that both targets can be concurrently and accurately decoded from the responses of relatively few neurons in the premotor cortex, we developed a real-time BMI capable of predicting both targets simultaneously prior to the monkey's motor response and then executing the targeted movements. In the associated experiments, we recorded a mean of 20 ± 2 cells per session from the premotor cortex of the same monkeys. Here, Poisson models were first fitted to the neural population activity during the working memory period prior to the "go" cue as the primates rehearsed a subset of target combinations that included either 4 or 8 possible sequences over an average of 26 ± 2 training trials per sequence (Fig. 1b).

Using the Poisson models, sequence decoding accuracies for the set of 4 and 8 sequences in these training sessions (found using leave-one-out cross-validation) were 79 ± 2 and 80 ± 3 % (Fig. 3; mean ± s.e.m.; one-sided *Z*-test, $P < 10^{-15}$), respectively. Following training, the primates performed the same task as before, but with the cursor now being sequentially positioned by the BMI on the targets decoded from the recorded neuronal activity during the single preceding working memory period (Fig. 1c). Here, BMI-generated cursor movements were set to occur immediately following the presentation of the "go" cue and the added delays were selected to match the reaction times that the monkeys normally experienced when moving the cursor themselves following the "go" cue (obviously, cursor movements could be generated without the added delays if desired).

Both monkeys performed the four-sequence set, and one monkey performed the eight-sequence set using the real-time BMI. Sequence accuracies for the set of four and eight sequences were 72 ± 2 and 71 ± 4 %, respectively, both of which were significantly above chance (Fig. 3; mean ± s.e.m., one-sided *Z*-test, $P < 10^{-15}$). These results established that two planned elements, i.e., the two intended sequential targets of movement, could be simultaneously predicted in advance of movement and then executed by a real-time BMI with high accuracy.

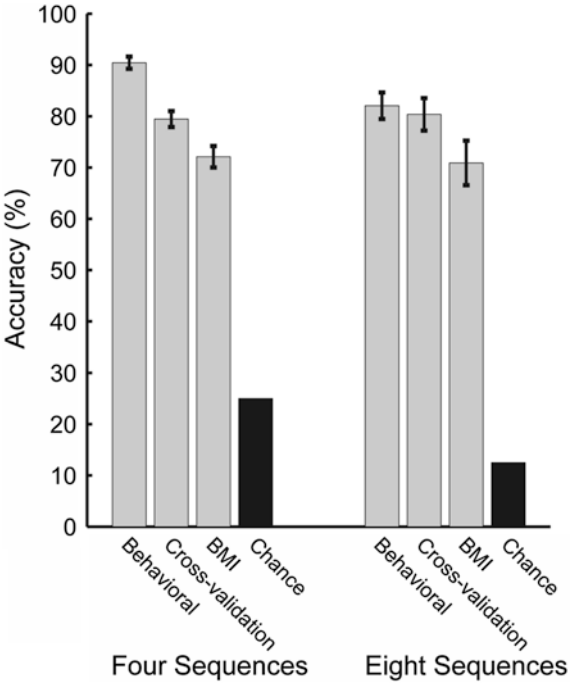

Fig. 3 Decoding accuracies on BMI trials. The *gray bars* indicate the monkeys' average behavioral accuracy, maximum-likelihood cross-validation accuracy on the training data, and real-time BMI accuracy, with each corresponding s.e.m. The *black bars* indicate chance level accuracies. Performances using four sequences are displayed on the *left*, and using eight sequences are displayed on the *right*

We also examined the time required by the concurrent decoder to decode the sequence. We found that the sequence decoding accuracy for the set of 4, 8 and 12 sequences reached 90 % of the maximum asymptotic accuracy possible, on average, 488 $\pm$ 135, 561 $\pm$ 119 and 641 $\pm$ 121 ms, respectively, after the initial presentation of the second target. In comparison, when performing the motor sequence, the minimum total time it took for the monkeys to both react to the two go cues and reach the two targets was, on average, 791 $\pm$ 93 ms.

2.4 Population Encoding Structure Reveals a Novel Partitioning Mechanism

Observing that both target locations could be accurately and concurrently predicted from the neural population responses, we further examined the spatial and temporal structure of their encoding. In particular, we investigated how neurons within the premotor cortex were able to add new information about the second target to working memory without compromising the integrity of information about the first target that was already being held.

We find that most cells encoded significant information about *only* the first (currently held) or *only* the second (newly added) target during the working memory period. Moreover, this partitioning remained stable throughout recordings

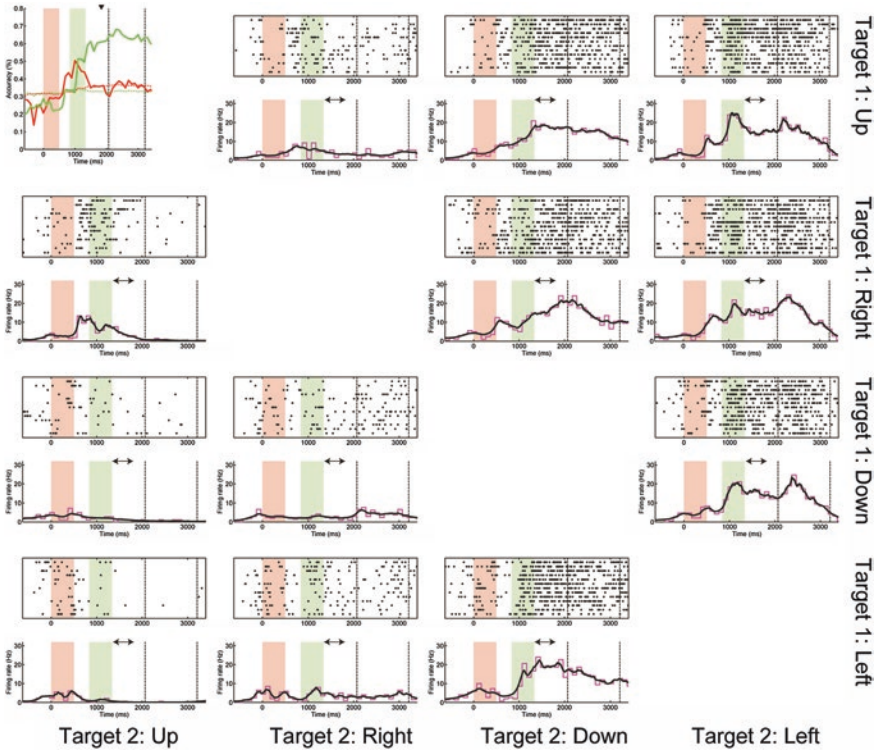

Fig. 4 Example of a second (added) target selective neuron. The subfigure at the *upper left corner* shows the first and second target accuracies of the cell as a function of time into the trial. The *vertical bars*/*lines* and their timings follow the same convention as Fig. 2. In all other subfigures, each *top* panel corresponds to a different sequence of movements with each row illustrating the spiking activity during a single trial and the *black dots* indicating the spike times. Each *bottom* panel indicates the corresponding mean firing rate estimates using the expectation-maximization procedure (*black curve*) and the corresponding peristimulus time histogram (PSTH) (*magenta curve*). The *arrow* indicates the working memory period. The subfigures in the same row correspond to sequences with the same first target location. The subfigures in the same column correspond to sequences with the same second target location. Note that repeated target locations were not used in the sequences, and hence there are 3 subfigures per row/column

per day. Of the 281 neurons recorded in all sessions, 46 % had a target accuracy significantly higher than chance for at least one of the two targets during the working memory period (one-sided Z-test, $P < 0.01$). Of these, 68 % encoded significant information about only the first currently held target, and 23 % encoded significant information about only the second added target (one-sided Z-test; $P < 0.01$; Fig. 4). The percentage of cells that encoded significant information about both targets was only 9 % (one-sided Z-test; $P < 0.01$) and, even among these, most had target accuracies much closer to one of the two subpopulations of cells that significantly encoded only one target (Fig. 5).

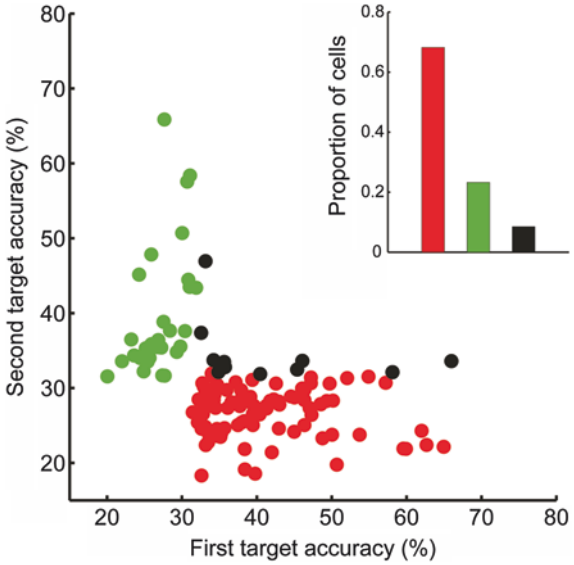

Fig. 5 Distribution of first and second target information across the population. Scatter plot of the first and second target accuracies for the 129 cells that encoded significant information about at least one target during the working memory period (across 12 sequences). Statistical significance of the target accuracies was tested here at the 0.01 level. *Red points* indicate cells that encoded significant information about only the first target, *green points* indicate those that encoded significant information about only the second target, and *black points* indicate those that encoded significant information about both targets. The *inset* indicates the proportion of cells that encoded significant information about only the first, only the second or both targets during the working memory period with the same coloring scheme, above

The two subpopulations of cells remained stable over time. In a given day's session, most neurons remained dedicated to encoding only the first (currently held) or only the second (added) target. For the two subpopulations of cells that encoded significant information about the respective first and second targets alone, most (89 %) provided substantially the same level of accuracy in decoding their respective targets in the first and second halves of the recording session (χ^2 test, $P > 0.05$).

2.5 *Effect of Adding Information to Working Memory on the Integrity of Existing Information*

In order to further examine how adding a new target to working memory affected the integrity of the currently held target, we disambiguated the process of holding information in working memory from that of adding information to it. The results were obtained from sessions in which the monkeys performed the standard

dual-target trials (as before), but also performed single-target trials in randomly interleaved fashion. Unlike dual-target trials, on single-target trials only the first target was presented and the second target presentation period was replaced with a blank-screen period of the same duration. The task timing was otherwise unchanged compared to the dual-target task.

We find that adding information about the second target location to working memory did not incur loss of information about the first target location. Of the cells that encoded significant information about the first target during working memory in single-target trials (one-sided Z-test, $P < 0.01$), most (74 %) provided the same level of accuracy in decoding the first target during working memory in dual-target trials, despite the addition of a second target (χ^2 test, $P > 0.05$). Moreover, for the whole population, there was also no significant difference in the first target accuracy during the working memory period when comparing dual-target and single-target trials across sessions (Wilcoxon's signed-rank test, $P = 0.69$). These results demonstrate that the subpopulation encoding the first target and their responses remained largely unchanged when the second target was added to working memory and, therefore, the addition of information about the second target did not comprise the integrity of information already held about the first target.

3 Conclusions

Collectively, our results establish the viability of concurrent decoding in a BMI. We find a novel functional structure within the premotor cortex that enabled accurate and concurrent decoding of two planned motor targets across multiple spatial locations. During working memory, premotor populations are largely partitioned into two fundamentally disjoint subpopulations of cells—one dedicated to encoding only the currently held (first) target and one dedicated to encoding only the newly added (second) target, irrespective of the specific sequence. Moreover, while the two target locations changed from trial to trial, the two encoding subpopulations did not. Interestingly, the subpopulation dedicated to encoding the first target and their responses remained largely unchanged when the second target was added to working memory, so that the process of adding information did not compromise the integrity of existing information. Also remarkably, only a small number of neurons were sufficient to accurately predict the location of both targets, making the decoding of such information highly robust.

We also developed a concurrent BMI that decoded the sequential motor plans in advance of movement, accurately, and robustly. Such a concurrent BMI allows the subjects to plan a sequential motor task simultaneously and will therefore decode this sequence concurrently. This is in contrast to requiring the subject to plan and execute the elements of a sequential plan one by one, as in prior BMIs.

Additionally, a concurrent architecture provides the prospect of BMIs that can enhance natural sequential motor function by considering the higher-level goal of the motor activity and then reformulating the motor plan accordingly. Because the

full motor plan is simultaneously decoded upfront and in advance of movement, the higher-level goal of the task can, in principle, be analyzed before execution. For instance, this could allow designing a BMI that can perform the task more quickly, more flexibly, or more efficiently than originally conceived. Such a BMI may, for example, alter the order in which the elements of the motor sequence are executed depending on rapid or unpredictable changes in the environment (e.g., to avoid unanticipated obstacles), or correct the original sequence based on the performance metrics of the task (e.g., proactively change a sequence of letters based on spelling rules). Significant technological innovations are obviously required for the realization of such BMIs. But our results demonstrate that the novel concurrent architecture that is a key requirement for such realization is feasible. As a simple but illustrative example of such a capability, we find that we could accurately decode the full sequence of two targets faster than it took the monkeys to select the sequence themselves.

Given these results, it is conceivable that a variety of higher-level motor functions could be achieved in the future by such BMIs exploiting concurrent decoding and the neural partitioning revealed in this study. As such, there may be broad implications for use in both clinical and non-clinical applications.

References

Averbeck BB, Chafee MV, Crowe DA, Georgopoulos AP (2002) Parallel processing of serial movements in prefrontal cortex. Proc Natl Acad Sci USA 99:13172–13177

Averbeck BB, Sohn J-W, Lee D (2006) Activity in prefrontal cortex during dynamic selection of action sequences. Nat Neurosci 9:276–282

Baldauf D, Cui H, Andersen RA (2008) The posterior parietal cortex encodes in parallel both goals for double-reach sequences. J Neurosci 28:10081–10089

Batista AP, Andersen RA (2001) The parietal reach region codes the next planned movement in a sequential reach task. J Neurophysiol 85:539–544

Boussaoud D, Bremmer F (1999) Gaze effects in the cerebral cortex: reference frames for space coding and action. Exp Brain Res 128:170–180

Brown EN, Frank LM, Tang D, Quirk MC, Wilson MA (1998) A statistical paradigm for neural spike train decoding applied to position prediction from ensemble firing patterns of rat hippocampal place cells. J Neurosci 18:7411–7425

Carmena JM et al (2003) Learning to control a brain-machine interface for reaching and grasping by primates. PLoS Biol 1:193–208

Chapin JK, Moxon KA, Markowitz RS, Nicolelis MAL (1999) Real-time control of a robot arm using simultaneously recorded neurons in the motor cortex. Nat Neurosci 2:664–670

Chase SM, Schwartz AB, Kass RE (2009) Bias, optimal linear estimation, and the differences between open-loop simulation and closed-loop performance of spiking-based brain-computer interface algorithms. Neural Netw 22:1203–1213

Crammond DJ, Kalaska JF (1994) Modulation of preparatory neuronal activity in dorsal premotor cortex due to stimulus-response compatibility. J Neurophysiol 71:1281–1284

Crammond DJ, Kalaska JF (1996) Differential relation of discharge in primary motor cortex and premotor cortex to movements versus actively maintained postures during a reaching task. Exp Brain Res 108:45–61

Crammond DJ, Kalaska JF (2000) Prior information in motor and premotor cortex: activity during the delay period and effect on pre-movement activity. J Neurophysiol 84:986–1005

Crutcher MD, Russo GS, Ye S, Backus DA (2004) Target-, limb-, and context-dependent neural activity in the cingulate and supplementary motor areas of the monkey. Exp Brain Res 158:278–288

Dempster AP, Laird NM, Rubin DB (1977) Maximum likelihood from incomplete data via the EM algorithm. J Roy Statist Soc B 39:1–38

Eden UT, Frank LM, Barbieri R, Solo V, Brown EN (2004) Dynamic analysis of neural encoding by point process adaptive filtering. Neural Comput 16:971–998

Ganguly K, Carmena JM (2009) Emergence of a stable cortical map for neuroprosthetic control. PLoS Biol 7:1–13

Hochberg LR et al (2006) Neuronal ensemble control of prosthetic devices by a human with tetraplegia. Nature 442:164–171

Hocherman S, Wise SP (1991) Effects of hand movement path on motor cortical activity in awake, behaving rhesus monkeys. Exp Brain Res 83:285–302

Jong PD, Mackinnon MJ (1988) Covariances for smoothed estimates in state space models. Biometrika 75:601–602

Kettner RE, Marcario JK, Port NL (1996) Control of remembered reaching sequences in monkey. II. Storage and preparation before movement in motor and premotor cortex. Exp Brain Res 112:347–358

Kim S-P, Simeral JD, Hochberg LR, Donoghue JP, Black MJ (2008) Neural control of computer cursor velocity by decoding motor cortical spiking activity in humans with tetraplegia. J Neural Eng 5:455–476

Kurata K (1993) Premotor cortex of monkeys: Set- and movement-related activity reflecting amplitude and direction of wrist movements. J Neurophysiol 69:187–200

Li Z et al (2009) Unscented Kalman filter for brain-machine interfaces. PLoS ONE 4:1–18

Lu X, Ashe J (2005) Anticipatory activity in primary motor cortex codes memorized movement sequences. Neuron 45:967–973

Messier J, Kalaska JF (2000) Covariation of primate dorsal premotor cell activity with direction and amplitude during a memorized-delay reaching task. J Neurophysiol 84:152–165

Moritz CT, Perlmutter SI, Fetz EE (2008) Direct control of paralysed muscles by cortical neurons. Nature 456:639–643

Mulliken GH, Musallam S, Andersen RA (2008) Decoding trajectories from posterior parietal cortex ensembles. J Neurosci 28:12913–12926

Musallam S, Corneil BD, Greger B, Scherberger H, Andersen RA (2004) Cognitive control signals for neural prosthetics. Science 305:258–262

Mushiake H, Inase M, Tanji J (1990) Selective coding of motor sequence in the supplementary motor area of the monkey cerebral cortex. Exp Brain Res 82:208–210

Mushiake H, Saito N, Sakamoto K, Itoyama Y, Tanji J (2006) Activity in the lateral prefrontal cortex reflects multiple steps of future events in action plans. Neuron 50:631–641

Nakajima T, Hosaka R, Mushiake H, Tanji J (2009) Covert representation of second-next movement in the pre-supplementary motor area of monkeys. J Neurophysiol 101:1883–1889

Ninokura Y, Mushiake H, Tanji J (2003) Representation of the temporal order of visual objects in the primate lateral prefrontal cortex. J Neurophysiol 89:2868–2873

Ohbayashi M, Ohki K, Miyashita Y (2003) Conversion of working memory to motor sequence in the monkey premotor cortex. Science 301:233–236

Saito N, Mushiake H, Sakamoto K, Itoyama Y, Tanji J (2005) Representation of immediate and final behavioral goals in the monkey prefrontal cortex during an instructed delay period. Cereb Cortex 15:1535–1546

Santhanam G, Ryu SI, Yu BM, Afshar A, Shenoy KV (2006) A high-performance brain-computer interface. Nature 442:195–198

Serruya MD, Hatsopoulos NG, Paninski L, Fellows MR, Donoghue JP (2002) Instant neural control of a movement signal. Nature 416:141–142

Shanechi MM, Hu RC, Powers M, Wornell GW, Brown EN, Williams ZM (2012a) Neural population partitioning and a concurrent brain-machine interface for sequential motor function. Nat Neurosci 15:1715–1722

Shanechi MM, Wornell GW, Williams ZM, Brown EN (2012b) Feedback-controlled parallel point process filter for estimation of goal-directed movements from neural signals. IEEE Trans Neural Syst Rehabil Eng. doi:10.1109/TNSRE.2012.2221743

Shanechi MM, Williams ZM, Wornell GW, Hu RC, Powers M, Brown EN (2013) A Real-time brain-machine interface combining motor target and trajectory intent using an optimal feedback control design. PLoS ONE 8:e59049.

Shanechi MM, Hu RC, Williams ZM (2014) A cortical–spinal prosthesis for targeted limb movement in paralysed primate avatars. Nat Commun 5:3237. doi:10.1038/ncomms4237.

Shima K, Tanji J (2000) Neuronal activity in the supplementary and presupplementary motor areas for temporal organization of multiple movements. J Neurophysiol 84:2148–2160

Shima K, Isoda M, Mushiake H, Tanji J (2007) Categorization of behavioural sequences in the prefrontal cortex. Nature 445:315–318

Smith AC, Brown EN (2003) Estimating a state-space model from point process observations. Neural Comput 15:965–991

Smith AC et al (2010) State-space algorithms for estimating spike rate functions. Comput Intell Neurosci 2010

Tanji J, Shima K (1994) Role for supplementary motor area cells in planning several movements ahead. Nature 371:413–416

Taylor DM, Tillery SIH, Schwartz AB (2002) Direct cortical control of 3D neuroprosthetic devices. Science 296:1829–1832

Truccolo W, Eden UT, Fellows MR, Donoghue JP, Brown EN (2005) A point process framework for relating neural spiking activity to spiking history, neural ensemble, and extrinsic covariate effects. J Neurophysiol 93:1074–1089

Velliste M, Perel S, Spalding MC, Whitford AS, Schwartz AB (2008) Cortical control of a prosthetic arm for self-feeding. Nature 453:1098–1101

Wessberg J et al (2000) Real-time prediction of hand trajectory by ensembles of cortical neurons in primates. Nature 408:361–365

Wolpaw JR, McFarland DJ (2004) Control of a two-dimensional movement signal by a noninvasive brain-computer interface in humans. Proc Natl Acad Sci USA 101:17849–17854

fMRI-Guided Subdural Visual Motion BCI with Minimal Invasiveness

Dan Zhang, Huaying Song, Rui Xu and Bo Hong

Abstract Electrocorticography (ECoG) is a promising technology for high performance brain-computer interfaces (BCIs). To implement practical ECoG based BCIs, minimizing the invasiveness of the electrode implantation is critical. In this study, we advanced our recently proposed 'N200 speller' BCI paradigm that utilizes the attentional modulation of visual motion response. Non-invasive functional magnetic resonance imaging (fMRI) was employed to localize the visual motion processing regions. The subdural electrodes within these fMRI defined regions were associated with a negative deflection around 200 ms post-stimulus, and a power increase of the high gamma (60–140 Hz) frequency range around 100–500 ms post-stimulus, when the corresponding visual motion stimuli were attended. In subsequent BCI analyses, these electrodes showed top classification accuracies among all electrodes, suggesting the optimal locations for electrode implantation can be determined prior to surgery using fMRI imaging. Our findings demonstrate the feasibility of implementing a minimally invasive ECoG based N200 speller.

Keywords Electrocorticography · Visual motion processing · N200 · High gamma · Functional magnetic resonance imaging

1 Introduction

Electrocorticography (ECoG) has attracted increasing interest as a neuroimaging approach for advanced brain-computer interfaces (BCIs) over the past decade. Compared to EEG, ECoG has two major advantages for implementing

D. Zhang · H. Song · R. Xu · B. Hong (✉)
Department of Biomedical Engineering, School of Medicine, Tsinghua University, Beijing, China
e-mail: hongbo@tsinghua.edu.cn

C. Guger et al. (eds.), *Brain-Computer Interface Research*, SpringerBriefs in Electrical and Computer Engineering, DOI 10.1007/978-3-319-09979-8_9

advanced BCIs. First, the spatial resolution of ECoG is much higher than that of EEG. ECoG records signals originating from brain tissues directly beneath the electrode surface (surface area of 1–10 mm^2) with little influence from adjacent tissues (Bullock et al. 1995; Nunez and Srinivasan 2006), whereas EEG's spatial resolution is at a multi-centimeter scale due to volume conduction of currents through tissues in the head. Such a fine spatial resolution makes ECoG ideal for capturing the cortical dynamics of sensory and cognitive functions that originate from relatively small brain regions (Liu et al. 2009; Mesgarani and Chang 2012; Vinjamuri et al. 2011). Second, low voltage, high frequency brain activity that is barely detectable in scalp EEG is readily observed in invasive ECoG recordings (Leuthardt et al. 2004). In the past few years, ECoG BCIs have achieved promising results using brain signals extracted from the motor cortex (Kubanek et al. 2009; Miller et al. 2010; Vinjamuri et al. 2011), language-related brain regions (Leuthardt et al. 2011; Pei et al. 2011a), and auditory and visual cortex (Brunner et al. 2011; Wilson et al. 2006).

Nevertheless, real-life application of ECoG BCI demands mitigation of its invasive nature by minimizing both the size of the involved brain regions and the number of implanted electrodes. To date, ECoG BCI studies have been carried out with epilepsy patients, who underwent open skull surgery and implantation of large electrode arrays for clinical purposes. However, surgery of this type is both unnecessary and risky for most potential BCI users (e.g. patients with amyotrophic lateral sclerosis). Instead, electrodes for BCI purposes can be inserted through a burr hole into the brain, thus implementing a 'minimally invasive' BCI, given that sufficient information can be extracted within a limited cortical area.

2 Motivation for a Minimally Invasive N200 Speller

Here we propose that the recently developed 'N200 speller' using motion onset visual evoked potentials (mVEPs) may serve as a suitable candidate for building minimally invasive BCIs (Guo et al. 2008; Jin et al. 2012). The N200 speller utilizes the modulation effect of mVEPs by overt attention (i.e., eye gaze) for a spelling application (Fig. 1a). The attended visual motion stimuli elicit a more negative peak around 200 ms post-stimulus (N200) over parietal-occipital areas than unattended stimuli, and BCI user intent is recognized based on this difference. BCIs based on mVEPs can be considered as an extension of the widely studied P300 BCI (Donchin et al. 2000; Farwell and Donchin 1988), which utilizes an attention-related positive event-related potential (ERP) peaking around 300 ms (P300) over the parietal cortex elicited by the attended visual flash stimuli. In terms of invasiveness, mVEP BCI is a better candidate than P300 BCIs, as visual motion processing (reflected by mVEPs in EEG) is believed to be highly focused in a small brain region known as the human middle temporal (MT) complex (Fig. 1b) (DeYoe et al. 1996; Huk et al. 2002; Zeki et al. 1991).

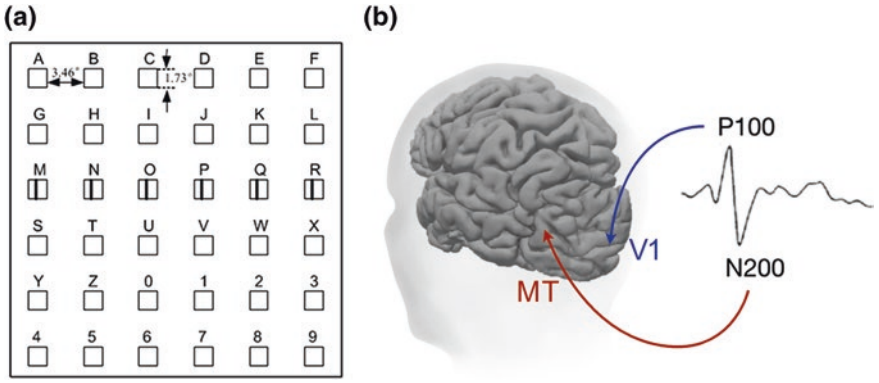

Fig. 1 The N200 speller BCI. **a** The N200 speller interface with the visual motion stimulus in the *third row*; **b** the hypothesized neural generator of the N200 component in the human MT complex

In the N200 speller, visual motion stimuli were presented as brief rightward motion (150 ms) of vertical bars in the rectangle regions beneath the symbols. Similar to the classical P300 speller, the visual motion stimuli were presented either by column or by row. The column and row stimuli corresponding to the attended symbol elicit stronger visual motion responses, constituting the basis for BCI classification. Hereby, a 36-choice spelling application can be realized on the basis of a series of binary decisions, based on whether the stimulus presented at certain time point is attended or not, by taking advantage of the visual speller design (Farwell and Donchin 1988; Hong et al. 2009). Compared with other types of ECoG BCIs for motor and speech decoding (Kubanek et al. 2009; Leuthardt et al. 2004, 2011), relatively less information is required for the operation of the N200 speller.

The N200 speller may further benefit from ECoG recordings with a broader frequency band response. Specifically, BCI classification may be facilitated by including the high gamma responses as a new feature, since visual motion processing is reflected in both low frequency mVEP responses (Matsumoto et al. 2004) and high frequency (50–120 Hz) power increases (Rauschecker et al. 2011). In the ECoG-based visual motion BCI, we expected to see not only an attention-related negative peak around 200 ms post-stimulus, but also a stronger high gamma response by the attended visual motion stimuli than the unattended ones.

3 ECoG BCI Experiment

Figure 1a shows the stimulation interface of the N200 speller. Visual motion stimuli were displayed on a 17-in. LCD monitor (DELL FP1708, USA) with 60 Hz refresh rate and 1,280 × 1,024 resolution. The viewing distance was 50 cm.

Patients participated in two offline experiment sessions. Each session consisted of six blocks, in which the patients were instructed to attend to one of the virtual buttons as a target. The patients were required to mentally count the number of times the moving bar appeared in the attended button without moving their mouths. During one block, the six column stimuli and the six row stimuli were presented in a random order and were repeatedly presented either 10 or 15 times. The repetition number was decided prior to the experiment, depending on the patients' physical state and willingness. In both sessions, the six virtual buttons on the diagonal of the speller matrix from top-left to bottom-right were sequentially used as the attentional target. A trial was defined as the EEG recording epoch relative to the stimulation of a single row or column stimulus, with trials of attended stimuli designated as target trials and trials of unattended stimuli as non-target trials.

To localize the functional regions of visual motion processing, patients participated in an additional fMRI experiment prior to their electrode implantation. A classical localizer paradigm for visual motion area MT (middle temporal) was employed (Huk et al. 2002). The patients passively viewed either static dots or center-out moving dots while having the fMRI scan (Fig. 2a).

Five epilepsy patients with subdural ECoG electrode coverage of human MT complex participated in this study. Two subjects (subject A and B) went through the fMRI experiment before electrode implantation surgery; the other three patients (subject C, D, and E) only had a structural MRI scan to evaluate their individual brain structures. The BCI experiment was carried out later in an offline manner, with ECoG recording. This study was approved by the Institutional Review Board of the hospital affiliated with Tsinghua University.

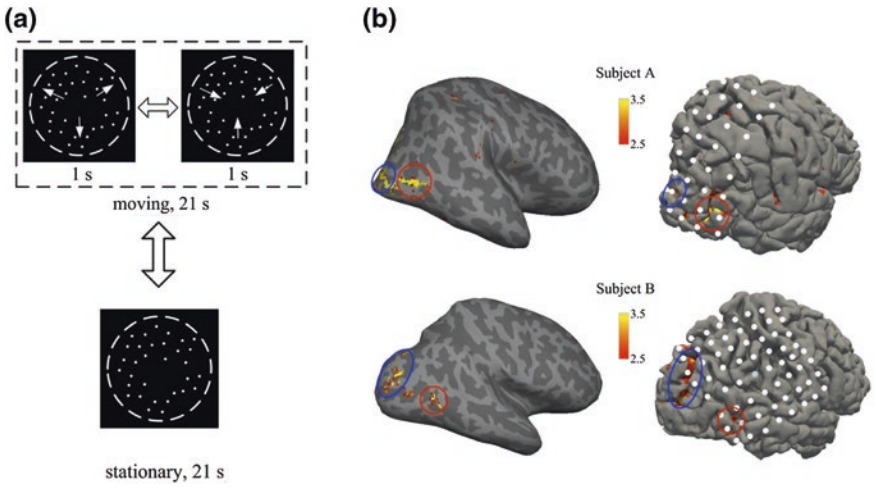

Fig. 2 **a** Visual stimuli used in the fMRI experiment for localizing the visual motion processing related brain regions; **b** fMRI BOLD activation patterns shown on inflated brain surfaces (*left column*) and on pial surfaces (*right column*, for the convenience of displaying the ECoG electrodes). The *red* and *blue circles* were used to mark out the BOLD activation of the MT complex and the early visual cortex, respectively

4 Intracranial Responses Within the fMRI Defined Visual Motion Regions

As shown in Fig. 2b, fMRI showed an enhancement of the blood oxygen level-dependent (BOLD) signal in the parietal-temporal-occipital junction (possibly the human MT complex), as well as part of the occipital cortices that is likely to be the early visual cortex. Within the fMRI-defined visual motion regions, the typical ECoG response is shown in Fig. 3. The ECoG responses were comprised of both a low frequency event-related potential (ERP) and a power increase at the high gamma frequency range (60–140 Hz). The observed negative deflection of the ERP amplitude around 200 ms after the stimulus onset resembles the scalp recorded N200 component in mVEPs, providing further evidence for the neural generator of the scalp N200 from the visual motion processing regions. More importantly, the high gamma power increase from post-stimulus 100–500 ms associated with overt visual attention suggests possibly distinct neural mechanisms underlying ERPs and high gamma responses. Therefore, the high gamma responses may have unique contribution to BCI classification.

The ERPs and high gamma responses can also be compared based on their spatial distributions. To describe the ERP/high gamma responses associated with the overtly attended visual motion stimuli, the squared Pearson product-moment correlation coefficient (r^2) was employed to characterize the difference in amplitude distribution between task and baseline conditions of the target trials (Pei et al. 2011b; Sheikh et al. 2003; Wonnacott and Wonnacott 1977). Here, we took the mean area under the post-stimulus 500 ms of target ERP/high gamma power waveforms to represent the task condition, and the mean area under the

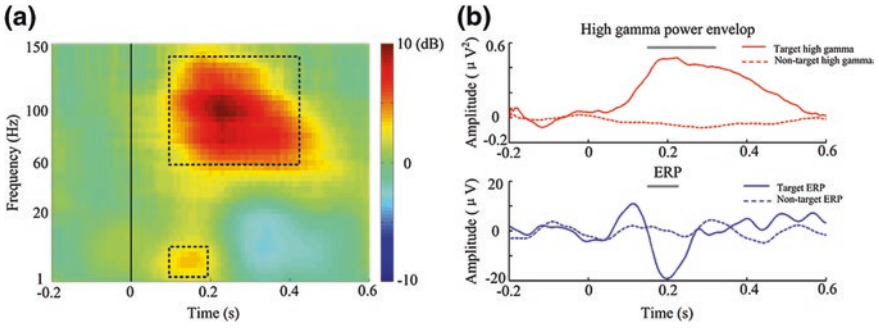

Fig. 3 **a** Typical time-frequency response to overtly attended visual motion stimuli. The frequency range and the time period of significant differences ($p < 0.05$, paired t-test, p-values corrected using the false detection rate (FDR) method) between the attended condition and the baseline are outlined by the rectangular boxes. The electrode was from patient B, placed over the parietal-temporal-occipital junctions (marked by *arrow* in Fig. 3a). **b** Averaged visual motion-related high gamma power envelopes and ERPs for target and non-target trials. The *grey line* indicates the time periods with significant differences between the target responses and the corresponding baseline ($p < 0.05$, paired t-test, FDR corrected)

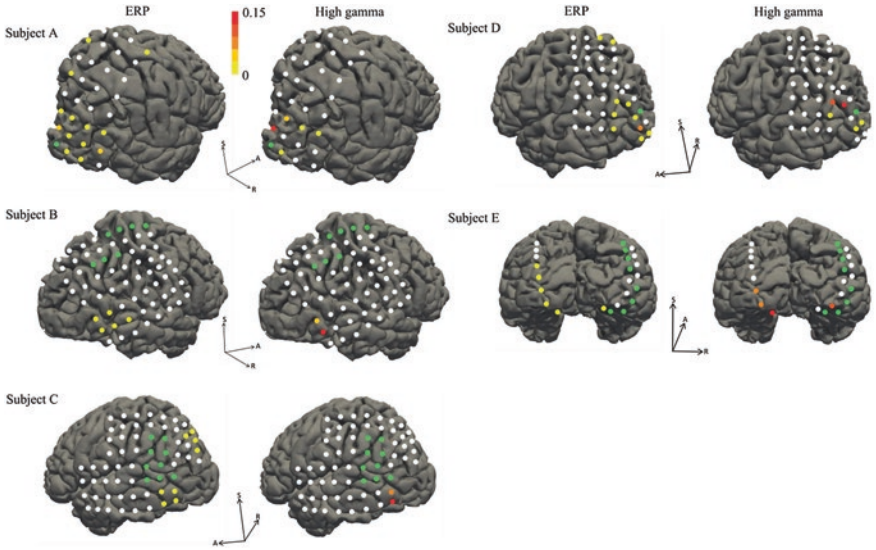

Fig. 4 r^2 values of ERP/high gamma activity, with *red* corresponding to the highest r^2 values and *yellow* to the lowest r^2 values. The r^2 values are only shown on electrodes with statistically significant responses, while other electrodes are marked in *white*. The seizure electrodes excluded for further analysis are marked in *green*

pre-stimulus 200 ms ERP/high gamma power to represent the baseline condition. As shown in Fig. 4, the ERP responses are more widely distributed, whereas the high gamma responses had a much more restricted spatial distribution, covering either the parietal-temporal-occipital junction, or more posterior part of the occipital cortex. Moreover, the high gamma responses elicited by the target stimuli were more prominent, as higher r^2 values were obtained compared to target ERP responses (Fig. 4, warmer color for larger r^2 value). The relatively restricted spatial distribution of the high gamma responses is in accordance with previous intracranial studies on motor functions, in which the authors concluded that the topographical distribution of high gamma responses were more discrete and somatotopically specific (Crone et al. 1998a, b). Hereby, our findings suggest that the observed high gamma responses are likely to be functionally specific for visual motion processing.

5 Feasibility of an fMRI Guided Minimally Invasive BCI

The major concern for a practical minimal invasive BCI is whether the position for electrode implantation can be determined prior to surgery using non-invasive methods. In previous ECoG BCI studies, the ECoG electrodes used for BCI classification were mostly selected afterwards from electrode grids placed purely for

diagnostic purposes (Brunner et al. 2011; Chang et al. 2011). Intuitively, electrode positions for BCIs could be determined based on the anatomical landmarks of the human brain, then placed over the intended brain regions using intraoperative stereotactic navigation. Such procedures have been successfully applied in studies focusing on the primary motor cortex for movement decoding (Leuthardt et al. 2009) and the posterior superior temporal gyrus for speech reconstruction (Chang et al. 2010; Pasley et al. 2012). However, anatomy based electrode localization does not ensure an accurate targeting of functional cortical areas, which is the basis for BCI decoding. Alternatively, non-invasive functional magnetic resonance imaging (fMRI) technology may provide useful information for determining the electrode locations of visual motion BCI prior to the electrode implantation. The direct functional mapping of fMRI on an individual basis is ideal for potential BCI users who may have brain functions remapped due to disease or injuries (Johansson 2011; Murphy and Corbett 2009). Although ECoG and fMRI signals reflect brain response in different modalities, it has been reported that gamma band responses in motor cortex, as well as theta and gamma band responses in the human MT complex, are correlated with fMRI signals in their corresponding brain regions (Hermes et al. 2012; Rauschecker et al. 2011).

Here, we demonstrate the feasibility of a minimally invasive visual motion BCI speller by comparing the location of the ECoG electrode selected for BCI classification with the fMRI activation map. Using both the ERP and the high gamma response as features for BCI classification (averaging over three trials, binary classification of target vs. non-target) (Zhang et al. 2013), all the single-electrode accuracies (attended vs. unattended) of subject A and B are shown in Fig. 5a. The electrodes with the highest accuracies (marked by the red asterisks) were within the fMRI-defined regions (shown as black bars; see Fig. 2b for the electrode locations). Although an fMRI scan was not performed for the other three patients (C, D, and E), the selected single electrodes with best high gamma response were also confirmed to be located either on the MT area or the secondary visual cortex, according to anatomical labels. The spatial locations of the best BCI electrodes are plotted in Fig. 5b, and the coordinates of the best BCI electrodes for all patients in Talairach space and the corresponding anatomical labels are given in Table 1. The best BCI electrodes for patients C and E were located in the early visual cortex, whereas the best electrode for patient D was near middle temporal gyrus, which is in the vicinity of human MT complex.

For all five patients, the average classification accuracies from the best single electrodes were 75.48 ± 4.18 % when using the ERP feature and 81.24 ± 6.23 % when using the high gamma feature. By combining the ERP and high gamma features together, significantly higher classification accuracies were achieved compared to the results using ERP/high gamma features alone (Fig. 5c, combined vs. ERP: 84.22 ± 5.54 % vs. 75.48 ± 4.18 %, $p < 0.005$, paired t-test; combined vs. high gamma: 84.22 ± 5.54 % vs. 81.24 ± 6.23 %, $p < 0.05$, paired t-test). In addition, high gamma features resulted in better classification accuracies than ERP features (81.24 ± 6.23 % vs. 75.48 ± 4.18 %, $p < 0.05$, paired t-test), which was consistent with the r^2 results. The superior

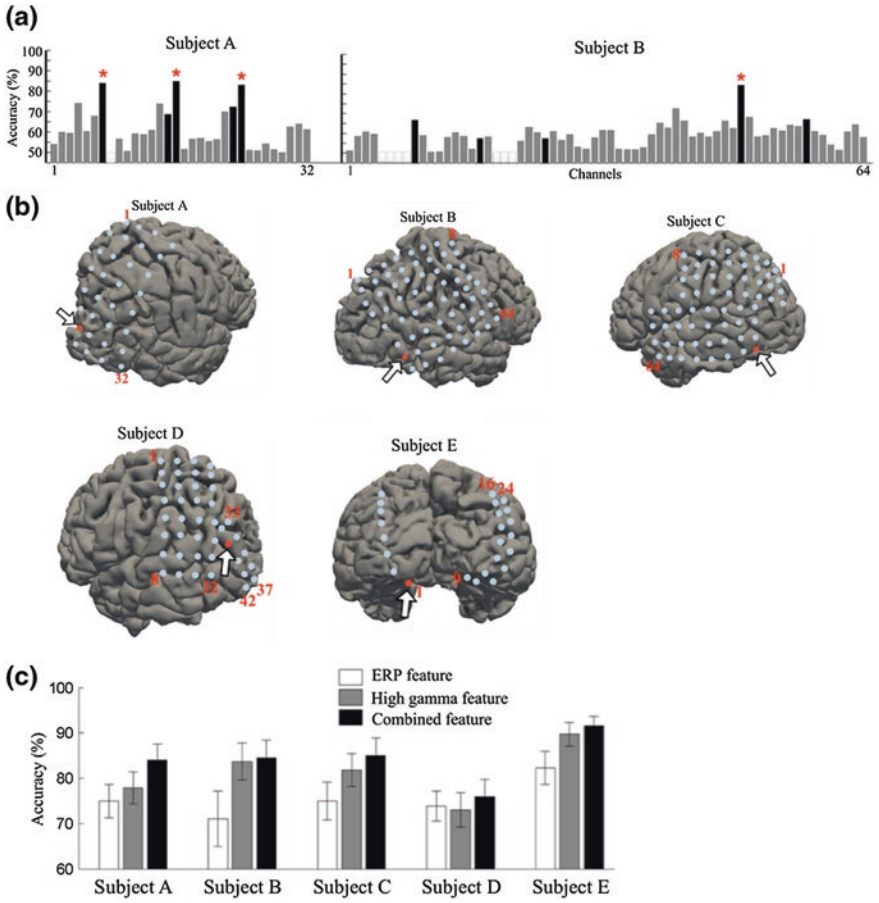

Fig. 5 **a** Single-electrode classification accuracy for subject A and B. Electrodes within the fMRI-defined regions are shown as *black bars*. **b** The spatial locations of the best BCI electrodes for individual patients, marked in *red*. **c** Individual classification accuracy using ERP features, high gamma features or combined features

Table 1 Talairach coordinates of the electrodes selected for BCI classification

Subject	Talairach coordinates of the selected electrodes	
A	Lateral occipital	(25.6, −89.1, 22.2)
B	Lateral occipital-middle temporal	(58.2, −63.9, 3.2)
C	Lateral occipital	(−51.4, −70.6, −9.3)
D	Lateral occipital-middle temporal	(−38.2, −80.5, 25.7)
E	Lateral occipital	(−10.6, −97.4, −14.5)

classification accuracy suggests that high gamma responses indeed contribute to BCI classification and sufficient information can be obtained for BCI control using a single-channel design.

6 Concluding Remarks

In the present study, we investigated the possibility of implementing a minimally invasive BCI through a novel 'N200 speller' BCI paradigm. The ECoG electrodes within the fMRI-defined visual motion processing regions were found to show both strong ERP responses and high gamma power increases associated with overt visual attention. Using both ERP and high gamma features for BCI classification, the electrodes with top classification accuracies were located within the fMRI-defined or anatomically defined visual motion regions. Our study demonstrates an implementation of an ECoG based visual motion BCI with a single subdural channel that can be implanted in a minimally invasive way employing pre-operative fMRI for target region localization.

Although the present study was conducted with epilepsy patients with electrode grids implanted, our results support a practical ECoG BCI for other patients (Fig. 6). A minimally invasive BCI can be implemented by inserting the single subdural electrode through a burr hole onto the surface of cortex that the non-invasive fMRI identifies as active during visual motion tasks. The reference electrode and the ground electrode can also be placed through the same burr hole, but on the outer surface of the skull. The BCI module, including an EEG amplifier and even a digital signal processing unit, can be implanted inside the body as well. Similar to impulse generators of a deep brain stimulation device package, such a unit can be placed under the skin of the chest, below the collarbone. The recognized mental states (i.e., which letter on the virtual keyboard is attended) can then

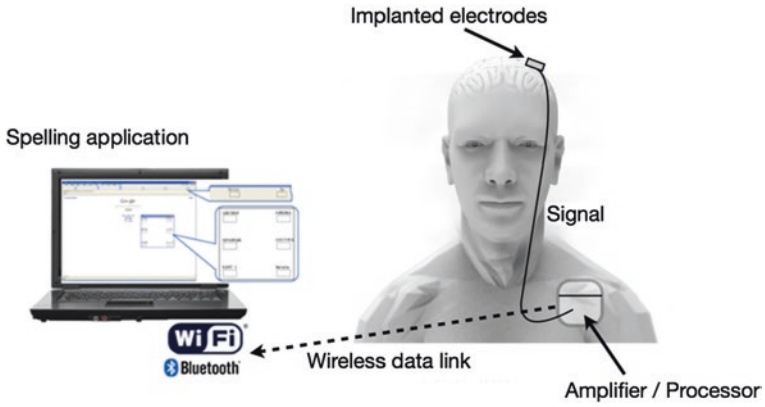

Fig. 6 Outlook: a fully implanted minimally invasive BCI at work

be transferred wirelessly to external communication devices, thus realizing a fully implanted BCI. Together with the durable and stable ECoG signal quality for long-term usage (Chao et al. 2010; Sperling 1997), a minimally invasive ECoG BCI is a promising tool for re-establishing a communication channel for disabled people.

Acknowledgments This work was supported by the National Natural Science Foundation of China under grant #61071003, National Program on Key Basic Research Projects of China (2011CB933204), and China Postdoctoral Science Foundation.

References

Brunner P, Ritaccio AL, Emrich JF, Bischof H, Schalk G (2011) Rapid communication with a P300 matrix speller using electrocorticographic signals (ECoG). Front Neurosci 5:5

Bullock TH, McClune MC, Achimowicz JZ, Iragui-Madoz VJ, Duckrow RB, Spencer SS (1995) EEG coherence has structure in the millimeter domain: subdural and hippocampal recordings from epileptic patients. Electroencephalogr Clin Neurophysiol 95:161–177

Chang EF, Rieger JW, Johnson K, Berger MS, Barbaro NM, Knight RT (2010) Categorical speech representation in human superior temporal gyrus. Nat Neurosci 13:1428–1432

Chang EF, Edwards E, Nagarajan SS, Fogelson N, Dalal SS, Canolty RT, Kirsch HE, Barbaro NM, Knight RT (2011) Cortical spatio-temporal dynamics underlying phonological target detection in humans. J Cogn Neurosci 23:1437–1446

Chao ZC, Nagasaka Y, Fujii N (2010) Long-term asynchronous decoding of arm motion using electrocorticographic signals in monkeys. Front Neuroeng 3:3

Crone NE, Miglioretti DL, Gordon B, Lesser RP (1998a) Functional mapping of human sensorimotor cortex with electrocorticographic spectral analysis. II. Event-related synchronization in the gamma band. Brain 121(Pt 12):2301–2315

Crone NE, Miglioretti DL, Gordon B, Sieracki JM, Wilson MT, Uematsu S, Lesser RP (1998b) Functional mapping of human sensorimotor cortex with electrocorticographic spectral analysis. I. Alpha and beta event-related desynchronization. Brain 121(Pt 12):2271–2299

DeYoe EA, Carman GJ, Bandettini P, Glickman S, Wieser J, Cox R, Miller D, Neitz J (1996) Mapping striate and extrastriate visual areas in human cerebral cortex. Proc Natl Acad Sci USA 93:2382–2386

Donchin E, Spencer KM, Wijesinghe R (2000) The mental prosthesis: assessing the speed of a P300-based brain-computer interface. IEEE Trans Rehabil Eng 8:174–179

Farwell LA, Donchin E (1988) Talking off the top of your head: toward a mental prosthesis utilizing event-related brain potentials. Electroencephalogr Clin Neurophysiol 70:510–523

Guo F, Hong B, Gao X, Gao S (2008) A brain-computer interface using motion-onset visual evoked potential. J Neural Eng 5:477–485

Hermes D, Miller KJ, Vansteensel MJ, Aarnoutse EJ, Leijten FS, Ramsey NF (2012) Neurophysiologic correlates of fMRI in human motor cortex. Hum Brain Mapp33:1689–1699

Hong B, Guo F, Liu T, Gao X, Gao S (2009) N200-speller using motion-onset visual response. Clin Neurophysiol 120:1658–1666

Huk AC, Dougherty RF, Heeger DJ (2002) Retinotopy and functional subdivision of human areas MT and MST. J Neurosci 22:7195–7205

Jin J, Allison BZ, Wang X, Neuper C (2012) A combined brain-computer interface based on P300 potentials and motion-onset visual evoked potentials. J Neurosci Methods 205:265–276

Johansson BB (2011) Current trends in stroke rehabilitation. A review with focus on brain plasticity. Acta Neurol Scand 123:147–159

Kubanek J, Miller KJ, Ojemann JG, Wolpaw JR, Schalk G (2009) Decoding flexion of individual fingers using electrocorticographic signals in humans. J Neural Eng 6:66001

Leuthardt EC, Schalk G, Wolpaw JR, Ojemann JG, Moran DW (2004) A brain-computer interface using electrocorticographic signals in humans. J Neural Eng 1:63–71

Leuthardt EC, Freudenberg Z, Bundy D, Roland J (2009) Microscale recording from human motor cortex: implications for minimally invasive electrocorticographic brain-computer interfaces. Neurosurg Focus 27:E10

Leuthardt EC, Gaona C, Sharma M, Szrama N, Roland J, Freudenberg Z, Solis J, Breshears J, Schalk G (2011) Using the electrocorticographic speech network to control a brain-computer interface in humans. J Neural Eng 8:36004

Liu H, Agam Y, Madsen JR, Kreiman G (2009) Timing, timing, timing: fast decoding of object information from intracranial field potentials in human visual cortex. Neuron 62:281–290

Matsumoto R, Ikeda A, Nagamine T, Matsuhashi M, Ohara S, Yamamoto J, Toma K, Mikuni N, Takahashi J, Miyamoto S, Fukuyama H, Shibasaki H (2004) Subregions of human MT complex revealed by comparative MEG and direct electrocorticographic recordings. Clin Neurophysiol 115:2056–2065

Mesgarani N, Chang EF (2012) Selective cortical representation of attended speaker in multi-talker speech perception. Nature 485:233–236

Miller KJ, Schalk G, Fetz EE, den Nijs M, Ojemann JG, Rao RP (2010) Cortical activity during motor execution, motor imagery, and imagery-based online feedback. Proc Natl Acad Sci USA 107:4430–4435

Murphy TH, Corbett D (2009) Plasticity during stroke recovery: from synapse to behaviour. Nat Rev Neurosci 10:861–872

Nunez PL, Srinivasan R (2006) Electric fields of the brain: the neurophysics of EEG. Oxford University Press, Oxford

Pasley BN, David SV, Mesgarani N, Flinker A, Shamma SA, Crone NE, Knight RT, Chang EF (2012) Reconstructing speech from human auditory cortex. PLoS Biol 10:1001251

Pei X, Barbour DL, Leuthardt EC, Schalk G (2011a) Decoding vowels and consonants in spoken and imagined words using electrocorticographic signals in humans. J Neural Eng 8:46028

Pei X, Leuthardt EC, Gaona CM, Brunner P, Wolpaw JR, Schalk G (2011b) Spatiotemporal dynamics of electrocorticographic high gamma activity during overt and covert word repetition. Neuroimage 54:2960–2972

Rauschecker AM, Dastjerdi M, Weiner KS, Witthoft N, Chen J, Selimbeyoglu A, Parvizi J (2011) Illusions of visual motion elicited by electrical stimulation of human MT complex. PLoS ONE 6:e21798

Sheikh H, McFarland DJ, Sarnacki WA, Wolpaw JR (2003) Electroencephalographic (EEG)-based communication: EEG control versus system performance in humans. Neurosci Lett 345:89–92

Sperling MR (1997) Clinical challenges in invasive monitoring in epilepsy surgery. Epilepsia 38(Suppl 4):S6–S12

Vinjamuri R, Weber DJ, Mao ZH, Collinger JL, Degenhart AD, Kelly JW, Boninger ML, Tyler-Kabara EC, Wang W (2011) Toward synergy-based brain-machine interfaces. IEEE Trans Inf Technol Biomed 15:726–736

Wilson JA, Felton EA, Garell PC, Schalk G, Williams JC (2006) ECoG factors underlying multimodal control of a brain-computer interface. IEEE Trans Neural Syst Rehabil Eng 14:246–250

Wonnacott TH, Wonnacott R (1977) Introductory statistics, 3rd edn. Wiley, New York

Zeki S, Watson JD, Lueck CJ, Friston KJ, Kennard C, Frackowiak RS (1991) A direct demonstration of functional specialization in human visual cortex. J Neurosci 11:641–649

Zhang D, Song H, Xu R, Lin Z, Hong B (2013) Toward a minimally invasive brain-computer interface using single subdural electrode: a visual speller study. NeuroImage 71:30–41

Multi-command Tactile and Bone-Conduction-Auditory Brain-Computer Interface

Tomasz M. Rutkowski, Hiromu Mori and Koichi Mori

Abstract We study the extent to which vibrotactile stimuli delivered to the head of a user can serve as a platform for a brain computer interface (BCI) paradigm. Six and ten head position setups are used to evoke combined somatosensory and auditory (via bone-conduction effect) brain responses, in order to define a multimodal tactile and bone-conduction-auditory brain computer interface (tbcaBCI) suitable for ALS-TLS patients with bad vision and suffering from an ear-blocking-syndrome. Experimental results on users performing online tbcaBCI, using stimuli with a moderately fast stimulus-onset-asynchrony (SOA), validate the tbcaBCI paradigm, while the feasibility of the concept is illuminated through information-transfer-rate analyses.

Keywords Tactile and auditory BCI · Somatosensory evoked potentials (SEP) · Auditory evoked potentials (AEP)

1 Introduction

The state of the art BCIs rely mostly on mental, visual and motor imagery paradigms, which require users to have healthy vision and often participate in long training. Recently alternative solutions have been proposed to utilize spatial, auditory

T.M. Rutkowski (✉)
Life Science Center of TARA, University of Tsukuba, Tsukuba, Japan
e-mail: tomek@bci-lab.info

T.M. Rutkowski
RIKEN Brain Science Institute, Wako-shi, Japan

H. Mori
Computer Science Department, University of Tsukuba, Tsukuba, Japan
e-mail: hiromu@bci-lab.info

K. Mori
Research Institute of National Rehabilitation Center for Persons with Disabilities, Tokorozawa, Japan
e-mail: mori-koichi@rehab.go.jp

C. Guger et al. (eds.), *Brain-Computer Interface Research*, SpringerBriefs in Electrical and Computer Engineering, DOI 10.1007/978-3-319-09979-8_10

(Halder et al. 2009; Lelievre and Rutkowski 2013; Rutkowski et al. 2009; Schreuder et al. 2010) or tactile (somatosensory) modalities (Mori et al. 2013a, b, c; Muller-Putz et al. 2006; van der Waal et al. 2012) in order to enhance brain-computer interface comfort or to boost the information-transfer-rate (ITR) (Schreuder et al. 2010) achieved by users. The concept described in this chapter of utilizing the brain's somatosensory (tactile) modality opens up the attractive possibility of targeting the tactile sensory domain, which does not rely on visual stimuli to elicit evoked potentials during visual computer applications or operation of robotic interfaces (prosthetic arm, vehicular robot, smart house appliance, etc.) or visual computer applications. The first successful trial to utilize steady-state somatosensory responses (SSSR) to create a BCI (Muller-Putz et al. 2006) targeted a very low stimulus frequency in a range of 20–31 Hz to elucidate the users' steady-state activity, which was then used to create BCI commands. A very recent report (van der Waal et al. 2012) proposed using a Braille stimulator with a 100 ms long static push stimuli delivered to six fingers to evoke a somatosensory response related P300. Very encouraging results were obtained with 7.8 bit/min on average and 27 bit/min for the best user. Here we propose to combine the two above-mentioned modalities in the tbcaBCI paradigm, which relies on P300 response evoked by the audio and tactile stimuli delivered simultaneously via the vibrotactile exciters attached to the head positions (see Fig. 1),

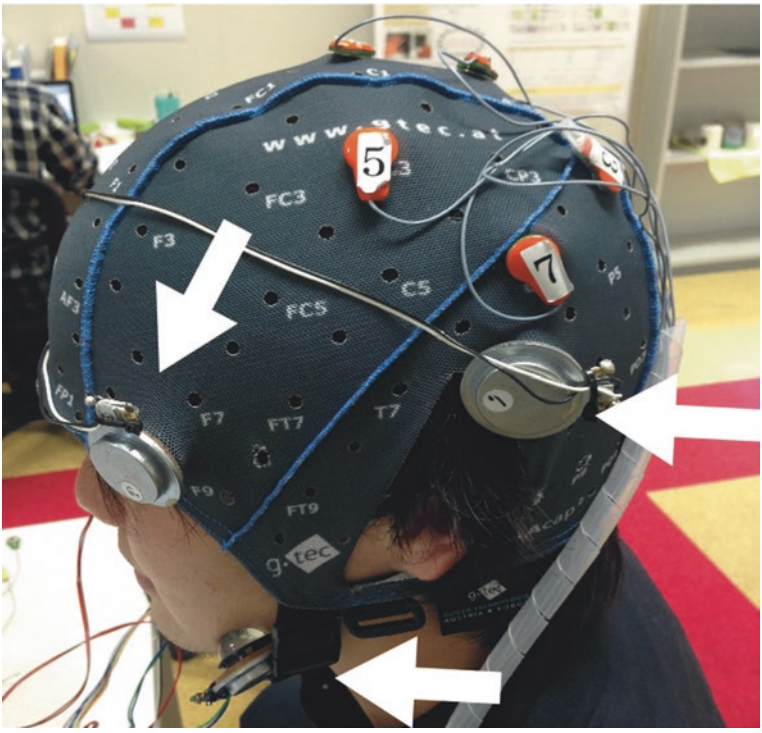

Fig. 1 User's head with EEG cap embedded with dry *g.SAHARA* electrodes (*orange*) and vibrotactile and bone-conduction exciters (indicated by *white arrows*) attached

thus benefiting from the bone-conduction effect for audio. This offers a viable alternative for individuals lacking somatosensory responses from the fingers or torso/chest body locations, which prevents them from utilizing tactile BCI solutions as proposed in Mori et al. (2013a, b), Severens et al. (2013), or for people suffering from the ear-blocking-syndrome (a middle ear effusion/negative pressure) (Gelinas 2007).

2 Materials and Methods

In the experiments described in this chapter, eleven BCI-naive users (mean age 21.82 with standard deviation of 0.87) and two experienced volunteers (mean age 32 with standard deviation of 14.14) took a part. All the experiments were performed at the Life Science Center of TARA, University of Tsukuba, Japan. The psychophysical and online EEG tbcaBCI paradigm experiments were conducted in accordance with WMA Declaration of Helsinki-Ethical Principles for Medical Research Involving Human Subjects. The experimental procedures were approved and designed in agreement with the ethical committee guidelines of the Faculty of Engineering, Information and Systems at the University of Tsukuba, Japan. The BCI-naive users performed the experiments for monetary compensation. The 100 ms long stimuli in the form of sinusoidal waves were delivered to each user's head areas via the tactile exciters *HiWave HIAX19C01-8* working in the range of 300–20,000 Hz. The vibrotactile stimulators were arranged as follows. The pairs of exciters were attached on both sides of the forehead, chin, and behind the ears respectively. During the online tbcaBCI experiments, the EEG signals were captured with a portable wireless EEG amplifier system, *g.MOBIlab+*, using eight dry *g.SAHARA* electrodes from g.tec, Austria. The electrodes were attached to eight electrode sites, *Cz, CPz, P3, P4, C3, C4, CP5,* and *CP6,* as in the 10/10 extended international system (see topographic plot in Fig. 2). The ground and reference electrodes were attached behind the left and right ears respectively. In order to limit electromagnetic interference, the user's hand was also grounded with a conductive armband connected to the amplifier's ground. No electromagnetic interference was observed from the vibrotactile activity on the head. The recorded EEG signals were processed by the in-house enhanced *BCI2000* application using an SWLDA classifier with features drawn from 0 to 600 ms ERP intervals. The sampling rate was set to 256 Hz, with a high pass filter at 0.1 Hz, and low pass filter at 40 Hz. The stimulus-onset-asynchrony (SOA) was 400 ms (250 ms for the two experienced users) and each stimulus lasted 100 ms. The user was instructed to spell six (or ten for experienced users) digit random sequences of numbers ranging from 1–6 (or 1–10), which were represented by the locations of the vibrotactile exciters on the head in each experimental session. Each target was presented five times in a single spelling sequence, and the averages of five ERP responses (single trials) were later used for the classification.

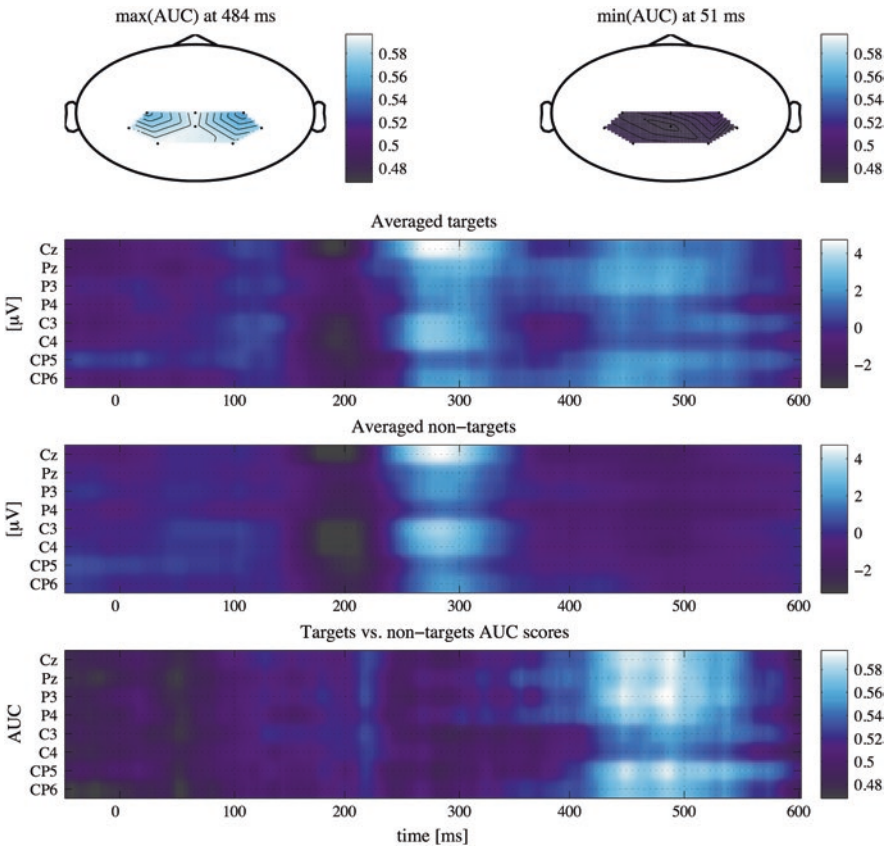

Fig. 2 AUC analysis of tactile and bone-conduction BCI target versus non-target response discrimination. The *top panels* present two topographic head plots with electrode positions and spatial maps of the response at maximum and minimum AUC values as obtained from the *bottom panel* time series depicting this quantity for each electrode separately. The *middle two panels* depict the ERP responses to targets and non-targets together. A resulting AUC analysis of the *two middle panel* plots is presented in the *bottom panel* of the figure

3 Results

The area under the curve (AUC) of the ROC for feature plots marking the most discriminable latencies is depicted in Fig. 2. Topographic plots of the AUC distributions are also presented in Fig. 2, supporting the choice of the eight dry EEG electrodes covering the vertex and the parietal cortex locations. The averaged ERP responses, from each EEG electrode depicted separately, with standard error bars from the eleven BCI–naive users are presented in Fig. 3 for the target and non-target digits. The results of online BCI interfacing sessions are summarized in Table 1 in the form of mean accuracies above the theoretical chance

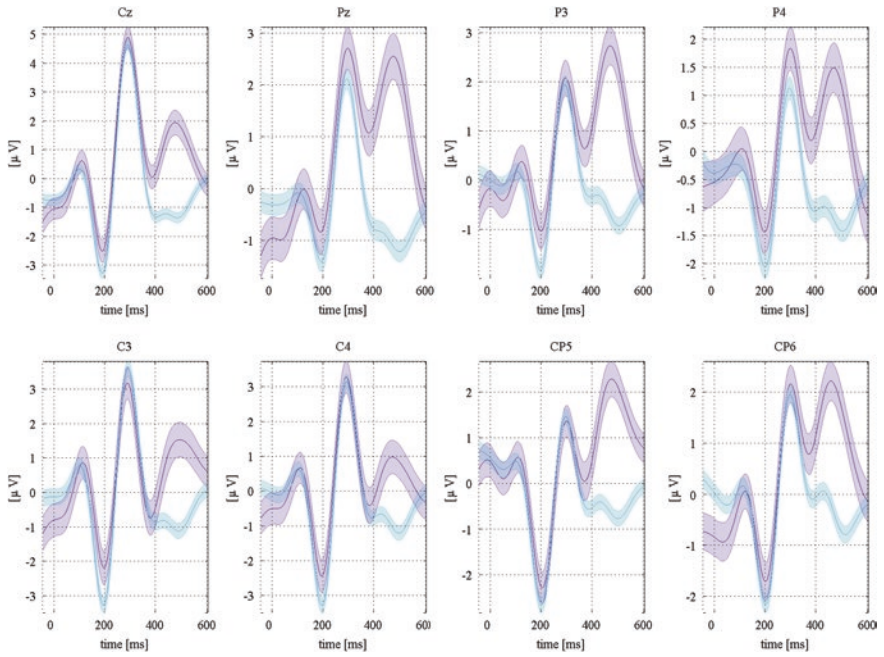

Fig. 3 Grand mean tactile and bone-conduction ERP visualization for all users, together with P300 responses for all electrodes used in the experiment. The eight EEG electrodes are depicted separately. The *purple lines* represent the targets, and the *blue lines* represent the non-targets. The P300 response is clearly visible in the 400–600 ms latency ranges

Table 1 Summary of the online tbcaBCI results with eleven BCI-naive and the two experienced users

Experimental parameter	Naive users	Experienced users
Number of commands	6	10
SOA (ms)	400	250
Number of averaged ERPs	5	5
Mean accuracy (%)	50	65
The best accuracy (%)	100	90
Mean ITR (bit/min)	3.22	7.17
The best ITR (bit/min)	12.90	12.17

level of 16.6 % or 10 %, for BCI-naive and experienced users respectively. In our experiments, only a single BCI-naive user obtained 100 % online spelling accuracy for the six digit sequence with averages of five trials. One user was also unable to attain any control at all, with 0 % accuracy.

These preliminary yet encouraging results are a step forward in the search for the new "non-vision-based" BCI paradigms.

4 Conclusions

This study demonstrated results obtained with a novel six-commands (or ten in case of BCI-experienced users) and the head locations based tbcaBCI paradigm developed and used in experiments with eleven BCI-naive and two experienced "body-able" users. The experiment results obtained in this study confirmed the validity of the tbcaBCI for interactive applications.

The results presented offer a step forward in the development of novel neurotechnology applications. Since the online BCI did not yield high information transfer rates overall, the current paradigm would obviously need improvements and modifications. These needs determine the major lines of study for future research. However, even in its current form, the proposed tbcaBCI can be regarded as a practical solution for ALS-TLS patients (locked into their own bodies despite often intact cognitive functioning), who cannot use vision or auditory based interfaces due to sensory or other disabilities.

We plan to continue this line of the tactile and bone-conduction-auditory BCI research in order to further optimize the signal processing and machine learning (classification) methods. Next, we will test the paradigm with ALS-TLS patients in need for BCI technology.

Acknowledgments This research was supported in part by the Strategic Information and Communications R&D Promotion Programme no. 121803027 of The Ministry of Internal Affairs and Communication in Japan, and by KAKENHI, the Japan Society for the Promotion of Science grant no. 12010738. We also acknowledge the technical support from YAMAHA Sound and IT Development Division in Hamamatsu, Japan.

References

Gelinas D (2007) Living with ALS—managing your symptoms and treatment. Online brochure, The ALS Association. URL http://www.alsa.org/assets/pdfs/brochures/alsa_manual3.pdf

Halder S, Rea M, Andreoni R, Nijboer F, Hammer E, Kleih S, Birbaumer N, Kiibler A (2009) An auditory oddball brain–computer interface for binary choices. Clin Neurophysiol 121(4):516–523. doi:10.1016/j.clinph.2009.11.087. URL http://www.sciencedirect.com/science/article/pii/S1388245709007512

Lelievre Y, Rutkowski TM (2013) Novel virtual moving sound-based spatial auditory brain-computer interface paradigm. In: Proceedings of the 6th international IEEE EMBS Conference on neural engineering. EMBS, IEEE Press, Sheraton San Diego Hotel & Marina, San Diego, CA, USA, pp 9–12. URL http://arxiv.org/abs/1308.2630

Mori H, Makino S, Rutkowski TM (2013a) Multi-command chest tactile brain computer interface for small vehicle robot navigation. In: Imamura K, Usui S, Shirao T, Kasamatsu T, Schwabe L, Zhong N (eds) Brain and health informatics. Lecture notes in computer science, vol 8211. Springer, Berlin, pp 469–478. doi:10.1007/978-3-319-02753-1_47. URL http://dx.doi.org/10.1007/978-3-319-02753-1_47

Mori H, Matsumoto Y, Kryssanov V, Cooper E, Ogawa H, Makino S, Struzik Z, Rutkowski TM (2013b) Multi-command tactile brain computer interface: a feasibility study. In: Oakley I, Brewster S (eds) Haptic and audio interaction design 2013 (HAID 2013). Lecture notes in computer science, vol 7989. Springer, Berlin, pp 50–59. URL http://arxiv.org/abs/1305.4319

Mori H, Matsumoto Y, Struzik ZR, Mori K, Makino S, Mandic D, Rutkowski TM (2013c) Multi-command tactile and auditory brain computer interface based on head position stimulation. In: Proceedings of the fifth international brain-computer interface meeting 2013. Graz University of Technology Publishing House, Austria, Asilomar Conference Center, Pacific Grove, CA, USA, p Article ID: 095. doi:10.3217/978-4-83452-381-5/095. URL http://castor.tugraz.at/doku/BCIMeeting2013/095.pdf

Muller-Putz G, Scherer R, Neuper C, Pfurtscheller G (2006) Steady-state so-matosensory evoked potentials: suitable brain signals for brain-computer interfaces? IEEE Trans Neural Syst Rehabil Eng 14(1):30–37. doi:10.1109/TNSRE.2005.863842

Rutkowski TM, Cichocki A, Mandic DP (2009) Spatial auditory paradigms for brain computer/machine interfacing. In: International workshop on the principles and applications of spatial hearing 2009 (IWPASH 2009)—proceedings of the international workshop, Miyagi-Zao Royal Hotel, Sendai, Japan, p P5

Schreuder M, Blankertz B, Tangermann M (2010) A new auditory multi-class brain-computer interface paradigm: spatial hearing as an informative cue. PLoS ONE 5(4):e9813. doi:10.1371/journal.pone.0009813. URL http://dx.doi.org/10.1371%2Fjournal.pone.0009813

Severens M, Farquhar J, Duysens J, Desain P (2013) A multi-signature brain-computer interface: use of transient and steady-state responses. J Neural Eng 10(2):026005. URL http://stacks.iop.org/1741-2552/10/i=2/a=026005

van der Waal M, Severens M, Geuze J, Desain P (2012) Introducing the tactile speller: an ERP-based brain–computer interface for communication. J Neural Eng 9(4):045002. doi:10.1088/1741-2560/9/4/045002. URL http://stacks.iop.org/1741-2552/9/i=4/a=045002

The BCI 2013 Award Winner and BCI Trends

Christoph Guger and Brendan Z. Allison

The preceding chapters described several of the most novel and promising BCI projects in 2013. The authors also extended the information in their original two-page submissions with additional details, related work, newer directions, and discussion. In this concluding chapter, we announce the 2013 Award winner, discuss trends reflected in the awards, and preview next year's BCI Award.

1 The BCI Award 2013 Winner

This year's jury had the biggest challenge in any BCI Award so far. With 169 submissions, reviewing and scoring all submissions and then selecting ten nominees was not easy. The jury then had to select a winner, who was publicly announced in front of hundreds of other BCI researchers at the Fifth Annual BCI Conference in Asilomar, CA in June 2013. The winner also earned $3000, the statue, and an invitation to the 2014 jury. Theresa Vaughan and the jury chose the winning project

C. Guger
g.tec Medical Engineering GmbH/Guger Technologies OG,
Sierningstrasse 14, 4521 Schiedlberg, Austria

B.Z. Allison (✉)
Cognitive Science Department, University of California at San Diego,
9500 Gilman Drive, La Jolla, CA 91942, USA
e-mail: ballison@ucsd.edu

B.Z. Allison
Electrical and Computer Engineering Department, Old Dominion University,
Norfolk, VA 23529, USA

C. Guger et al. (eds.), *Brain-Computer Interface Research*, SpringerBriefs
in Electrical and Computer Engineering, DOI 10.1007/978-3-319-09979-8_11

because it scored high on all of the Award Criteria, and was particularly novel and promising, with significant potential to help a broad number of people.

The winning project was:

"**A learning-based approach to artificial sensory feedback: intracortical microstimulation replaces and augments vision**"

M.C. Dadarlat[a,b], J.E.O'Doherty[a], P.N. Sabes[a,b]
[a]Department of Physiology, Center for Integrative Neuroscience, San Francisco, CA, US
[b]UC Berkeley-UCSF Bioengineering Graduate Program, University of California, San Francisco, CA, US

2 Trends Reflected in the Awards

The BCI Awards help identify major trends in BCI research. Our BCI Award books have included tables that analyze different characteristics of the submitted projects. These tables help identify characteristics of BCI systems used in top BCI labs, thus reflecting which types of BCIs are most common in submitted projects. For example, Table 1 demonstrates that BCIs submitted to the BCI Awards typically analyze brain signals in real-time. This year, only 5.3 % of the submitted projects focused only on improved signal processing algorithms without real-time validation. The fact that over 150 real-time BCIs were submitted this year demonstrates an impressive growth of BCI system capabilities over the last few years.

Table 2 shows the different input signals used in submissions across the years, with the last row presenting the number of projects that focused on developing new electrodes for BCI systems. Most of the projects use the EEG as input signal because it is relatively cheap and easy to measure. The table shows also that ECoG based systems are used despite their invasive nature, due to their better signal quality, higher spatial resolution and their ability to utilize high-gamma activity as a control signal. The percentage of projects using spike activity decreased slightly in 2013, but is still greater than projects that used fMRI or NIRS. 22 projects used other signals, such as physiological signals from the autonomous nervous system.

Table 3 summarizes the different mental activities used for control across different submissions that relied on EEG activity. In 2013, as with prior years, motor imagery based BCI system were strongly represented with about 25.4 % of the

Table 1 Real-time BCIs and off-line algorithms in projects submitted to the BCI Awards

Property	N	2013 % (N = 169)	2012 % (N = 68)	2011 % (N = 64)	2010 % (N = 57)
Real-time BCI	156	92.3	94.1	95.3	65.2
Off-line algorithms	9	5.3	4.4	3.1	17.5

In all tables in this chapter, N reflects the number of submissions

Table 2 Type of input signal for the BCI system

Property	N	2013 % (N = 169)	2012 % (N = 68)	2011 % (N = 64)	2010 % (N = 57)
EEG	115	68	70.6	70.3	75.4
fMRI	7	4.1	1.5	3.1	3.5
ECoG	16	9.4	13.3	4.7	3.5
NIRS	5	3	1.5	4.7	1.8
Spikes	12	7.1	10.3	12.5	–
Other signals	22	13	2.9	1.6	–
Electrodes	11	6.5	1.5	1.6	–

Table 3 Type of control signal used for EEG based BCIs

Property	N	2013 % (N = 169)	2012 % (N = 68)	2011 % (N = 64)	2010 % (N = 57)
P300, N200	20	11.8	30.9	25	29.8
SSVEP/SSSEP/cVEP	24	14.2	16.2	12.5	8.9
Motor imagery	43	25.4	30.9	29.7	40.4
ASSR	3	1.8	–	1.6	–

submissions, followed by SSVEP/SSSEP/cVEP and P300/N200 based systems. The increase in SSVEP/SSSEP/cVEP based systems in 2012 and 2013 stems partly from on new stimulation principles like the code based stimulation (c-VEP), which leads to higher accuracy and faster election. A few ASSR BCIs were submitted, as in 2011.

Table 4 presents the overall application of the BCI, such as communication, control of a device or facilitating or studying rehabilitation. Table 4 shows that

Table 4 Type of application

Property	N	2013 % (N = 169)	2012 % (N = 68)	2011 % (N = 64)	2010 % (N = 57)
Control	34	20.1	20.6	34.4	17.5
Platform technology	28	16.6	16.2	9.4	12.3
Stroke neural plasticity	22	13.7	26.5	12.5	7
Wheelchair robot prosthetics	20	11.8	8.8	6.2	7
Spelling	14	8.3	25	12.5	19.3
Internet or VR game	10	5.9	2.9	3.1	8.8
Learning	9	5.3	1..5	3.1	–
Monitoring	8	4.7	4.4	1.6	–
Stimulation	6	3.6			

(continued)

Table 4 (continued)

Property	N	2013 % (N = 169)	2012 % (N = 68)	2011 % (N = 64)	2010 % (N = 57)
Authentification speech coma	5	3	–	9.4	–
Connectivity	4	2.4	1.5		
Music	3	1.8			
Sensation	2	1.2	–	1.6	–
Vision	2	1.2	1.5		
Epilepsy	2	1.2			
Depression	–	–	1.5	–	–
Simulation	–	–	1.5	–	–
Neuromarketing	–	–	1.5	–	–
Simulation	–	–	1.5	–	–
Mechanical ventilation	–	–	–	1.6	–

most of the BCI projects still focus on systems to control external devices such as cursors, computers, etc. 16.6 % of the projects developed new platforms for either real-time or off-line BCI analysis. The percentage of stroke rehabilitation projects this year declined relative to 2012, but 2013 had far more total submissions than 2012. Wheelchair control increased slightly from 8.8 to 11.8 %. Interestingly, spelling applications dropped from 25 % to only 8.3 %, which reflects that the field is branching out into new directions. Furthermore, some applications appeared for the first time 2013, while some applications from previous years were absent.

3 Conclusion and Future Directions

The CEO of g.tec, Dr. Christoph Guger, once said that "The Annual BCI Research Award allows us to look back at highlights of BCI research in 20 years and see how the field changed". Indeed, the Annual BCI Awards, supplemented by this book series, have so far been successful in encouraging and documenting the top BCI-related research projects and teams. The 2014 BCI Awards use the same jury selection procedure, award criteria, award, and other details as previous BCI Awards.

g.tec has announced the jury and schedule for the 2014 BCI Award. The Host Institute is the Institute for Knowledge Discovery in the Technical University of Graz in Austria. The Chairman of the Jury, Gernot Mueller-Putz, has selected the following jury:

Deniz Erdogmus
Peter Brunner
Tomasz M. Rutkowski
Mikhail A. Lebedev
Philip N. Sabes

Submissions were due on July 1, 2014, and nominees were informed in August. The winner will be announced at an award ceremony at the Sixth Annual BCI Conference that TU Graz will host from September 16–19. Since the 2013 Award received 169 submissions, the 2014 Award should be very competitive. Submission guidelines and other information about the 2014 Award, and other annual BCI Awards, can be found on bci-award.com.

The jury's Award Criteria are identical to prior years. Hence, anyone considering a submission to a BCI Award may want to review the projects that have been nominated in earlier BCI Awards and consider how these projects scored well on the Award Criteria. For example, submissions should describe how the project is novel in different ways, operates in real-time, helps real-world users, and/or improves speed, accuracy, and/or usability.

Overall, this is a thrilling and dynamic time for the BCI research community. With so many new groups, ideas, and BCI directions, it can be difficult to identify the most impressive projects and trends. In this book, we reviewed the top BCI projects from 2013 and discussed BCI trends and broader ramifications. We enjoyed developing this book along with our contributors, and are very grateful to them for their contributions to our book and the research community. We are especially grateful to the jury for their major efforts to identify ten nominees and then the best project. We also wish to thank our many other colleagues in BCI research around the world for their ongoing efforts to make BCI systems into practical, helpful tools for more users. We also thank you, the reader, and sincerely hope you enjoyed this book.